KTH Royal Institute of Technology

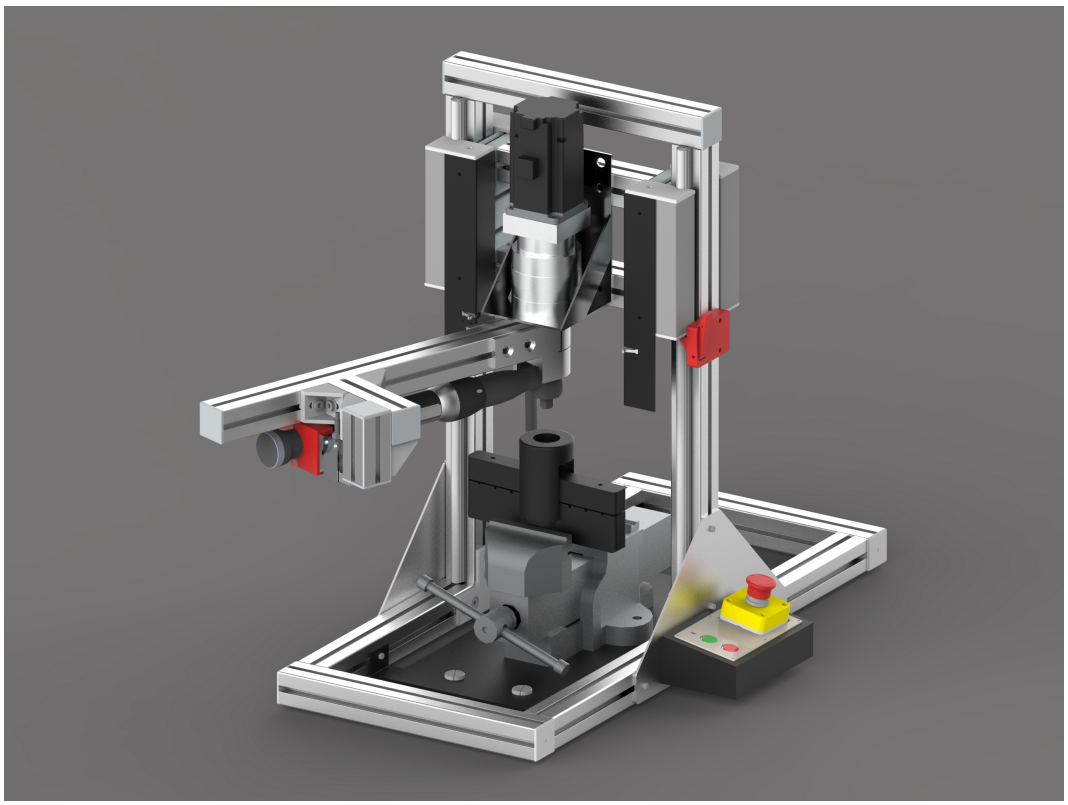

MF2059: Mechatronics Advanced Course, Autumn Semester

Atlas Copco HK Project

Power Tool Test Rig for Ergonomic Assessment and Optimisation of Tightening Algorithms

Submitted by: Samuel Eriksson
Petter Falkenstrand
Annie Farell
Tim Gidlöf
Anton Hylander
William Marin
Denis Ramsden
Erik Rudqvist
Signe Stéen

Supervised by: Daniel Frede

Submitted on: December 19, 2021

Abstract

Powered hand tools are highly common in industries for tightening bolts and nuts, but with them comes health issues for the operator. By using a powered hand tool, like a nutrunner, the operator is exposed to intense reaction forces and vibrations from the tool. Improving these types of tools and its internal tightening algorithm is of great interest as it can relieve the operator. In the present, the exposed reaction force is measured on operators while using the tool which is time-consuming and risky, especially in more extreme cases. This project was founded on the question; “How can a test rig be designed that could simulate a human operator using a nutrunner?” The goal was to develop an automated platform for repetitive ergonomic assessment of hand-held power tools. The main stakeholder requirements from Atlas Copco was that the test rig should simulate a human operator, provide a systematic and repetitive test method and be robust enough to handle extreme tightening cases. The project started in the early spring of 2021 with state of the art in the fields: tightening techniques, ergonomics of powered hand tools, operator models, damping systems and existing test rigs. From the state of the art four design concepts were developed and evaluated against the stakeholder requirements. In the final design, a servo motor and a load cell were used to actively control the rotation of the tool using a simulation of a mass-spring-damping system. The mass-spring-damper system had been verified to resemble a human operator well and the parameters in the model were calculated from using a grey-box on recorded data of reaction forces on a human operator. During the autumn of 2021, the test rig was assembled and tests were performed. The result showed that the test rig gave repetitive results. Almost all stakeholder requirements were fulfilled by the end of the project and some suggestions were made for further improvements. The final test rig could simulate a human operator well and hopefully, this new platform can help the process of improving the algorithms of the tools, which in the end will make a large difference in the operators working conditions.

Acknowledgements

We would like to thank Atlas Copco for offering this interesting project to us, as well as our contact person Sofia Olsson along with the other stakeholders Ava Mazaheri, Romain Haettel, Johan Nåsell and Martin Karlsson at Atlas Copco, giving us feedback and support throughout the project. We would also like to thank our supervisor Daniel Frede for supporting and helping us, for example by giving us advice on how to handle different issues of the project. We would also like to thank the expert panel at Kungliga Tekniska Högskolan (KTH) for giving us their input on different parts of the project where assistance was needed. Hans Johansson and Mikael Hellgren helped us with safe electrical connections and noise problems, and for that we are very thankful.

Contents

List of Figures

List of Tables

Abbreviations

ADC	Analog-to-Digital Converter
BOM	Bill of Materials
CTS	Carpal Tunnel Syndrome
EMC	Electromagnetic Compatibility
EMG	Electromyography
GPIO	General-Purpose Input/Output
HAVS	Hand-Arm Vibration Syndrome
IRTT	Inline Rotary Torque Transducer
KTH	Kungliga Tekniska Högskolan
MSD	Musculoskeletal Disorder
PMSM	Permanent Magnet Synchronous Motor
PWM	Pulse-Width Modulation
QS	*Quick Step*®
RCBO	Residual Current Breaker with Over-current
RMSE	Root Mean Square Error
SOTA	State Of The Art
TT	*Turbo Tight*®

1 Introduction

This section introduces the project with a background and important information to know before reading the report about the project. The section also presents the project description, the requirements and delimitations of the project, conducted interviews during the project, and a description of the report disposition to work as a reader's guide.

1.1 Background

Atlas Copco's Industrial Technique business area provides industrial power tools and systems, industrial assembly solutions, quality assurance products, software, and service through a global network. Atlas Copco's customers often work in physically demanding environments on the human body, such as assembly work. Therefore, it is crucial for the company to continuously develop and improve the ergonomics for the operators using Atlas Copco's handheld tools. This project is mainly focused on vibrations and reaction forces from the tool during bolt tightening. In addition, weight, noise, and physical design are also some significant ergonomic parameters.

The project has several stakeholders at Atlas Copco who provide additional relevant information and support. The stakeholders at Atlas Copco are both the team working with developing tightening algorithms and techniques, and the team working with ergonomics.

1.1.1 Nutrunners

A nutrunner is a tool used in the industry for tightening bolts and nuts. There are two main types of tools, classified by the way they are held by the operator: pistol grip and right angle grip. See figure figure 1 for a comparison of the two grip types.

Figure 1: Examples of a pistol grip nutrunner [1] (left) and a right-angle nutrunner [2] (right).

A right angle nutrunner is preferred for tightenings that require high torque. Compared to a pistol grip nutrunner, it has three times lower vibrations during a tightening and the risk for white finger syndrome is more than three times smaller.[3]

1.1.2 Tightening Techniques

There are many methods for tightening bolts. The most common ones are torque control, angle control, and yield control. Torque control measures the tightening torque and stops tightening when a predetermined torque is reached. This is very simple, but as the friction in the joint can vary widely, the tension in the bolt is difficult to predict. In angle control, the nut is turned to a specified angle. The angle can be difficult to measure precisely, and the required tightening angle can vary between different joints. Yield control requires measurement of both torque and angle. By monitoring both the torque and the nut angle, it is possible to detect when the yield point of the bolt is reached.[4]

Atlas Copco uses the previously mentioned tightening strategies with extra functionality and more advanced control. This report considers three different Atlas Copco tightening strategies: *Turbo Tight®*, *Quick Step*, and *TensorPulse*. *Turbo Tight®* calculates the rotational energy in the tool (motor rotor and gearbox) and predicts when the bolt will be fully tightened. The goal is to let the rotational energy inside the tool power the last bit of the tightening process and thus achieve a very small reaction force to the operator. *Quick Step* has two phases. In the first phase, the bolt is tightened to a first torque, and in the second phase, the speed is reduced and the final torque is reached. This decreases the effects of joint relaxation, but it is not as fast as *Turbo Tight®* and has a larger reaction force [5]. *TensorPulse* tightens the bolt using pulses. The pulses lower the impulse acting on the operator but give rise to vibrations.

1.1.3 Ergonomics of Bolt Tightening Tools

When a nutrunner is tightening a bolt or a nut, a reaction torque occurs as an effect on the tool and the operator. As a consequence, the operator needs to apply an equal and opposite force at the tool handle to counteract the reaction torque. This can be seen in figure 2.[6] Apart from the reaction torque and the reaction force, the operator is also exposed to vibrations when using a bolt tightening tool. All these types of exposures contribute to risk factors of the operator's health.

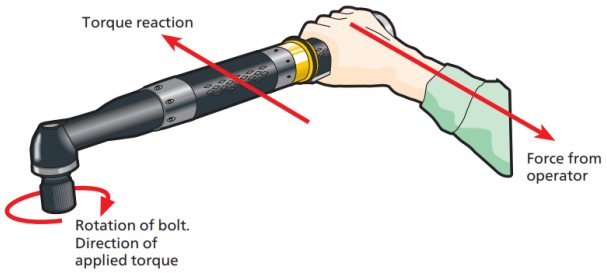

Figure 2: Reaction torque on the operator and resulting reaction force from the operator. [7]

When evaluating the ergonomics of a nutrunner, the vibrations on the operator are of interest. When the operator is using the tool, vibrations are planted through the fingers, hands and arms. These types of vibrations are also called hand-arm vibrations. Hand-arm vibrations are today regarded to be significantly related to serious disorders from workplaces.[8] Hand-Arm Vibration Syndrome (HAVS) is a condition of several serious symptoms for damage caused by vibrations. The most common symptoms are tingling and numbness in the fingers, loss of strength in the hands and white fingers. White fingers is both painful and very serious.[9] Another term for white fingers is Raynaud's phenomenon, which is a disorder of decreased blood circulation in the fingers or toes. If white fingers are not discovered at an early stage, it can result in permanent limitation of blood circulation in the fingers.[10]

Today there are strong regulations and strict standards for both manufacturing new vibrating hand-tools and how these tools should be used from a health perspective. The EU has a legal act called *The Directive 2002/44/EC*, which among other things, lists the minimum standards of acceptable vibrations exposures. The Directive selected the the action value of vibration exposure to be 2.5 m/s^2 and the limit value of vibration exposure to 5 m/s^2, see figure 3. These values are average A-weighted values over an eight-hour working day. From experiences, the right angle nutrunners at Atlas Copco are considered to expose the operator to low vibrations.[8] However, it is still important to have vibrations in mind when evaluating ergonomics in nutrunners.

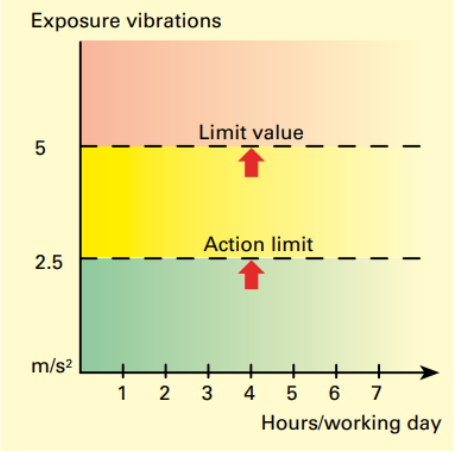

Figure 3: Action value and Limit value for vibrations exposure.[8]

Another common hand condition from working with powered hand tools like nutrunners is Carpal Tunnel Syndrome (CTS). The syndrome is caused by damage or compressing of the median nerve, which is the major nerve through the hand. The median nerve gets compressed when the operator is working with a bent wrist.[11] Some symptoms of CTS are pain, numbness, and tingling through the hands and arms.[12] In figure 4, the placement of the median nerve and the areas of the hand that affect damages on the nerve are illustrated.

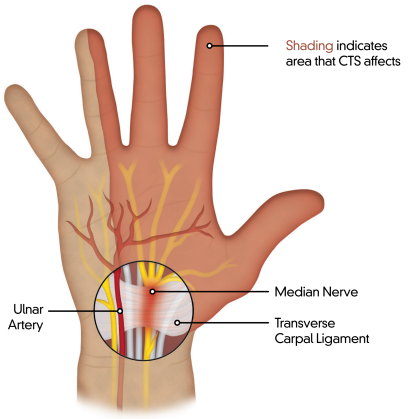

Figure 4: Illustration of damages on the median nerve and Carpal Tunnel Syndrome. [13]

Since the syndrome occurs when the wrist is twisted and exposed to intense loads, the design of the handle is of great importance. To minimise the strain of the operator, the design of the tool handle should enable the operator to keep the wrist straight. Another design factor of the tool that affects the load on the wrist is the weight. If a powered hand tool is too heavy for the operator, it can result in injuries on the wrists as well as decreased precision ability. This can, in turn, affect the quality of the operation.[6] Another aspect that also affects the strain of the hands and wrists

is the position of the operator's centre of body mass. If the operator is standing in a stable position and using a two-hand grip on the nutrunner, the operator can receive reaction forces better and decrease the level of tension in muscles. When an operator is using a nutrunner with only one hand, the operator's capability of handling the torque is significantly reduced.[11] Figure 5 demonstrates an operator holding the tool with a two-hand grip. Lastly, some other design factors that affect the ergonomics of a nutrunner are grip shape, the centre of gravity of the tool, noise and lubrication between components.[11]

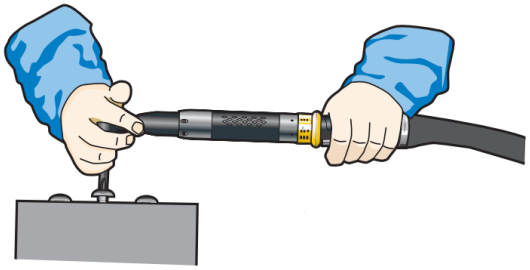

Figure 5: Operator holding a nutrunner with a two-hand grip. [7]

Besides damaging the median nerve, another health risk when using a nutrunner is crushing or injuring the fingers. If the reaction torque on the operator is larger than 60 Nm, a reaction force bar is recommended to minimise the risk of injuries.[11]

Lastly, an important part when evaluating the ergonomics of an operator's work situation is to take the repetitive motions into account. Very common ergonomic risk factors, in general, are the high repetition rate of monotonic motions and lack of recovery between uses of the tool. When the muscles of an operator get exhausted from repetitive motions it can lead to upper Musculoskeletal Disorder (MSD). MSDs include a wide range of injuries on parts like joints, ligaments, muscles and nerves. When the operator is using the nutrunner, the operator needs to increase the grip force in the hand and activate the muscle groups in the forearm during the rundown phase of the bolt tightening. This is to resist the resulting reaction torque from the nutrunner.[14] After many repetitions of using a nutrunner, these muscle groups can get exhausted and potentially injured if the muscles do not recover.

1.1.4 The Value of Improving Ergonomics in Tools

Including ergonomics in the process of developing and evaluating products used by operators has an enormous value in several aspects. Firstly, it can secure the operator's safety, physical health and mental well-being. By improving the ergonomics in nutrunners, the risks of serious conditions like hand-arm vibrations syndrome, CTS and musculoskeletal disorders can be minimised. Secondly, when the operator feels safe and comfortable when using the tools, job satisfaction can be improved. Great job

satisfaction can, in turn, also increase job motivation and result in great productivity and quality of the operations. This can, in turn, create good benefits for the employees at companies.[6] Atlas Copco has throughout the years seen that there is a great economic benefit of including ergonomics in product development.

Atlas Copco has a long and rich history of including ergonomics in the development of hand-held powered tools. In the 1950s, Atlas Copco began to apply ergonomics in drill development. Medical experts were a part of the designing process and gave their opinions on different grip types. The resulting product was a great success and became very popular on the market.[11] Today, ergonomics is a strong part of Atlas Copco's brand and is an important factor for their successful tools. Although the ergonomics of the existing nutrunners has been improved throughout the years, there is still a strong strive at Atlas Copco to continue improve the tools. In the end, these improvements would help and relieve the operator.

1.2 Project Description

The vibration and reaction force levels the operator is subjected to depend on several factors, for example, the tool type, the pre-programmed tightening algorithm, the joint type and the operator himself. The operator's impact on the vibration and reaction force levels varies uncontrollably from test to test, as it depends on how much the operator resists the movements of the tool. To perfect Atlas Copco's ergonomic measurement methods and develop their tightening algorithms, the company needs a controlled test environment with a repetitive model of an operator. As mentioned in section 1.1.4, there is a large incentive to develop ergonomic tools. It has large benefits for the operator and the assembly line as a whole, and that is why Atlas Copco needs a test rig for reliable ergonomic assessment. Atlas Copco is currently in possession of a simple nutrunner test rig, see figure 6. It has only passive components and is therefore limited in its functionality.

Figure 6: One of the current test rigs at Atlas Copco.[15]

1.2.1 The Team's Strengths

The HK project team's strengths are that the group consists of nine diverse, fifth-year students who have high knowledge in different technical areas. The group is good at communicating and cooperates well. The team has also had similar goals and therefore has been able to agree on the project in a good way. The group members also contribute their fair share and offer each other support. Throughout the project, the team has stayed organised thanks to having regular meetings with meeting protocols, a thorough time plan, as well as a shared calendar.

1.2.2 Goals and Impacts of the Project

The goal of this project is to develop an operator-independent test rig for ergonomic assessment and optimisation of new tightening algorithms. The test rig will provide a systematic, repetitive test method to output comparable test results and offer a platform for optimising tightening algorithms.

1.2.3 Deliverables and Most Important Issues

This report is written during the autumn term of 2021 and is a project that was initialised during the spring term of 2021. The group will focus on constructing the test rig. The main goal of this report is to present the final product and the process of reaching the final product. The key parts of the State Of The Art (SOTA) analysis made during the spring term 2021 are included in the report as well, supporting the decisions made to reach the final product.

Included in the final report is also a short description of the design concepts produced during the spring term, as well as the GANTT schedule of the entire project (appendix B) and the required components with a summary of total costs(appendix G).

1.3 Requirements

By close communication with the stakeholders, the stakeholder requirements have continuously been refined and updated during the course of this project. The requirements are divided into different subcategories such as Operator Model, Physical Requirements, Stakeholder Suggestions, Measurement, Wishes, Safety, and Costs.

Operator Model:

- Simulate a human operator accurately (compared to Atlas Copco test data)
- Enable repetitive and accurate test results (of reaction forces and accelerations)
- Being able to test new tightening strategies (redundancy, not just one tightening technique)

Physical Requirements:

- Be robust enough to operate during heavy vibrations
- An Inline Rotary Torque Transducer (IRTT) must fit between the tool and the bolt
- Be robust enough to withstand extreme cases (reaction torques up to 100 Nm)
- Fit a beam test joint (a special part supplied by Atlas Copco)
- Adjust for height difference from bolt tightening

- Work for different tightening strategies (Quickstep, TurboTight and TensorPulse)
- Be able to send data to a Dewe43
- Work with three different angle tools: STR series ETV STR61-50-10, ETV STR61-70-13, ETV STR61-100-13
- 60° rotary displacement

Stakeholder Suggestions:

- Have a lifespan of >10 000 test runs
- Movable by two people
- Short list of components and/or low manufacturing complexity
- Easy maintenance (in terms of sustainability)
- Independent installation of tool (ease of use)

Measurement:

- Accurately measure reaction torque on nut
- Accurately measure vibrations of the tool
- Accurately measure reaction force to the operator

Wishes:

- Work with pistol grip tools
- Simulate different types of operators (different model parameters, at least as continued work)
- Different operator positions can be tested, horizontally and vertically

Safety:

- Protect against injuries, e.g., finger injuries, while running the test rig
- Have an emergency system that stops all operations
- Noise levels below harmful threshold

Costs:

- Enable component and implementation costs within budget

1.4 Delimitations

After some initial research, the project group decided to focus on the main requirements and put some of the wishes aside to reduce the complexity of the construction. The pistol grip tools have not been considered when designing the rig. The main focus has instead been put on the different angle tools, and that the rig should have the ability to change operator characteristics such as inertia, stiffness etc.

The operator model used in this project is a spring-mass-damper system, emulated by an actuator to have the ability to actively control the system. Other operator models, such as active models are discussed but not realised in this project.

1.5 Interviews

During the SOTA review, which is explored further in section 2, a few interviews were conducted. These were carried out to gain knowledge and utilise experience already developed by experts within the fields relevant to the project.

Claes Tisell, lecturer in Systems and Component Design, and Henrik Sandberg, professor in Decision and Control Systems, were interviewed, and a brief summary of these conversations are provided below. Also, a session was held with our stakeholder Sofia Olsson, where the project members, for example, were allowed to test a nutrunner. A summary of this is also provided below.

1.5.1 Interview with Claes Tisell

During the meeting, the realisation of the operator model was discussed. It was also discussed how the data provided by Atlas Copco, showing the reaction force on an operator during nut tightening, can be used to determine the parameters for the operator model. Claes provided the group with contact information to researchers at KTH specialising in biomechanics, active damping, ergonomics, as well as electric and mechanical components.

1.5.2 Interview with Henrik Sandberg

During the meeting, it was discussed how an electric motor could be controlled to simulate a mass-spring-damper system. It was also discussed which type of controller that should be used. Henrik provided the group with educational material written by Bo Bernharsson and Karl Johan Åström about active damping. He also recommended research done by the Robotics Lab at Lund University that might be relevant for this project.

1.5.3 Bolt Tightening with Sofia Olsson

Early on, it was discovered that the project group would benefit greatly in the concept phase if some hands-on experience with the tools in question could be acquired. Therefore, a session was scheduled with Sofia Olsson from Atlas Copco to let each group member try a couple of different tightening techniques with a right angle nutrunner. In figure 7, one of the project members is demonstrating the two-hand grip most commonly used during tightening with a right angle nut-runner.

Figure 7: Project members tested to use a nutrunner from Atlas Copco.

During this session, Sofia also provided a lecture regarding the testing procedures at Atlas Copco in addition to the chance of testing a nutrunner. What software they use, what the results are used for etc. One of the key points from the lecture was Dewesoft, a software for processing data. This was extra fruitful as this is one of the interfaces that the test rig will need compatibility with.

At a later stage of the development process, another meeting was scheduled with Sofia Olsson. While the first meeting was more about how to operate a nutrunner and understand what forces could be expected from it, the second meeting was more technical about how to configure the tool. These configurations were mainly how to enable functions like remote start and create our own tightening programs, which was very helpful to automate and validate the results of the test rig.

1.6 Readers guide

The report divides into nine chapters, where each chapter aims to facilitate the understanding when reading the paper and let the reader gain information about the different parts of the project to understand the final results, including the discussions and conclusions given at the end of the report. The report has the following structure.

Introduction
The introduction (section 1 gives the reader a light overview of the project, where the

reader can find an introduction to the project, some background information, drawn requirements and limitations, and a few interviews conducted during the spring term.

State of the Art
The chapter State of the Art (section 2) presents preliminary research necessary for this project. The chapter includes studies of the following areas relevant to the project: operator models, damping systems, existing test rigs and sensors, to provide insightful information for the subsequent steps of the project.

Methodology
The methodology chapter (section 3) focuses on the project structure, including the project planning, team composition, workflow, internal and external communication, to mention a few. Prior courses in project management have influenced the decisions made throughout this project.

Design Concepts
The design concepts chapter (section 4) presents the different design proposals made at the beginning of the project. The group at KTH made four design proposals during the spring term, including a concept evaluation to conclude a final design proposal, which is presented in this chapter as well. The section 5 then explains the implementation of the final design proposal.

Implementation
The implementation chapter (section 5) contains the final physical construction in detail, including the used electronics with schematics, the operator model, the control scheme of the operator model, software and safety features. The stakeholder requirements viewable in section 1.3 led to the different selections of components and design decisions regarding the previously mentioned parts of the implementation.

Verification
The section on verification (section 6) describes the verification method of the test rig. The verification includes verifying the different subsystems and the complete rig as a whole, including checking the ability to follow the reference generated by the operator model, generating repetitive tests, and matching data collected from a human operator. The presentation of the results of the verification is viewable in the section 7.

Results
The section results (section 7) presents all results of the project, how the final test rig turned out, including results of the verification of performance of the test rig. The section of verification of performance includes the reference tracking, which means how well the test rig followed the generated reference, as well as the repetitiveness, where the repetitiveness is compared to the initial settings of the common gain and P-controller gain. In addition, a human operator is also compared with the test

rig, to see how well the rig measures up to a human. Which of the stakeholder's requirements are met are also described in the results. A discussion of the results is then viewable in the section 8.

Discussion and Conclusions
The section discussion (section 8) discusses the results of the project mainly in the areas where results are presented in section 7, which are the final rig, the verification of performance and the stakeholder requirements. Conclusions are then drawn from these discussions respectively.

Future Work
The section future work (section 9) gives recommendations of how the test rig can be developed further to improve it, with a focus on further verification, and suggested recommendations on different parts regarding the test rig.

2 State of the Art

Section 2 covers the preliminary research made, the state of the art analysis, to later be able to utilise this information in the concept design and thereby the required research for this project to be able to become successful.

2.1 Operator Models

This section presents different methods of simulating the behaviour of the human operator by using operator models, what considerations have to be made when choosing an operator model and how the parameters for the operator model can be determined. This is to find a suitable operator model for use in the test rig.

2.1.1 Human Reaction Time

The reaction time is defined as the time it takes from a stimulus to when a response is performed. During nutrunner operation, stimuli could be the onset of torque build-up.

A study performed by Oh and Radwin indicated that there is a time delay between torque build-up and when a muscle activity burst occurs, defined as Electromyography (EMG) latency. In the study, the muscle EMG activity was measured during nutrunner operation. It was concluded that the EMG latency is greater for softer joints with larger torque build-up time and that a harder joint with shorter torque build-up time results in a lower EMG latency.[16]

2.1.2 Definition of an Operator Model

An operator model is a mathematical model used to describe the behaviour of the human operator. These models can be used to estimate the force the human operator applies to the tool during bolt tightening. Multiple different operator models use different methods of simulating the human operator. Some models are more biologically based on simulating the muscles and tendons, while others are at a higher level, lumping the effects of the different muscles and tendons together. When choosing an operator model, the aspects to take into consideration are the complexity of the model, the accuracy of the model and how the parameters of the model can be determined for different operators. Three of the most common operator models will be described below.

2.1.3 Mass-Spring-Damper Model

One of the most commonly used operator models in nutrunner test rigs is the mass-spring-damper model shown in figure 8. The model uses a spring, mass and damper to simulate the dynamics of the human hand-arm system. Instead of simulating all

muscles, the influences of joints and tendons in the human arm are lumped together into three parameters. These parameters are the spring constant, damping constant and mass. By lumping the parameters together, the complexity of the model is reduced as only the value of these three parameters has to be determined. But at the same time, this results in the model ignoring physiological phenomenons [17] and, according to Johan Nåsell at Atlas Copco, the model will only be an accurate representation of the real system for the first 200 milliseconds of the tightening sequence.

The equation describing the dynamics of the operator using the mass-spring-damper model is shown in equation (1), the relation between the tool angle θ and the mass-spring-damper system displacement x is shown in equation (2).

$$F(t) = m\frac{d^2x}{dt} + d\frac{dx}{dt} + kx \tag{1}$$

$$x = \theta l \tag{2}$$

where F is the force applied to the tool handle by the operator, x is the displacement of the mass-spring-damper system, m is the mass, d is the damping constant, and k is the spring constant.

Figure 8 presents how the operator model will be simulated using a mass-spring-damper system, where θ is the angle of the tool and l is the length between the axis of rotation of the tool to the point where the operator grips the handle.

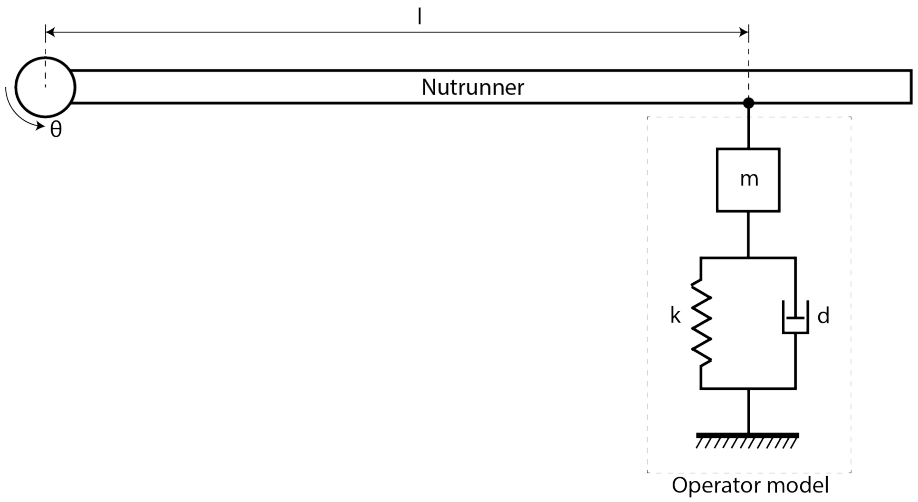

Figure 8: Depiction of the spring-mass-damper operator model with spring constant k, damper coefficient d, mass m, length l and angle θ.

2.2 Damping Systems

A damping system is an assembly that, through its setup and system model, reduces the vibrations of the system it is integrated into. However, depending on the mentioned setup, a damping system can achieve tasks beyond only reducing the vibrations. The three main setups of a damping system are the passive, the semi-active and the active setup. These are described further in this chapter.

2.2.1 Passive Damping

A passive damping system depends only upon components that have time-independent characteristics. Therefore, the agency of a passive system is quite limited. One of the main use cases of a passive system is therefore simple vibration reductions. This is not to say that a passive system is useless. On the contrary, its simplicity often makes it the preferred solution for such use cases [18].

2.2.2 Semi-Active Damping

When the limited agency of a passive damping system is hindering, the semi-active set-up is the next option. The key feature that differs between the passive system and the semi-active system is the ability to change the damping coefficient. The coefficient is changed using a small source of power, and with that in different ways, change the amount of power dissipated inside the damper.

2.2.3 Active Damping

The third and most sophisticated variant of damping systems used in the industry is the active damping system. It has, in addition to the existing damping system, a control structure that can in real-time adjust the oscillating behaviour of the system by either modifying the damping coefficient or by generating additional force, which cancels out the undesired motion and helps the system to follow the desired trajectory.

2.2.4 Implementation of Active Damping

The additional force mentioned in section 2.2.3 is applied by either a linear actuator in parallel with a passive or a semi-active system or by a linear actuator that builds up the complete suspension system by itself.

In the automotive industry, it is common to use hydraulic actuators in parallel with the suspension system. By doing so, it is possible to real-time adjust the behaviour of the suspension system, and this allows the vehicles to counteract body roll and other irregularities on the road to make the ride more comfortable for the passengers. Another way of achieving the active part is by implementing a servo-motor with a ball-screw mechanism parallel with the passive part. This principle was tested by

Masaaki Tawana and Taro Shimogo when they researched the active suspension of truck seats that showed great results [19]. Audi has also achieved active suspension on their A8-line cars by mounting one geared electric motor in parallel with the suspension system on each wheel [20].

There are also examples where the complete suspension system of each wheel is built up by a single actuator. Bose researched for 30 years before the year 2007 when they revealed their electromagnetic suspension system for cars. This electromagnetic suspension system replaces all the parts of a conventional suspension system and did show great handling performance during harsh driving conditions. [21] The electromagnetic system has many benefits over hydraulic systems, but in the end, the weight and the price of the system caused it to never reach the automotive market [21] [22].

2.2.5 Permanent Magnet Synchronous Servo Motors

Permanent Magnet Synchronous Motor (PMSM) is a high-efficiency motor often used in industry. The motor works by inducing a rotating magnetic field in the windings inside the stator. Permanent magnets are placed inside the rotor, and the interaction between the permanent magnetic field of the rotor and the rotating magnetic field of the stator is what creates the torque and gets the rotor to rotate. The rotor will rotate with the same frequency as the rotating magnetic field hence named synchronous. So by varying the frequency of the magnetic field, the rotor speed can be controlled. The change of frequency is, however, a complex task, so to fully be able to operate the PMSM a variable frequency drive or servo driver is required. The control of the motor can then be done with either a trapezoidal or sinusoidal control, and the choice of method is dependent on the task the motor is to perform.

The main advantages of using a PMSM motor is that it has high efficiency compared to other equivalent electric motors used in the industry, the full torque can be delivered at low speeds and the ratio between performance and weight is high. [23]

2.3 Existing Test Rigs

Some test rigs were available at Atlas Copco before the start of this project, on which this project is based. With access to information on past and present test rigs, it became easier for the team at KTH to develop a useful test rig for Atlas Copco. Some of Atlas Copco's existing test rigs are described below.

2.3.1 Atlas Copco's Current Test Rig

Atlas Copco's current test rig shown in figure figure 6 consists of a beam test joint (measures clamping force), dampers, springs, a mass of about one kilogram and

the tool (nutrunner). The dampers are mounted close to the centre of rotation of the nutrunner to reduce the damping effect because it turned out to be quite high. The test rig is supposed to allow movements and vibrations horizontally around the axis of the beam test joint and prevent vertical movement. Rubber bands were temporarily attached to the front rods of the frame to reduce vertical movements. The only programmed software used was modifications for the controller to send out CAN messages of torque, speed, position and current measurements. [15]

Some conclusions drawn regarding this test rig were that it had high repeatability, but the reliability of the experiments needed improvement. It was also concluded that it would be interesting to investigate how changing the mass (or the springs or the dampers) would affect the use of the test rig. Other ideas for future work were safety measures, an analytical model for the tool and human operator and machine learning.

2.3.2 Pneumatic Variant of Test Rig

S. Mukherji constructed a test rig for a right angle nutrunner (manufactured by the company Stanley, but the tool is similar to Atlas Copco's).[24] The operator is modelled as a spring-mass-damper system. A pneumatic cylinder was used as a semi-active spring. The mass could be varied using small removable weights in a cart. The test rig could handle torques of 60 Nm at the nut, and the tests were highly repeatable. However, the rig did not contain a damping element and therefore had some oscillations. The rig is shown in figure 9.

H. Ay et al. constructed a similar rig to Mukherji.[25] The rig also had a pneumatic cylinder used as a semi-active spring and a variable mass using weights. The damping was not adjustable, but the inherent damping of the pneumatic cylinder was found to be close to the human arm model. The system was automated and could simulate a human operator with high accuracy.

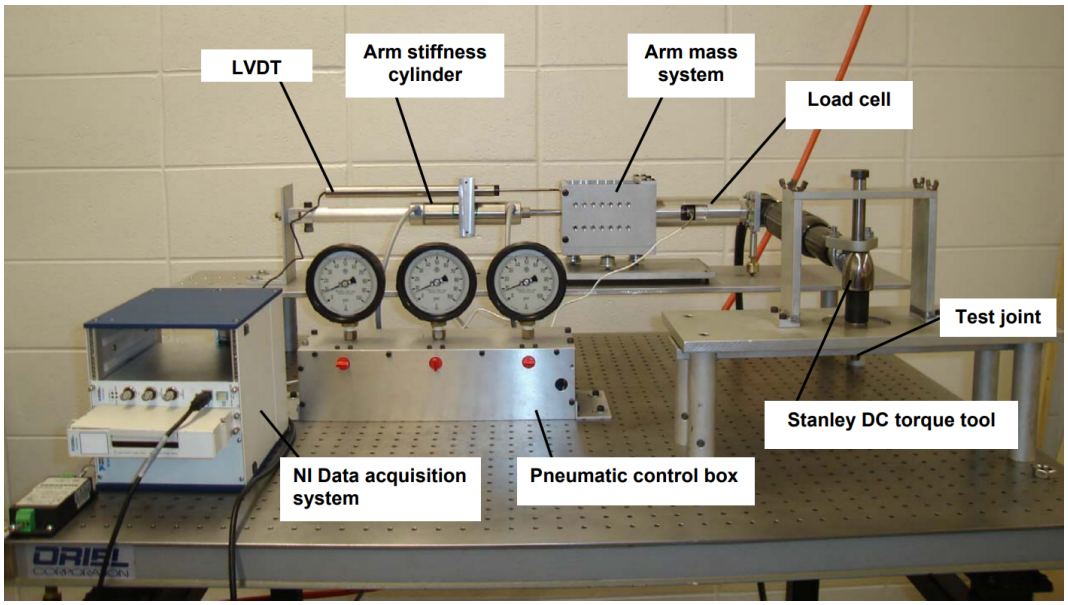

Figure 9: Pneumatic test rig constructed by S. Mukherji.[24, p. 53]

2.4 Sensors

This section describes the relevant theory behind the sensors that have been used in this project, such as load cells, encoders, filters, as well as Dewe43A and Dewesoft.

2.4.1 Load Cells

A load cell is a force transducer that converts a force, torque or pressure into an electric signal. A commonly used load cell is called a strain gauge. A strain gauge uses a thin wire that is strained when a force is applied to the measured object. When the wire is strained, its electrical resistance increase and by measuring an electric signal that goes through the wire, the applied force can be calculated. By combining several wires in one sensor, the force can be measured in multiple dimensions. Generally, the strain gauge has been attached to a metal body that is designed to be able to deform slightly. For small deformations, metal is linear elastic which means that body will behave like a spring and return to its original shape after being unloaded. However, if the load gets too high, the body will be permanently deformed, and the sensor will give invalid measurements.[26]

2.4.2 Encoders

A rotary encoder is a digital sensor that can be used to measure the angle and speed of a rotor shaft. It is characterised by sensing a pulse when the shaft has rotated a certain angle which also can be used to calculate the speed.

A common type is the optical encoder, where a disc with a series of holes is mounted onto the rotary shaft. A light-emitting diode is placed on the opposite side of a photodiode. Each time a hole passes the light diode, the light will pass through the hole and onto the photodiode that generates a pulse.

Another type of encoder is inductive. Inductive encoders generally have lower resolution than optical but are much simpler in their design. There are different variations of inductive encoders, but common for most of them is that movement in different ways can affect a magnetic field, which is used to calculate the angle. [26]

2.4.3 Filters

A very commonly used filter is the low pass filter. Simply, it filters away signals of high frequencies while lower frequencies remain unchanged. The limit for the frequencies filtered away is specified by the cutoff frequency, which is the frequency where the signal is attenuated with 3 dB. A low pass filter can be implemented digitally in software or analogously in hardware. If it is implemented analogously, it can be divided into two types: active and passive. The benefit of a passive filter is that it is very simple to implement. The active filter is more complicated to implement since it uses op-amplifiers but results in lower impedance which is preferable in many applications.[27]

A common application for a low pass filter is to filter away the noise. Noise is typically a high-frequency character, and there will always be noise when measuring a signal.[28] Because of this, a low pass filter can be used after a load cell when measuring, for example, a force. Another implementation is as an anti-aliasing filter. A microcontroller reads a signal digitally, and the bandwidth of the signals it can read is limited by the Nyqvist criteria. An anti-aliasing filter is a low pass filter that filters away all signals outside the bandwidth, which otherwise would be miss-interpreted by the microcontroller as part of the signal.[29]

2.4.4 Dewe43A and Dewesoft

The Dewe43A that can be seen in figure 10 is a product designed by Dewesoft to allow the user to collect data with high precision and that is synchronised with time. The company also provides free software called Dewesoft X3 that can be used to visualise and analyse the data. The Dewe43A has eight analogue input channels that can measure voltages with 24-bit resolution. It also has eight encoder inputs and two CAN ports.

An important feature of the Dewe43A is that it can be used to amplify signals, which is important since the signals from all the sensors can be very small.

Another aspect with the Dewe43A is that it is not designed to provide data in real-time. Because of this, it is not suitable to use it when implementing real-time applications like active damping. A microcontroller needs to be used for that instead, to receive and transmit signals. In that case, extra amplifiers need to be used to scale the signals so that it corresponds to the microcontrollers reference voltage.[30]

Figure 10: Dewe43A board.[31]

3 Methodology

This section will mainly focus on the project structure concerning the project planning, team composition, workflow, and internal and external communication. The decisions made throughout the project were heavily influenced by prior courses in project management and from previous personal experiences from various projects.

3.1 Project Organisation

The project began in March 2021. The first phase was to pursue a state of the art research to gain knowledge and insight about what was expected from the students. The workload during the SOTA was divided into three research areas: ergonomics, bolt tightening, and active damping. The team, which consisted of nine students were divided into three subgroups with three students in each group. Each subgroup was responsible for one of the research areas.

After the SOTA, it was time to generate design proposals for the test rig. The previous subgroups were broken up and mixed into three new constellations, which ensured that all subgroups had the necessary knowledge from each research field to generate proper design ideas for the test rig. During this process, all subgroups worked independently to avoid being influenced by each other. By doing this, the team could produce a couple of different design approaches, which later got evaluated by using an evaluation matrix that was based on the project requirements and also by having continuous discussions with the stakeholders of the project. This evaluation method did not only help the team to compare different designs but also generate ideas on how to improve the proposals further. The inspiration for this working method comes from the agile project management methodology, which encourages continuous learning and is proven to be very effective when pursuing a complex project in which changes often occur along the way.

By August 2021, a final design concept had been chosen, and the development phase of the rig could begin. To stay productive and effective while also minimising potential risks and mistakes, the team decided to fully incorporate an agile project management structure. This way of working comes with many benefits, such as allowing for complete transparency, stakeholder focus, adaptability and shared ownership.

3.1.1 Transparency

A core part of agile project management is the emphasis on a shared understanding of the different processes of the project. This was achieved by having weekly team meetings, in which everyone could share what they have been working on, how it went and what they will do for the upcoming week. All of this was documented in a

shared kanban board which increased transparency. Doing this allowed every team member to have complete insight into all the different development processes. This also made it possible for the team members to be flexible and help out on different types of engineering tasks without having to spend a lot of time catching up on what previous work had been performed by other project members.

3.1.2 Stakeholder Focus

In most engineering projects, the stakeholders have different kinds of requirements, which will ensure that the final product meets their expectations. For a complex project, this might be easier said than done since there are a lot of internal and external factors that can affect the project outcome. By scheduling at least one stakeholder meeting per week, the team could frequently deliver small updates about the progress. The stakeholders could therefore be updated about the direction of the project and continuously provide the team with important feedback. By doing this, the team could be confident that they were always working towards a final product that would meet the stakeholders' requirements.

3.1.3 Adaptability

There are many unknown factors in complex engineering projects which cannot be fully considered before developing the product. Because of this, it is essential that the team work in a way that allows for adaptations along the way. This was achieved by trying to produce small work batches to see if an alternative engineering solution was practical in reality. It could be anything from manufacturing a new design of 3D printed components to evaluating the potential improvement in performance, implementing additional low pass filters to see how it affected the readability of sensor signals or trying out different cables to reduce the external electromagnetic interference. Some of these solutions were successful right away, while others required further improvements before they could be implemented. By continuously evaluating small work batches, the team could avoid mistakes early in the development process.

3.1.4 Shared Ownership

In traditional project management, all information within the project has to go through a project manager, whose job is to allocate different work tasks to the team members. This method can, however, be very inefficient since the project direction is heavily influenced by one single person. In contrast, the agile working method enables the entire team to be part of the decision-making process. The method decreases the risk of group thinking while allowing people with experience in a specific technical field to get their opinion across. This was proven to be very successful for this project since the group could together conduct productive

meetings and have discussions with regarding critical problems. By also allowing team members to work with different parts of the test rig, the project was not as dependent on a single person to perform a specific task, since other team members could step in if necessary.

3.2 Engineering Approach

With a design concept in place, the whole test rig could be broken down into smaller subsystems and then into single components. This method is referred to as the V-model, which increases the visibility of the project and decreases the risk of producing sub-optimal parts which might be detected later on in the project, see figure figure 11. It also makes it easier for the team to evaluate the workload for different tasks. Depending on the criticality and complexity of a specific task, either one or multiple people could be working on a single assignment. All of this was carefully documented in a kanban board to keep track of the progress. Once a subsystem got completed, it was tested and verified to see how it would work with other subsystems. For example, when the test rigs frame was complete, the team could perform tests to verify if the structure was robust enough to hold the remaining parts of the test rig.

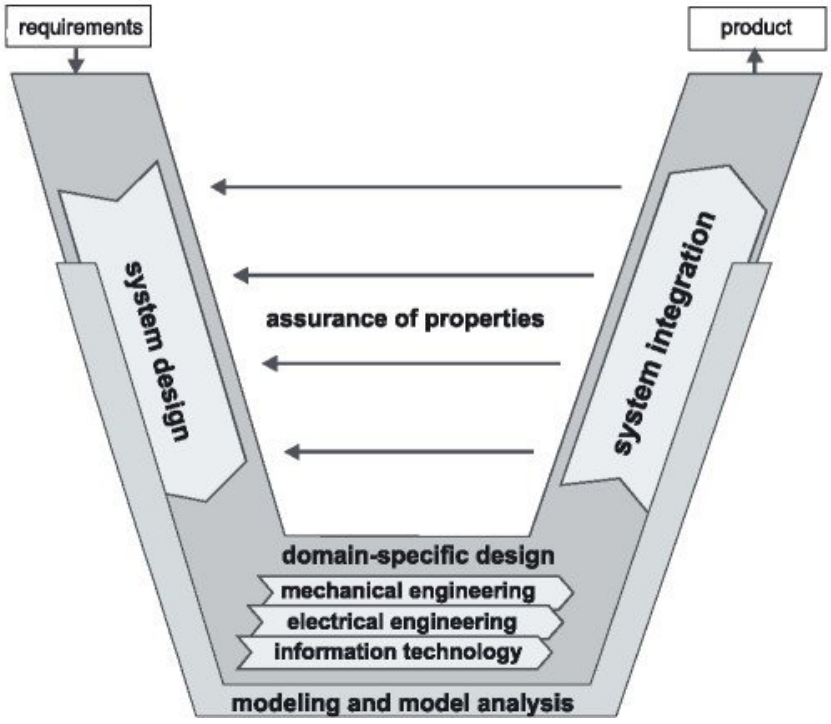

Figure 11: V-Model.[32]

3.3 Time Planning

In addition of using a kanban board for generating an overview of the tasks that had to be preformed, a GANTT chart was also used for time planning. Its main purpose was to help keep track of important deadlines. It included all key activities as well as estimations on how much time to spend on each subsystem, see appendix B. During the weekly meetings, the whole team checked the GANTT chart to see how it related to the actual progress of the test rig.

3.4 Communication

Since communication is a vital part of any successful project, a communication plan was established early on to ensure that internal information among project members and external information between stakeholders was done in a structured way, see table table 1.

Table 1: Communication plan

Audience	**Why?**	**When?**	**How?**
Atlas Copco	Keep project owner up to date and ensure realistic expectations	Once a week	Teams/mail
Project members	Discuss time planning, problem and activities to be performed	Ongoing	At KTH/Discord
Coach	Get continuous feedback on the progress of the project	Once a week	Zoom/mail
Component resellers	Get necessary components on time	When necessary	Mail

Apart from verbal communication tools, Google Drive and Google Calendar were also frequently used to store project files, facilitate collaboration and schedule meetings.

4 Design Concepts

The bulk load of the SOTA regarding test rigs in terms of hand tools, and most of the concept creation process based on the SOTA, was performed in a prestudy during the spring of 2021. This section recaps this work and moves it forward by narrowing the four different concepts down to a final one, which will be realised in later chapters.Initially, three concepts were created. However, during the evaluation process, a fourth concept was conceived, which is basically a mix of the three initial concepts. These four concepts are recapped below in the sections 4.1-4.4.

4.1 Design Concept 1

The central idea behind design concept one, a somewhat improved version from what can be seen in figure 12), is that the force from the operator model will be applied to the tool handle via a rotating beam that follows the movement of the tool. The rotating beam has the same rotational axis as the tool and is fixed to the tool handle via a clamp. A force sensor is attached between the clamp and the rotating beam to measure the reaction force on the operator. A cup attached to the rotating beam presses on the tool head, thus mimicking the operators resting hand.

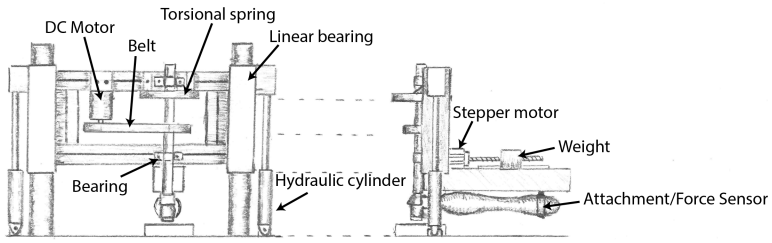

Figure 12: Spring 2021 concept 1 drawing, compare with figure 13 for updated version.

To generate the force from the operator model, a servo motor and a gearbox are attached to the rotational axis of the rotating beam. Two alternative ways of mounting the output shaft of the gearbox to the rotating beam are proposed. The first alternative is to mount the output shaft directly to the rotating beam via a custom bracket, as can be seen in figure 21. However, then the weight of the tool and the rotating beam will cause a bending torque on the gearbox shaft. The other alternative is to extend the gearbox shaft and have an external bearing above the rotating beam to reduce the bending torque acting on the gearbox shaft, as can be seen in figure 13.

The rotating beam, servo motor and gearbox is mounted on linear rails, allowing them to move vertically, which makes it possible for the tool to move down during a tightening, and it also makes it possible to fit different extensions between the

tool and socket. To reduce the weight resting on the tool head two gas springs are attached to the sliding assembly.

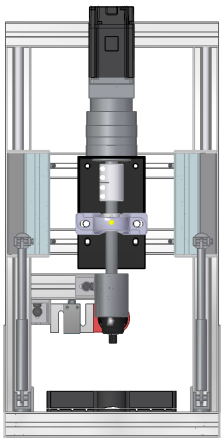

(a) Front view of concept 1.

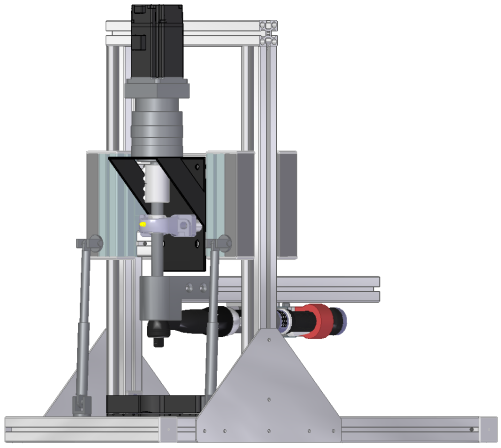

(b) Corner view of concept 1.

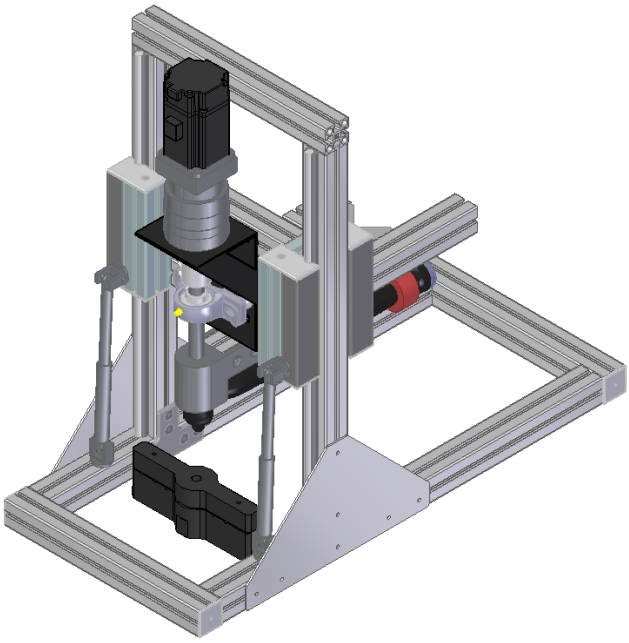

(c) Isometric view of concept 1.

Figure 13: Concept 1 design illustration.

4.2 Design Concept 2

The main idea of design concept two is that the test rig would apply the force at the handle of the tool, which would visually mimic a human operator. The test rig in this concept controls and absorbs reaction forces with the help of a mass-spring-damper system, in which a pneumatic cylinder is used to actively regulate the various forces, which arise when tightening the screw. The idea is that the pneumatic cylinder

should have an equivalent to adjustable damping constant, which would make the test rig semi-active and able to preset parameters, and then let the cylinder regulate accordingly.

The construction of the test rig in design concept two is the following: the tool handle is mounted in a bracket on a carriage that runs along a circular rail, which enables the carriage to follow the rotational movement of the tool. The tool attachment on the carriage has a vertical rail which enables the tool to move down vertically during the tightening phase. This can be seen in figure 15. One end of the pneumatic cylinder is attached to the carriage, and the other end is mounted on a plane with a circular joint. This construction enables the pneumatic cylinder to rotate vertically and horizontally and is thus able to dampen the system smoothly. See figure 14.

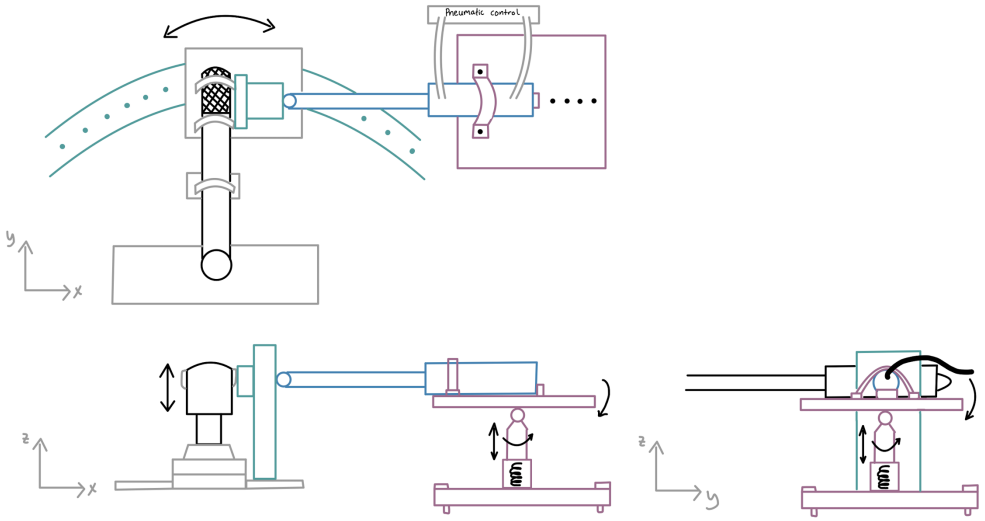

Figure 14: Design Concept 2: drawing with front view (xz-plane), side view (yz-plane) and top view (xy-plane).

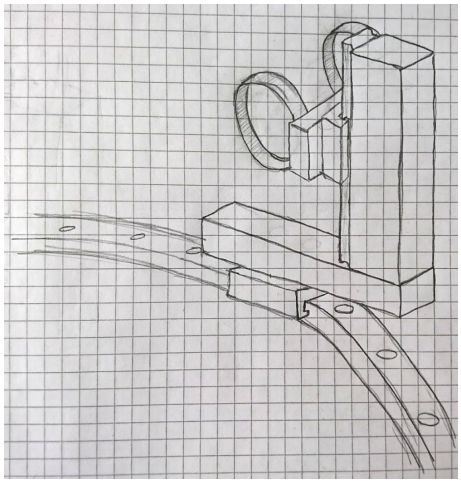

Figure 15: Detailed view of carriage and the tool attachment on vertical rails.

4.3 Design Concept 3

The main idea of design concept three is to apply a reaction force at the tool handle and dampen the movement of the tool actively by using an electric motor through a belt drive system. The electric motor was meant to be modelled in a way that the system dynamics mimic the dynamics of a mass-spring-damper system. The motor applies force on the belt drive through a gearbox and a rotational gear to which the belt is attached. This belt is, in turn, connected to a carriage where the handle is attached as well. The carriage slides on a linear rail, which can be seen in figure 16. The motor torque controls the belt position, which results in the reaction force at the tool handle. The linear rail limits the rotational motion of the rig since the nutrunner travels in a circular path. However, to allow the tool to rotate, the carriage have a slot and a pin on the tool handle bracket, allowing the tool to move in both x-direction and y-direction as pictured in figure 17. The construction has a helix screw and springs that push the tool's head onto the socket and beam test joint. The helix screw intends to stabilise the tool to prevent unwanted vibrations, and the helix screw is adjustable up and down to enable changing the tools.

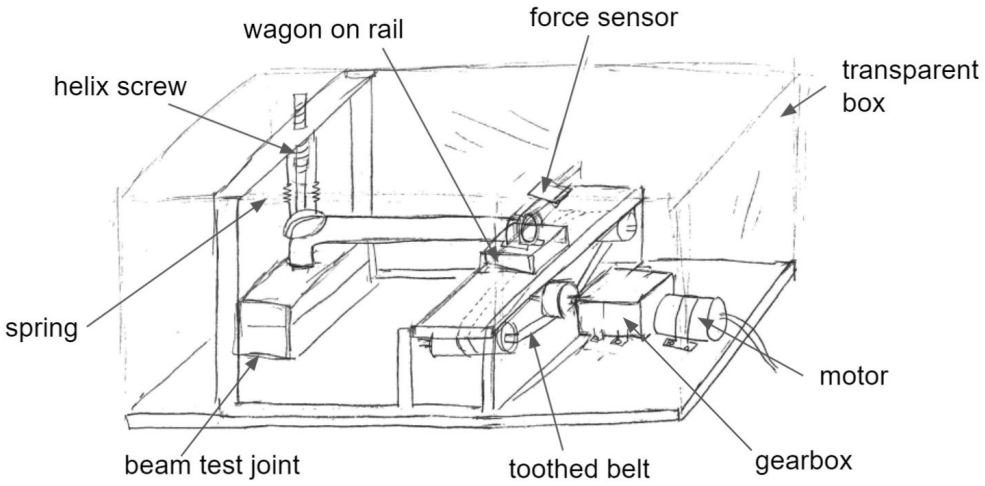

Figure 16: Overview of concept 3 with all important features marked out.

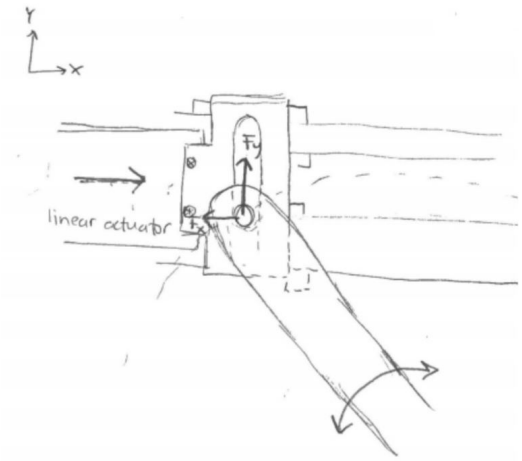

Figure 17: Detailed view of the tool handle and the carrier.

4.4 Design Concept 4

Later on in the concept evaluating process, a fourth design concept was developed. The benefits and drawbacks were summarised of the previous concepts, and the benefits from each concept formed the fourth concept. Different mechanical solutions from the concepts were combined into this concept. This concept has a rotating beam, inspired from the first concept, circular rails from the second concept and a belt drive system from the third concept. This combined construction illustrated in figure 19. The aluminium structure can rotate with the tool. It is fastened to a circular rail to keep it centred around the nut. A load cell measures the force between the tool handle and the operator, and when the tool rotates, it drives a servo. Like the previous concepts with motors, the servo motor in this concept has a control system based on the dynamics of a mass-spring-damper system to simulate the operator.

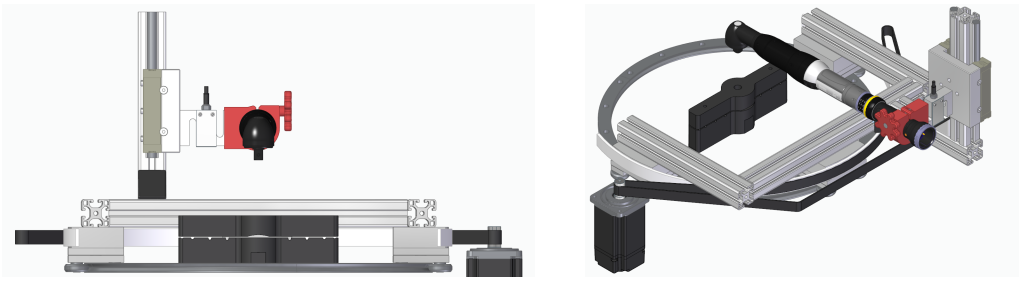

(a) Front view of combination concept.

(b) Isometric view from back of combination concept.

Figure 18: Combination concept design illustration.

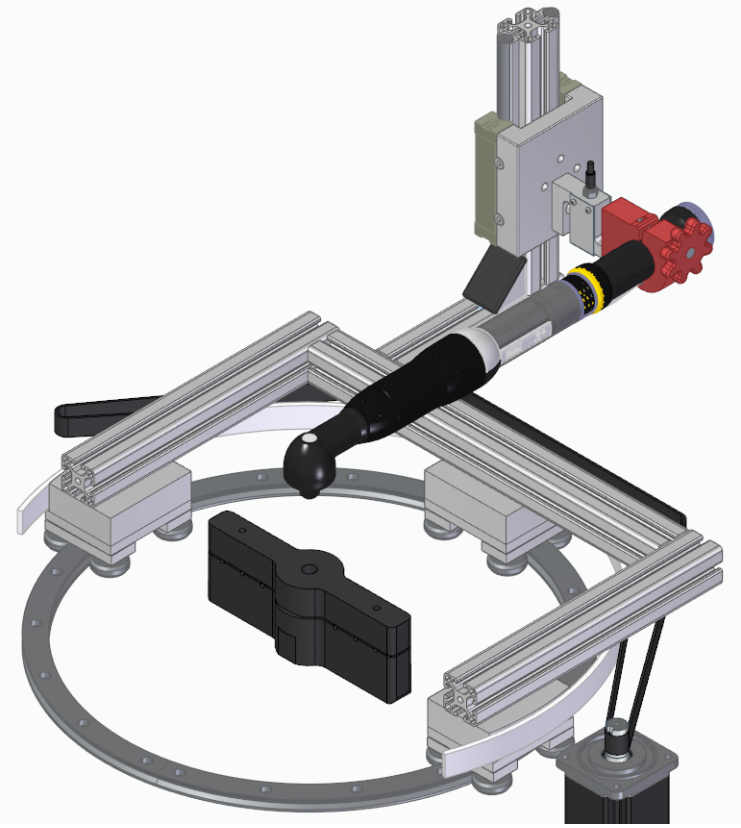

Figure 19: Isometric view from front of combination concept.

4.5 Concept Evaluation

Chapter 3.1 mentions that during the Spring of 2021, a concept generation phase was initiated and that there was a substantial evaluation phase following subsequently to that. This chapter delves deeper into that process.

4.5.1 First Round of Concept Evaluation: Pro-Con Lists

Initially, as mentioned in 4, there were only three concepts, each one corresponding to a subgroup. The evaluation process was commenced with these as contenders. To start, these were compared to each other with the help of a simple pro-con list. The final list was quite lengthy and can be found in appendix C, here only a selection of the most vital attributes are presented.

Pros of Concept 1:

+ The height of the rig is movable, which enables the rig to follow the tool down during bolt tightening and to fit different types of beam test joints.
+ This height regulation also enables the rig to fit different types of beam test joints and various sensors.

Cons Concept 1:

- The beam that the tool is attached too can be heavy. This can affect the inertia and the results of the tests.
- The concept will require a large gear ratio, which can increase the inertia of the system a lot, as the inertia of the motor is proportional to the gear ratio squared.

Pros Concept 2:

+ Easy to use semi-active system which has been proven to work (section 2.3).
+ Using a pneumatic cylinder semi-actively is robust for extreme cases, since it does not need be actively controlled and requires no power during test runs.

Cons Concept 2:

- Semi-active systems limits the modelling of a human operator. For example, the stiffness and damping can change during rundown which is hard to simulate with pneumatic.
- Friction forces in the rail might affect the test results, and if the nut is not perfectly centred the linear bearing might bind up.

Pros Concept 3:

+ A passive system with springs and dampers can be implemented parallel to the active system. This would also decrees the torque requirement on the motor.

Cons Concept 3:

- The tool has limited rotation range since the tool attachment point in the wagon has limited vertical translation space.
- As for concept 1, the inertia of the motor will have a large effect on the total system inertia, as there is a high gear ratio.

These pros and cons were then considered within the group, but also presented to the stakeholders. They had plenty of feedback, not only regarding the pros and cons, but also concerning the concepts themselves. The input revolved around the construction and some ideas on how to improve the different concepts. Below are a couple of the bullet points summarising the feedback.

- The stakeholders liked the different ideas from all the concepts.

- One idea from the stakeholders was to have a permanent passive system parallel to an active system, to decrease the requirements on the active system.
- A suggestion was to use a plate coupling between the passive and the active system and to connect the active system at a specific time.
- One solution might be to regulate the height of the beam test joint and not the rig itself during tightening.
- The tool does not need to start from degree 0 but it can start from example -20 and when rotate to 20 degrees (40 degrees rotation in total).
- In terms of motor requirements, the motor needs to counteract the tools movement by applying a larger torque to stop the tool rotating.
- It was more important to have a robust rig than it would be easy to change tool and to move the rig.
- It was also more important to be able to test different tightening techniques than to test different operators.
- The project group need to have in mind that the rig needs to have space for a tool battery or space for a power cable.
- Concept 1 would probably require a gear ratio since the torque requirement on the motor could be very large. If a gear box would be used it would affect the inertia of the system.
- The group also needs to check that the motor for concept 1 would be fast enough, this with also having the extra inertia in mind.
- For the rails in concept 2 and 3, the project group needs to have the friction in mind.
- A cylinder can effectively damp vibrations.

4.5.2 First Round of Concept Evaluation: Evaluation Matrix

In addition to the pro-con list, an evaluation matrix was constructed, see figure 20. This was done in a systematic way to evaluate the different concepts objectively. The matrix was built with weights to emphasise attributes and stakeholder requirements deemed more important, and they were set according to the categories presented below.

- 5 - Extremely important
- 4 - Very Important
- 3 - Important

- 2 - Desirable, but not so important
- 1 - Desirable, but not important

Requirement Category		Stakeholder requirements	Weight	Concept 1		Concept 2		Concept 3	
		The test rig should...		Concept Point	Score	Concept Point	Score	Concept Point	Score
	1	Simulate an human operator accurately (compared to Atlas Copco test data)	4		0		0		0
	2	Enable repetitive and accurate test results (of reaction forces and accelerations)	5		0		0		0
Operator Model	3	Being able to test new tightening strategies (redundancy, not just one tightening technique)	2		0		0		0
	4	Be robust enough to operate during heavy vibrations	4		0		0		0
	5	An IRTT must fit between the tool and the bolt	5		0		0		0
	6	Be robust enough to withstand extreme cases (reaction torques up to 100Nm)	3		0		0		0
	7	Fit a beam test joint	5		0		0		0
	8	Adjust for height difference from bolt tightening	4		0		0		0
	9	Work for different tightening strategies (Quickstep, turbotight, tensorpulse?)	3		0		0		0
	10	Be able to send data to a Dewe43	5		0		0		0
	11	Work with threee different angle tools: STR series (ETV STR61-50-10, ETV STR61-70-13, ETV STR61-100-13)	2		0		0		0
Phyisical Requirements	12	60 degree rotary displacement	3		0		0		0
	13	Have a lifespan of >10 000 uses	3		0		0		0
	14	Movable by two people	4		0		0		0
	15	Short list of components/low manufacturing complexity	3		0		0		0
	16	Easy maintenance (in terms of sustainability)	3		0		0		0
Our Suggestions	17	Independant installation of tool (ease of use)	4		0		0		0
	18	Accurately measure reaction torques on nut	3		0		0		0
	19	Accurately measure vibrations	2		0		0		0
Measurment	20	Accerately measure reaction force	5		0		0		0
	21	Work with pistol grip tools	1		0		0		0
	22	Simulate different types of operators (different model parameters at least as continued work)	2		0		0		0
Wishes	23	Different operator positions can be tested, horizontally and vertically	1		0		0		0
	24	Protect against finger injuries	4		0		0		0
	25	Have an emergency system that stops all operations	5		0		0		0
Safety:	26	Noise levels below harmful threshold (noise level under XX db)	4		0		0		0
Costs:	27	Enable component and manufacturing costs within budget	3		0		0		0
					0		0		0
				Total Score:	0	Total Score:	0	Total Score:	0

Figure 20: Evaluation matrix template, with weights and different categories.

Each group member completed the evaluation matrix individually, and subsequently, all the matrices were compiled into a final result. The final result turned out to be very even between the concepts, but concept 1 got the highest score for most of the project members. This result, in combination with the stakeholder feedback and the pro-con lists, determined concept one as the preferred concept. However, the group and Atlas Copco saw benefits and drawbacks in each concept, and to extract all the benefits, a fourth concept was conceived. Concept four was a mix of the previous three concepts and was described in some more detail in 4.4.

4.5.3 Second Round of Concept Evaluation

The conception of concept four commenced a second round of the concept evaluation, with concepts one and four as contenders. Concepts two and three were not included again as they were already eliminated in the first round. However, the thought process was that their strengths would be included in concept four and so indirectly be re-evaluated.

The second round began with general thoughts regarding the concepts and a somewhat unstructured pro-con list. However, to systematise the process, another weighted evaluation matrix was introduced. The second evaluation matrix was not quite as thorough as the first one but was still based on the same concept of weighting different attributes to emphasise which ones are most important. It can be seen in table 2. As is apparent, not all attributes of concepts one and four were scored or weighted. This was since the group found difficulty in distinguishing a difference in

performance regarding these attributes between the two remaining concepts. A more detailed explanation of each test rig attribute in this second evaluation matrix can be seen in Appendix F.

Table 2: Weighted attribute comparison between concept 1 and concept 4, an evaluation matrix.

Second evaluation matrix			
Test-rig attribute	Weight	Concept 1	Concept 4
Low moment of inertia*	3	9	3
Repetitiveness*	-	5	5
Extreme cases*	-	5	5
Easy access to nut*	1	3	2
Easy access to tool*	1	2	3
Robustness*	-	5	5
Vibration resistance*	3	-	-
IRTT Compatibility*	3	9	6
Vertical adjustment*	3	9	6
Component availability*	3	1	3
Complexity	1	3	3
Mobility*	1	-	-
Cost	-	6	4
SUM		95	63

* Further explained in appendix F

According to this evaluation matrix, it is clear that concept one was still favoured, but the final blow to concept four did not hit until an inquiry into the cost of the circular rails, one of its major components, was performed. The price was much higher than first expected and did not fit into the budget, which resulted in concept four being discontinued, indirectly pushing concept one forward as the concept that would continue to see development.

4.6 Final Design Proposal

Through the extensive evaluation process described in 4.5, the group landed in following up on concept one, shown in figure 13. However, due to budgetary reasons, in combination with difficulty finding the right components, a shortened version of concept one was developed. This version has a shortened axle, and the motor mount is flipped to save on parts, which also results in a simpler construction and is illustrated in figure 21. The final design proposal also added a base plate and a vice to hold the beam test joint. A height stop was added to be able to lock the sliding mechanism in the upright position, mechanical stops were added for increased safety, and a button interface was added to control the rig.

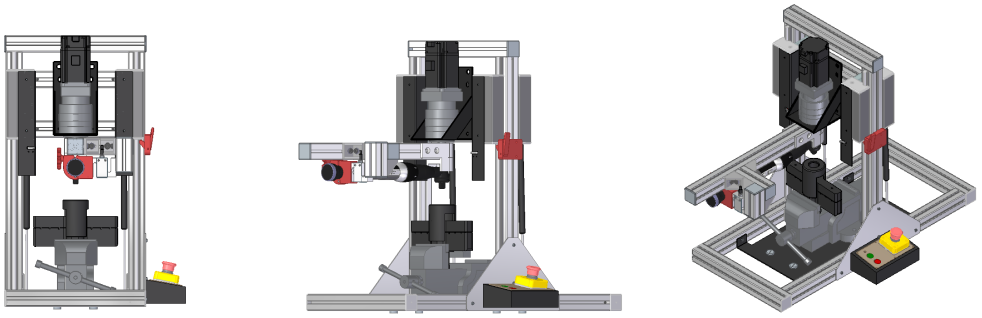

(a) Front view of the final concept. (b) Corner view of the final concept. (c) Isometric view of the final concept.

Figure 21: Final concept design illustration.

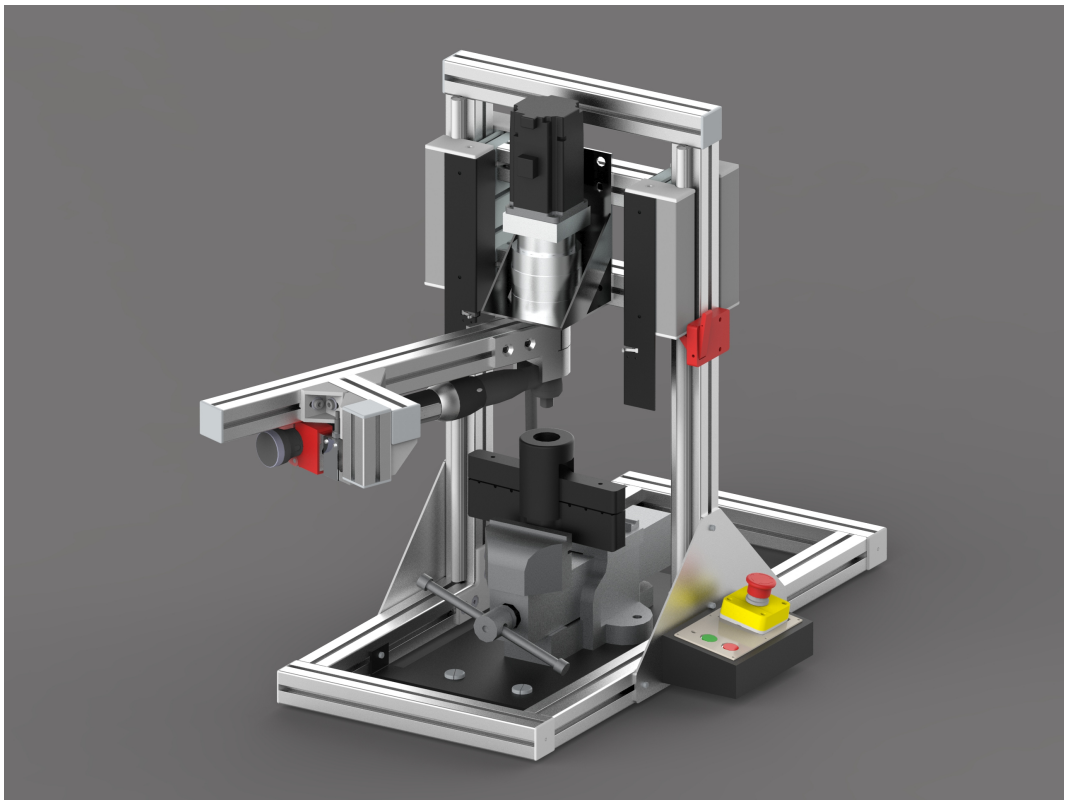

Figure 22: Render image of the final concept.

5 Implementation

This section contains the final physical construction in full detail, the used electronics with schematics, the operator model and control scheme, software and safety features. The component selection and design decisions regarding the test rig were based on the stakeholder requirements. A Bill of Materials (BOM) was made to keep track of all purchased components and costs, which is attached in appendix G.

5.1 Construction Overview

The final construction of the test rig can be seen in Figure 23 and 24. Figure 23 shows the different components of the rig and figure 24 shows different views of the rig. More details about the construction of the test rig will be described in the following subsections.

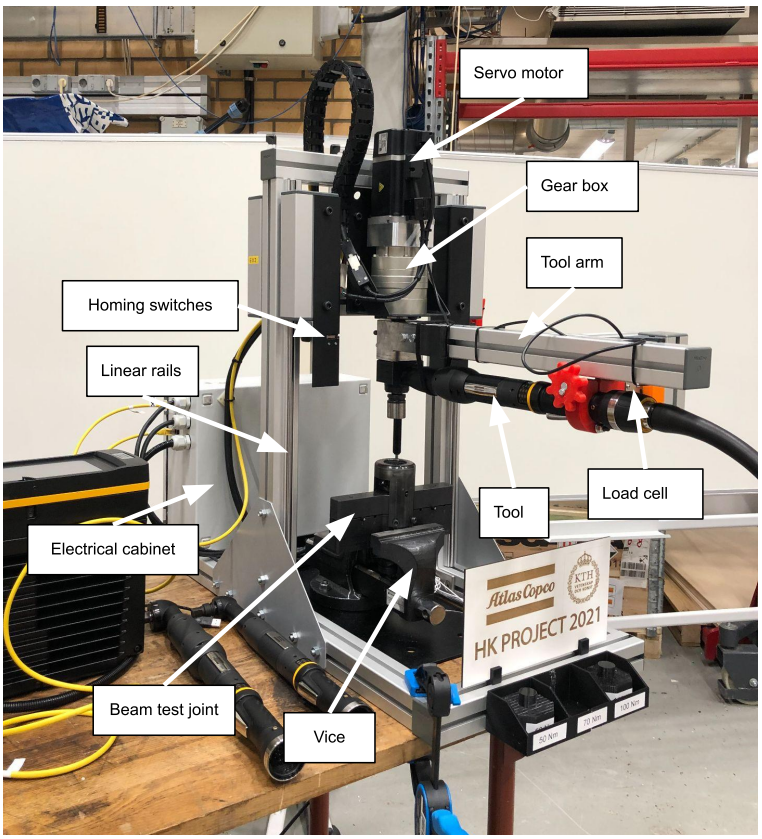

Figure 23: Overview of the components of the test rig.

(a) Corner view of the final test rig.

(b) Front view of the final test rig.

(c) Isometric view of the final test rig.

Figure 24: Overview of the final test rig.

5.2 Frame

The physical foundation of the test rig consists of aluminium profiles that form a frame, see figure 25. Aluminium profiles were suitable for the test rig since they are lightweight, compatible with linear components, and have easy and flexible attachment solutions.

Two important physical requirements for the test rig were that it should be robust enough for exposure to high reaction torques and heavy vibrations during operations. To fulfil these requirements, the frame was designed to have a large rectangular base that would stabilise and absorb reaction forces from tightenings. The two vertically mounted aluminium profiles with linear rails were placed in the centre of the base frame to ensure stability.

Figure 25: The frame of the test rig, built by aluminium profiles.

5.2.1 Mechanical Stops

To protect the linear rails and the test rig if the tool arm would collide with the frame, two mechanical stops were implemented. The mechanical stops was attached to the rig, which can be seen in figure 26. The mechanical stops was made by water cutting two steel plates with 2 mm thickness. These were then bent with a press brake to fit the rig. Cut outs were made for screws holes and to fit the electrical switches for the homing sequence, which will be described later in section 5.8.3.

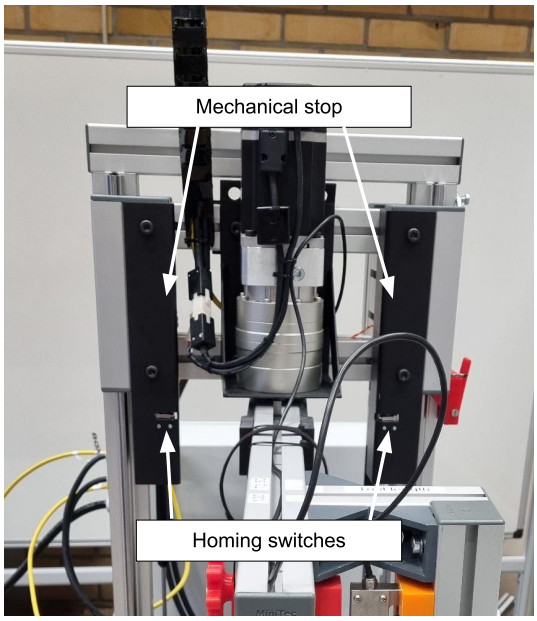

Figure 26: Mechanical stop.

5.2.2 Fastening Mechanism

A vice was used to fix the beam test joint to the rig. This vice is fastened to a custom made bottom plate that is fastened to the frame of the rig by using four M8 screws in each corner of the base plate into the slots of the aluminium profiles. This makes it possible to move the frame of the rig in relation to the vice, which is required since the centre of the tool always needs to match the centre of the beam test joint, even for different sizes of the beam test joint.

The bottom plate also has a pattern of four holes that fits the standard pattern of a Siegmund table used by Atlas Copco. These holes can be used to fasten the whole rig to the table by using four screws. Figure 27 shows the bottom plate mounted to the frame of the rig. The vice is also fastened to the base plate, and the beam test joint is mounted to the vice.

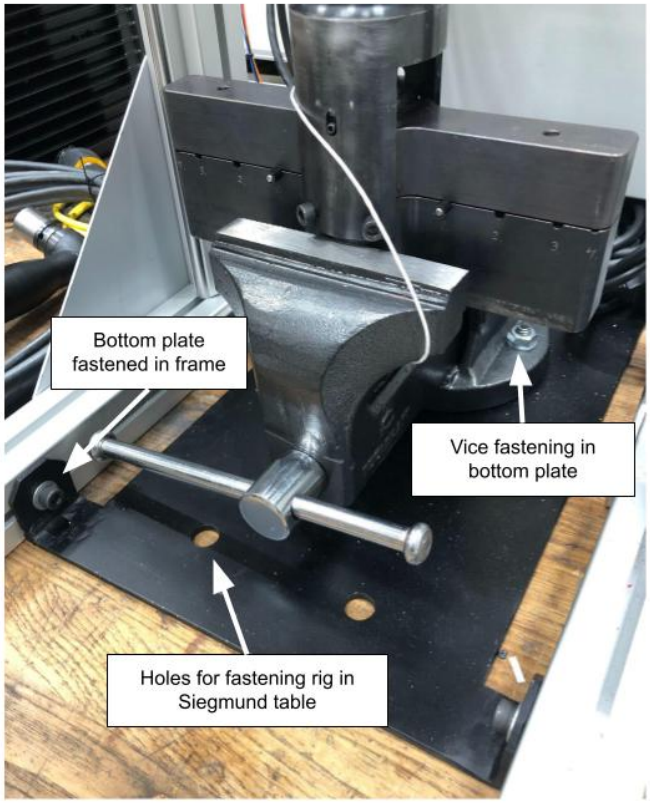

Figure 27: Bottom plate with vice and beam test joint.

5.3 Height Adjustment Mechanism

A few requirements were demanding for the ability to move the tool up and down. The first one is that a nut, when tightening, will have some vertical movement. And so, for the tool to follow suit, it will have to move vertically as well. Another reason would be that in some test tightenings, an in-line torque sensor attached between the nut and the nutrunner is desired and is called vertical flexibility. The frame of the test rig and its linear rails were designed so that an IRTT sensor could fit between the beam test joint and the tool, which can be seen in Figure 28.

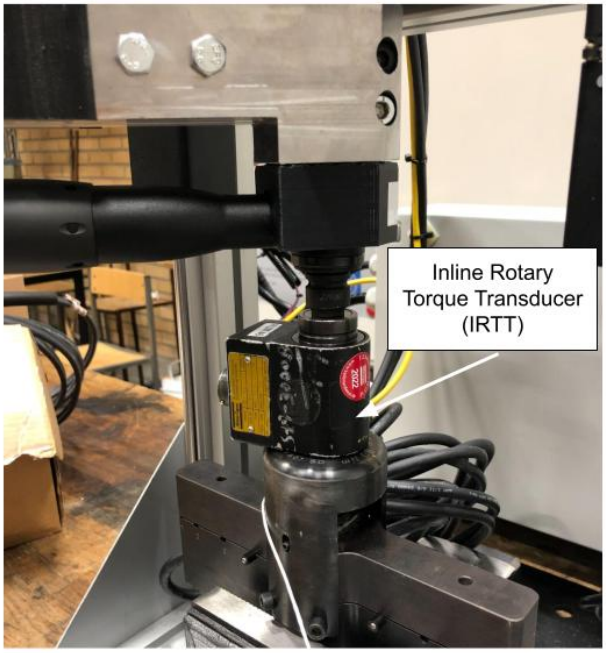

Figure 28: Height adjustment enables the rig to fit an IRTT sensor

The vertical flexibility was implemented on the rig with two linear rails as the base. They allow continuous movement along the vertical axis. A cart is attached to the rails and is the attachment point for the entire mechanised system, i.e., the motor assembly and tool arm. However, the cart has nothing that supports it, which means it will always run towards the nut. To make it easier for the user to change tool and to get access to the beam test joint a height stop was implemented, which can be seen in figure 29. To release the cart from this specific height a lever, connected to a spring, has to be pulled out and then the cart will be free to slide down along the rails.

(a) Height stop in top view (b) Height stop in beside view

Figure 29: Height stop for the vertically moving cart

Another point of interest here is the fact that when the cart is not propped up by the height stop, the entire weight of the cart, the motor assembly, and the tool arm will rest on the beam test joint and the tool during the nut tightenings. This would not comply very well with modelling a human operator as a human arm only has a weight of around 2-3 kg, while the cart of the test rig has a weight of around 20 kg. So to resemble a human arm, two gas cylinders were implemented, as can be seen in Figure 30.

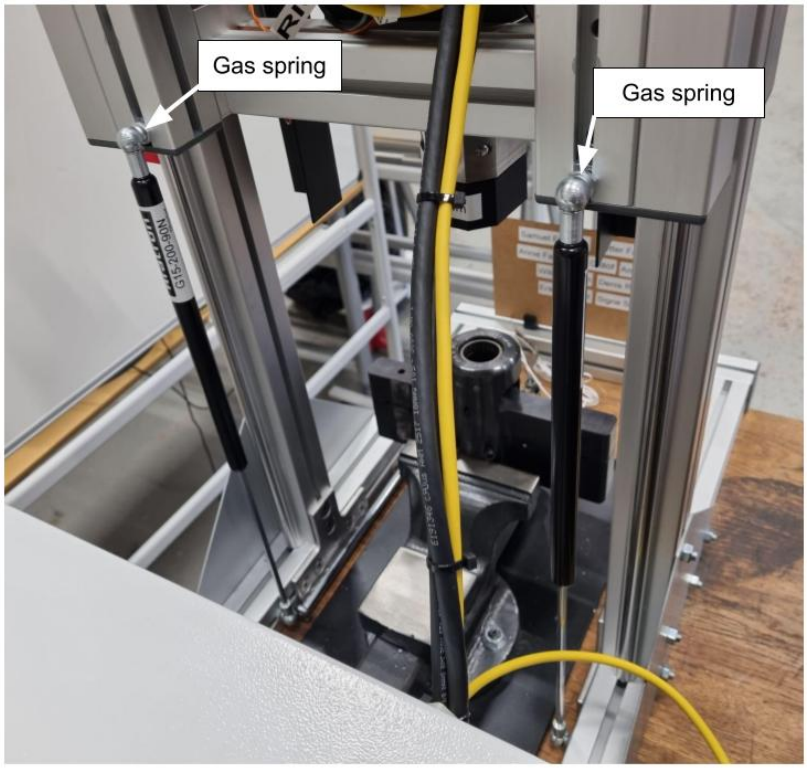

Figure 30: Two gas cylinders decreasing the weight on the tool and beam test joint.

The gas cylinders are of pushing configuration. As illustrated, the gas cylinders assist the tool and test beam joint in holding the vertically moving cart up, effectively taking weight off of the cart, making it lighter. Each gas spring were configured to push with 90 N each and to have a stroke of 200 mm.

5.4 Motor Assembly

There are two main components in the motor assembly. These are the servo motor and the gearbox, which will be presented in the following sections.

5.4.1 Servo Motor

The motor used in the project is a 750W AC servo motor produced by Hiwin, and the main argument for choosing this motor was its capability of delivering high torque and high speed. It has a peak max torque of 7.2 Nm and can deliver in the span from zero up to 3000 rpm, which is the max speed. The motor is also equipped with a 13-bit quadrature encoder to read rotor position. More details of the motor can be found in appendix C. The motor is mounted via a motor mount onto the sliding cart described in section 5.3, so it can freely move along together with the nutrunner.

Since the stakeholders required the rig to withstand reaction torques up to 100 Nm, as mentioned in 1.3, the motors torque of 7.2 Nm is not sufficient. Hence the need for a gearbox.

5.4.2 Gearbox

The gearbox implemented in the project is a planetary gearbox produced by Nidec, and it has a gear reduction ratio of 20. The resulting maximum torque results in 144 Nm, which is more than enough according to the requirements discussed in section 1.3, and the max speed is reduced to 150 rpm. The gearbox is mounted in line with the motor, and the outgoing shaft is the direct attachment point for the tool arm, described in the next section. The motor mount, pictured in figure 31a, is made of 2 mm steel that was water cut and then bent into shape, and the two side supports were welded on.

(a) The complete motor assembly with the motor, gearbox and mounting plate.

(b) The machined custom adapter.

Figure 31: Illustrations of the different parts in the motor assembly.

To be able to mount the beam directly onto the outgoing shaft of the gearbox, a custom adapter of steel was machined in the workshop at KTH. It has a hole of 22 mm with a key slot in the top surface and a 45 mm wide slot for the beam to fit in.

The adapter also has a slot along the full length of the hole, which allows the adapter to be clamped onto the shaft. This custom adapter, pictured in figure 31b, is the connection between the motor assembly and the tool arm, which will be explained in more detail in the upcoming section.

5.5 Tool Arm

Figure 32a shows some of the components that were used to build the tool arm. To the left is one of the nutrunners that the arm is supposed to hold. The arm was designed to comply with three different models of angle tools, all of which are of different sizes. To the right is the arm itself which is made of an aluminium profile attached to an assembly of smaller aluminium profiles and angle brackets. A force sensor was placed between the assembly and the tool handle and can be seen at the top of the left image. The assembly was attached to the arm with screws through the angle brackets to enable the arm to hold different tools. These are easy to loosen, which makes it easy to move the assembly along the arm, allowing for various tool lengths. The figure to the right, figure 32b, shows the tool arm, which illustrates how the nutrunner is attached to the rig.

(a) A nutrunner and components used to build the tool arm.

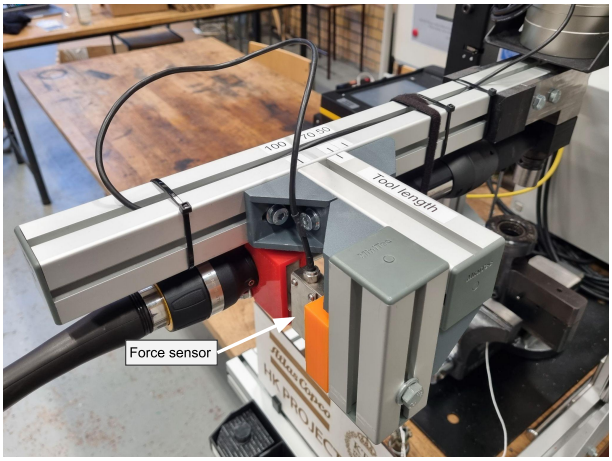

(b) Isometric view of the tool arm.

Figure 32: Illustrations of the tool arm.

Since the size of the head also varies for each model of the angle tools, a custom attachment between them had to be manufactured for each model to achieve the best fit. This was important because a bad fit could affect the motion of the tool during tests. Since the forces acting on these attachments were relatively small, they were manufactured using 3D printers. In figure 33a to the left, two of these attachments can be seen. A carrier was also designed to hold the attachments that are not in use, which can be seen in the figure as well. The labels make it easy to keep track of which attachment belongs to which tool. Similar labels were also put on the tool

arm to make it easier to switch between different angle tools, which can be seen in 33b. The placement of tool handle attachment can be changed on the tool arm by loosening the angle brackets. In this way the tool arm can be adjusted for different tools with different tool lengths.

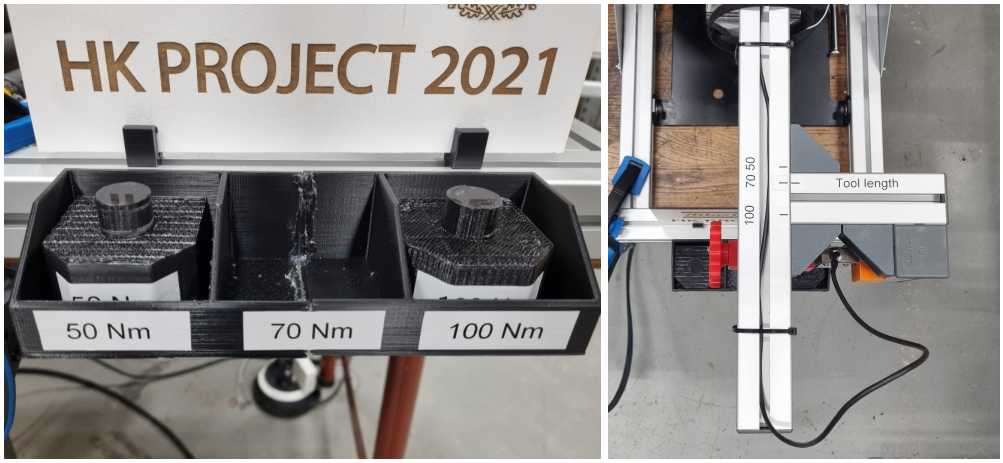

(a) Custom made attachments for each tool.

(b) Top view of the tool arm.

Figure 33: Tool arm marks

5.6 Electronics

The electrical system consists of two main parts: a high voltage side with the servo motor and driver and a low voltage side with the microcontroller and sensors. The general layout of the electrical system is shown in figure 34. The blue components are driven by 230V AC, the red components are 12V, and the orange connections are 3.3V. Signals are green, and the external 24V signal to the Power Focus 6000 is black. The figure also shows three main groups of components; those in the electrical cabinet, those on the box on the rig, and those on the "button interface" (where the rig is operated from). In the coming sections, the subsystems of the electrical system will be explained.

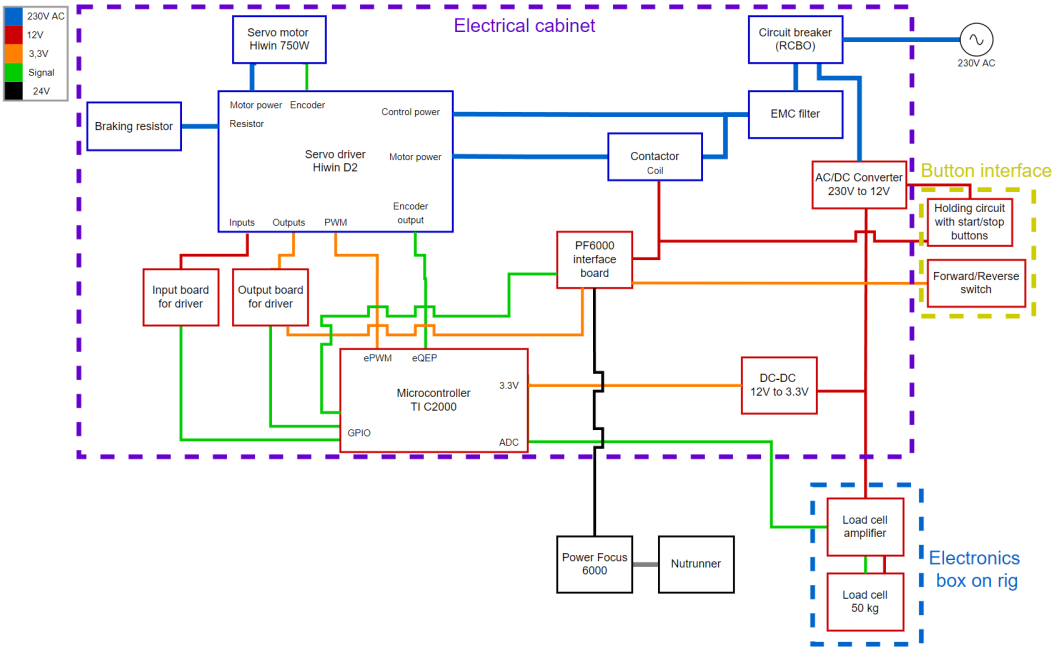

Figure 34: General layout of the electrical system. A complete schematic is available in appendix A.

Figure 35 shows the inside of the electrical cabinet. The cabinet houses the servo driver as well as the microcontroller with all peripherals. There are many components, all of which are explained in detail later in this section. The complete schematic is available in appendix A, however figures 35 and 36 shows how everything is put together in reality to aid the understanding of the whole system.

In figure 36 only the 230V AC connections are shown. Mains voltage (230V) can be hazardous, therefore the group consulted electronics professor Hans Johansson to connect the 230V AC safely. A Residual Current Breaker with Over-current (RCBO) protects against overcurrent and earth leakage. The RCBO also acts as a power switch for the whole system. The contactor is used to electronically switch the current to the motor and is operated by 12V. As the servo drive creates a lot of electric noise, an EMC filter is used to filter the AC to the servo drive, which reduces the noise emitted from the servo drive to the grid.

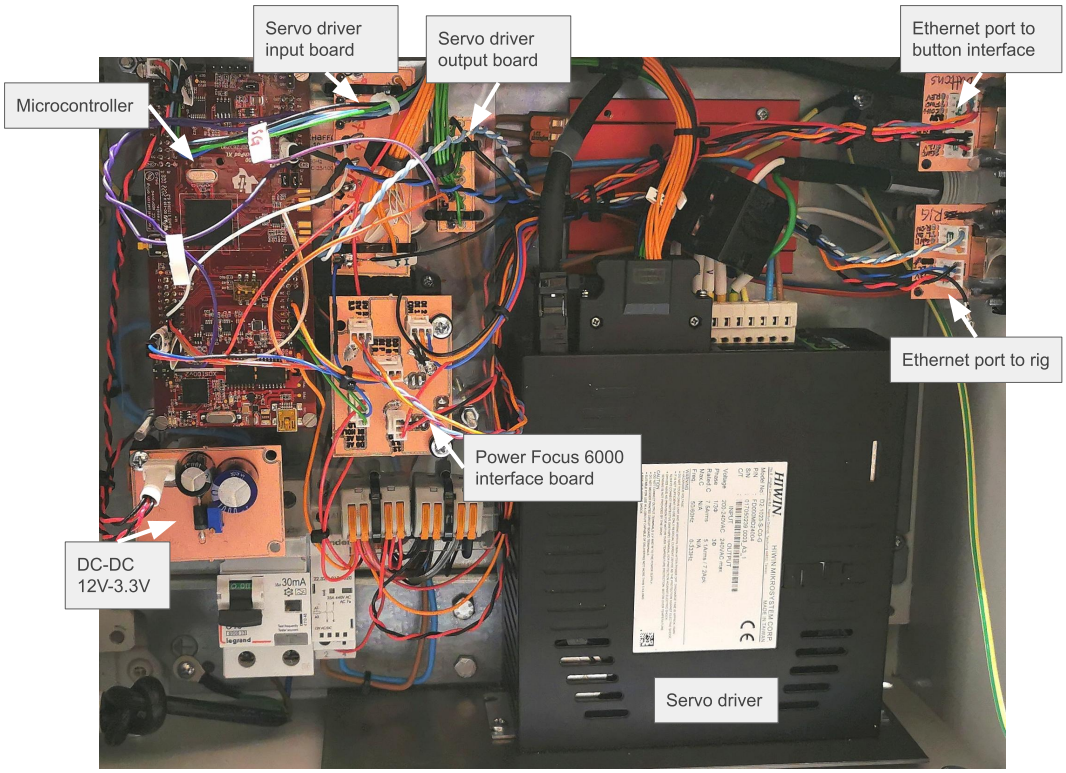

Figure 35: Inside the finished electrical cabinet.

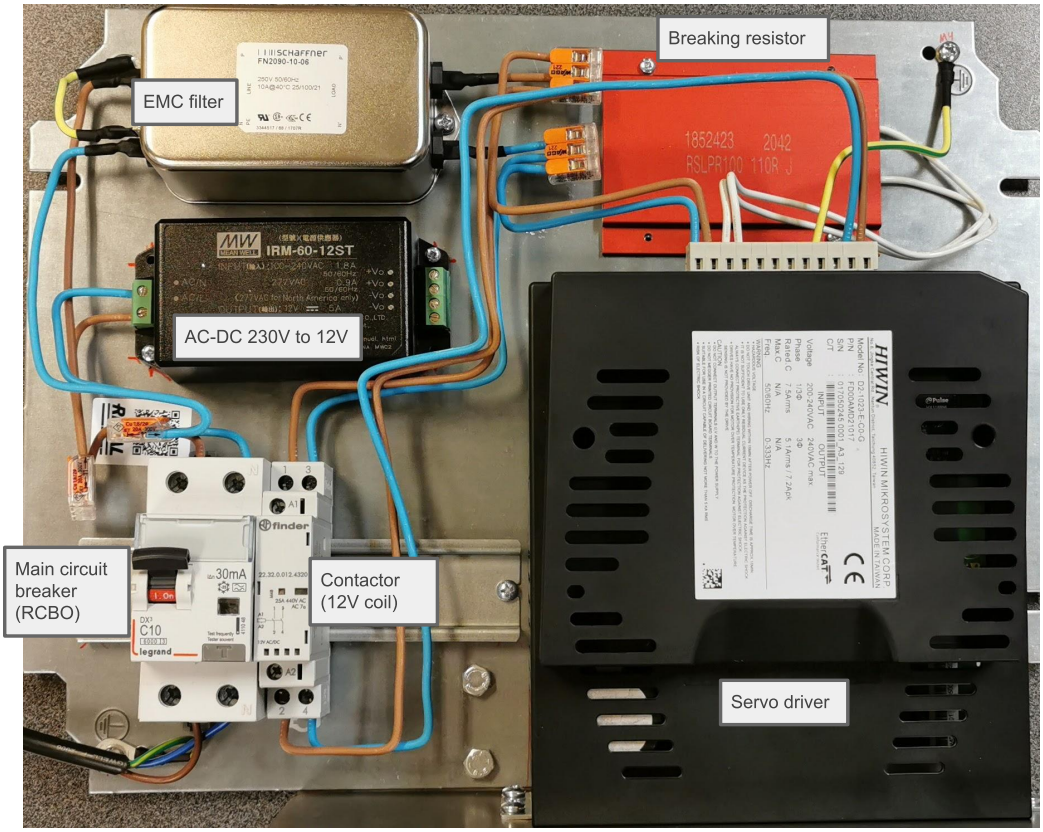

Figure 36: Inside the electrical cabinet, with only the 230V AC connections shown.

5.6.1 Servo Motor and Driver

The servo drive is from the manufacturer Hiwin Mikrosystem. The model is D2T and has a rated output of 1kW. [33] When controlled in velocity mode, the drive accepts a Pulse-Width Modulation (PWM) signal to control the speed of the motor. The motor is also from Hiwin and is rated for 750 W continuous power at 3000 rpm. [34] It is equipped with a 13-bit quadrature encoder (10 000 pulses per revolution), which is read both by the driver and the microcontroller.

Figure 37 shows how all peripherals are connected to the servo driver. Schematics of the input and output boards will be shown in the following sections. The driver can be configured through the software "Lightening" (explained in detail in section 5.8.8) connecting via USB to a computer.[35] All inputs and outputs can be configured as they are not "locked" to a specific function.

The inputs (1 to 7) are configured as:

In 1: Axis enable. Enables the power to the servo drive.

In 2: Right limit switch (inverted).

In 3: Left limit switch (inverted).

In 4: Start homing. Signals drive to start the homing procedure.

In 5: Switch to secondary mode. Switch from the primary mode (position) to the secondary (velocity) to accept PWM input.

In 6: Reset. Reset the drive, e.g. to clear errors.

In 7: Switch HI/LO pulse command (inverted). Enables the low speed pulse command, which makes the relatively slow PWM frequency of 50kHz to be read by the drive.

Of all the outputs only number two is used. Output number two signals when the homing procedure is finished.

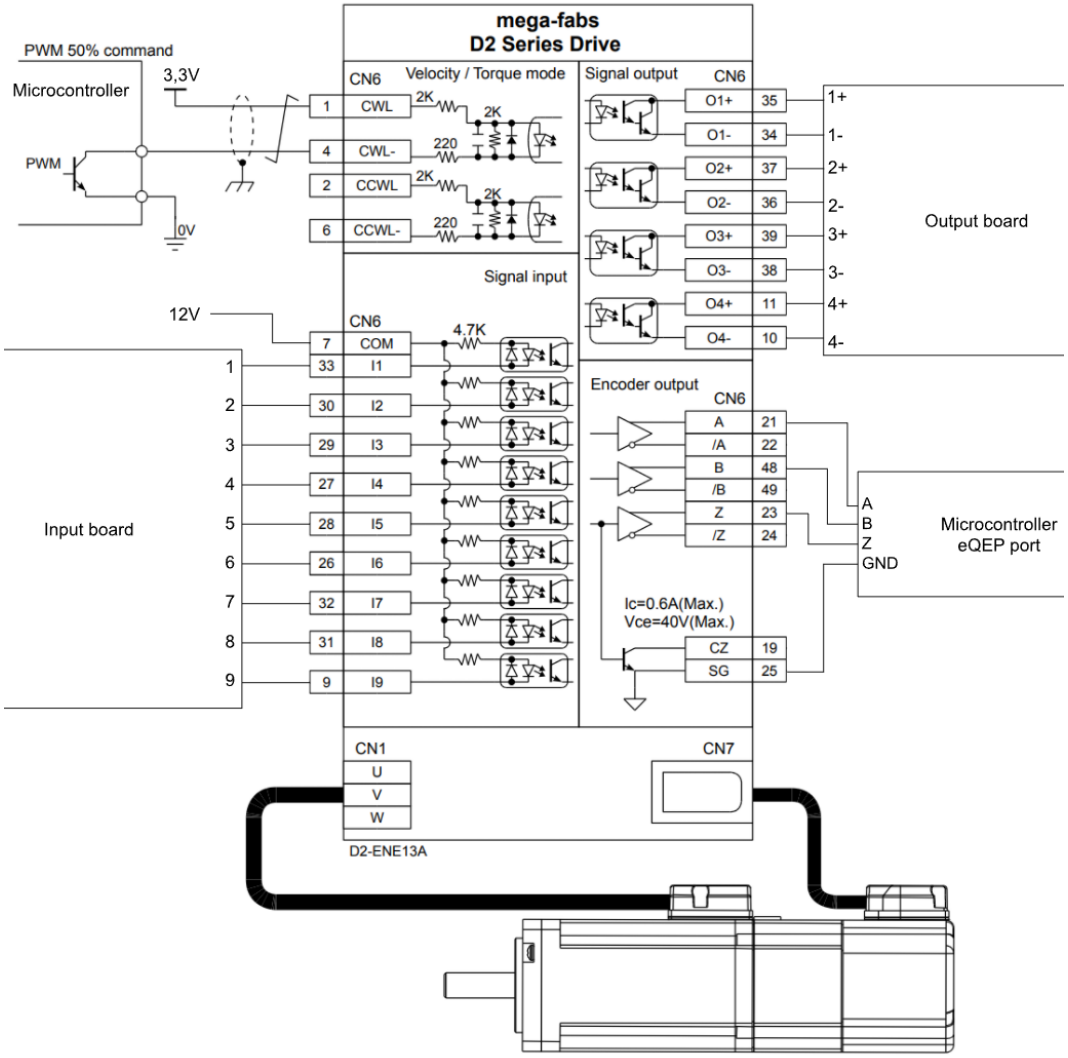

Figure 37: Connections to the Hiwin D2 drive, excluding 230V power and brake resistor. The image is a modified version of Figure 4.6.3.1.1 in the drive manual (D2 Series Servo Drive User Manual V2.1 (EN))[35].

5.6.2 Input and Output Board for Servo Driver

To be able to interface the microcontroller with the servo driver, two boards were constructed ("input board" and "output board" in figure 37). The input board consists of MOSFETS that are activated by the microcontroller, letting 12V flow through the inputs to the servo and thus activating the servo inputs. The schematic is shown in figure 38. The output board consists of pull-down resistors, which give a high voltage (3,3V) to the input of the microcontroller when the servo output is high. The schematic of the output board is shown in figure 39. In the two schematics, GPIO1 to GPIO9 are used to denote any input or output pins on the microcontroller. GPIO1 to GPIO4 are not the same ports on the microcontroller in the two schematics.

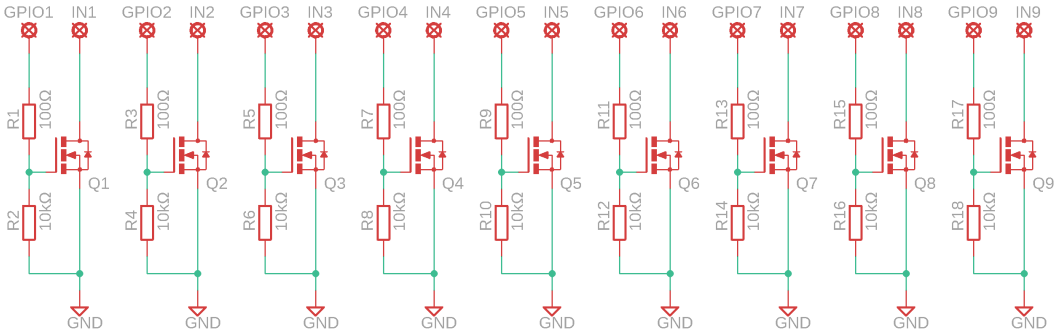

Figure 38: Schematic of the input board. It is the same pattern repeated once for every input, i.e., one MOSFET for every input on the servo driver.

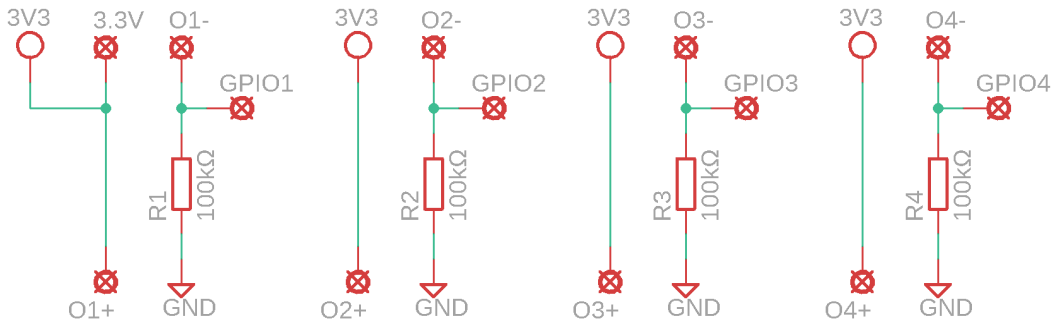

Figure 39: Schematic of the outboard board. It is the same pattern repeated once for every output.

5.6.3 Holding Circuit with Emergency Stop

As can be seen in figure 34, the contactor supplying the servo driver, and subsequently the servo motor, is controlled by a holding circuit. The idea behind a holding circuit is that once it is triggered, it remains in its on-state until powered down. Then after being powered down, no matter in what manner, it will need to be powered back on again by the press of the on-button. This is accomplished with the use of a self-feeding relay, which can be seen in figure 40.

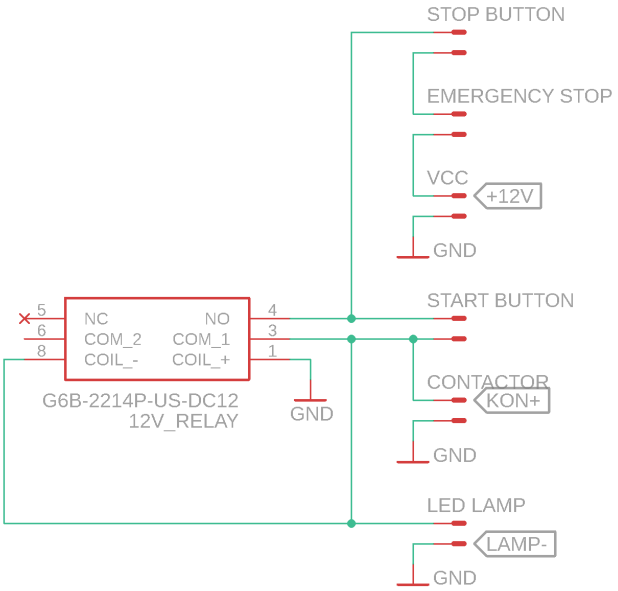

Figure 40: Schematic of the holding circuit.

This is advantageous from a safety standpoint. As can be seen in figure 40, this holding circuit involves three buttons: a start button, a stop button, and an emergency stop button. This scheme originates from one of the stakeholder requirements to implement an emergency stop button.

The emergency stop button needs to be reset if activated, and this is where the safety aspect comes in. It is not desirable to power up the test rig automatically again by only resetting the emergency button. Instead, it should be required to consciously press the on-button again, which is achieved through the use of this holding circuit.

By implementing the emergency button into the holding circuit that controls the contactor, the emergency button indirectly controls the power to the servo driver and servo motor. It is only when the holding circuit is feeding power to the contactor that it allows for power transfer in the 230V system.

The box with the holding circuit and buttons can be seen in figure 41. The green button activated the holding circuit (Start), the red button deactivates it (Stop). The emergency stop is the large red and yellow button. The "controller" is connected to the box, which has a rocker switch. When pressed forward or backwards, the tool will tighten or loosen, respectively.

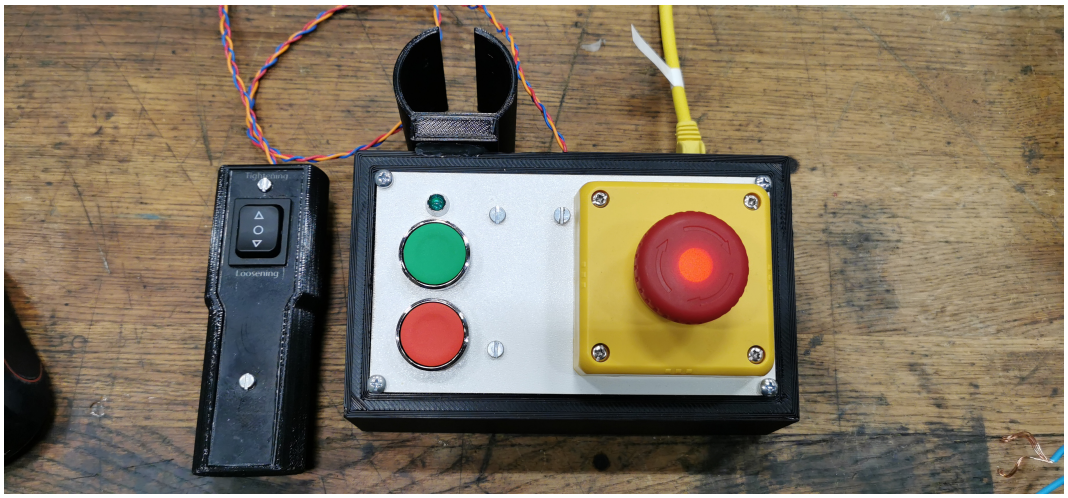

Figure 41: The button interface from which the rig is operated.

5.6.4 Power Focus 6000 Interface Board

The tool controller, Power Focus 6000 (PF6000), controls the tool. The PF6000 is configured for remote start, i.e., the button on the tool does not need to be pressed for the tool to start. To start a tightening or loosening sequence with the tool, a 24V signal is switched on the PF6000 to the DI1 and DI2 ports. Digital in 1 (DI1) is configured for tightening, and digital in 2 (DI2) is configured for loosening. To control the 24V switching with the microcontroller, NPN and PNP transistors are used. PNP transistors are needed because of the high side switching. The transistors are on a circuit board, shown in figure 42.

Another function of the interface board is to read the status of the holding circuit and send it to the microcontroller. A MOSFET (Q4 in figure 42) reads the 12V of the holding circuit and sends 3.3V to the microcontroller if the holding circuit is activated. The holding circuit also controls the Axis Enable signal through MOSFET Q3. As the MOSFET is on when the holding circuit is enabled, the servo motor can only be activated when the holding circuit is on. This is useful because residual energy (stored in capacitors) in the servo controller can actuate the motor for several seconds even though the contactor is off, and there is no voltage to the servo drive. In the worst case, this could lead to damage of the rig or personnel, even though the emergency stop has been pressed.

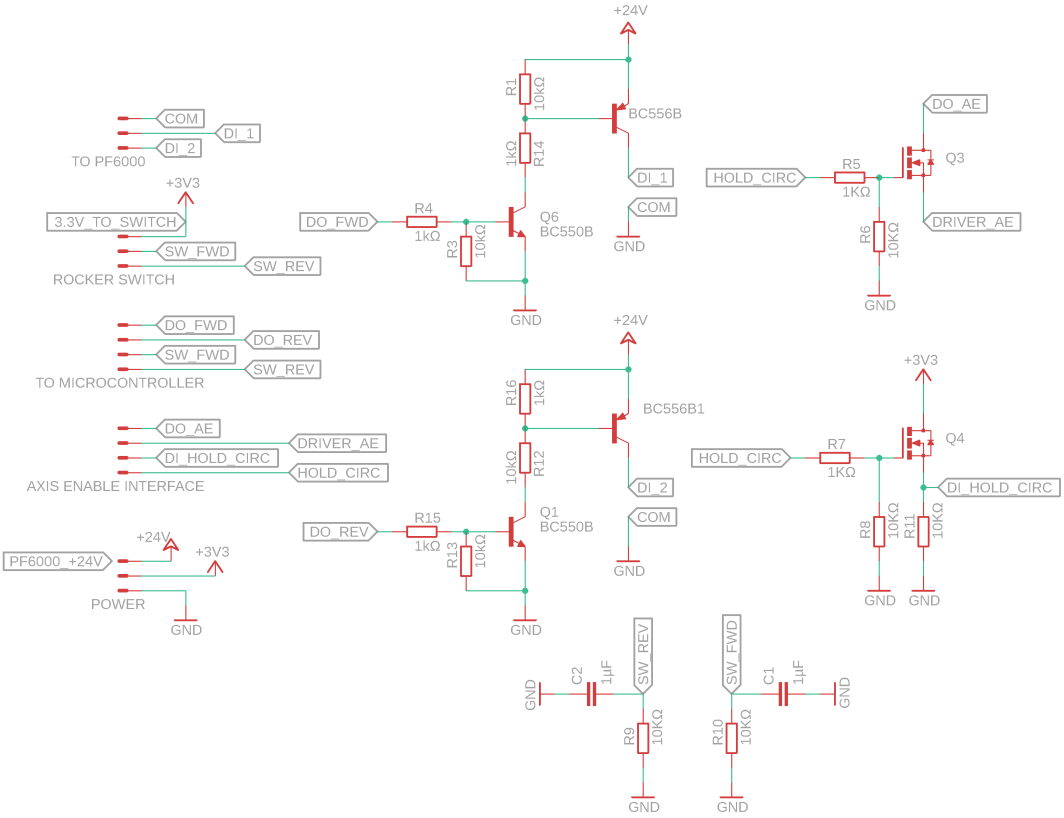

Figure 42: Schematic of the Power Focus 6000 interface board.

5.6.5 Load Cell Amplifier

To amplify the load cell signal to a level that can be read by the microcontroller, a load cell amplifier is used. The schematic is shown in figure 43. The main part of the amplifier is the INA126 instrumental amplifier.[36] It amplifies the differential signal of the load cell to a single-ended signal. On the board, there are two potentiometers to adjust the offset and the gain. The offset is the voltage that will be outputted when the load cell is not loaded. In this case, it is half of 3.3V, as the microcontroller ADC has a range of 0 to 3.3V. The gain is the amount of amplification to apply to the load cell signal.

When the gain and offset has been set, the load cell must be calibrated, as the actual gain is not known. This was done by using weights to load the load cell while measuring the load with a scale and observing the signal value from the load cell amplifier. After this procedure, a conversion factor can be calculated to convert Volts (or bits in the ADC) to Newtons in the microcontroller.

The amplifier also has over-voltage protection that never lets the load cell signal go above 3.3V. If the voltage gets any higher, an OP-amp sends a signal to a MOSFET that pulls the load cell signal to ground. As the OP-amp reacts quickly and the load

cell signal is low pass filtered, the output is stable around 3.3V for as long as the overvoltage protection is activated.

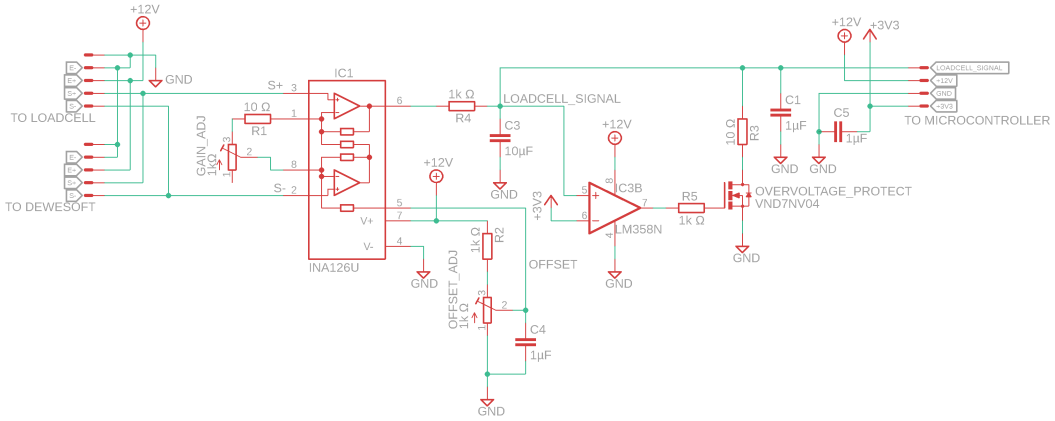

Figure 43: Schematic of the load cell amplifier.

5.6.6 Microcontroller

The microcontroller is a "C2000 Delfino MCU F28379D LaunchPad" from Texas Instruments.[37] It was chosen because it is widely supported by MATLAB and Simulink, with the possibility to compile programs for it directly from Simulink. This way, virtually no actual programming needs to be made. When using Simulink, the microcontroller can be controlled in external mode, meaning that data can be logged to a computer, and parameters can be changed in real-time. To use this functionality, the package "Simulink embedded coder" must be installed.

There are four kinds of signals handled by the microcontroller:

1. General-Purpose Input/Output (GPIO): Input and output signals on the GPIO ports, e.g. to activate inputs and to read outputs on the servo drive.
2. Analog-to-Digital Converter (ADC): The analogue signal from the load cell is converted to a digital signal.
3. PWM: To control the speed of the servo motor, a PWM is sent from the ePWM module.
4. Quadrature interface: The A and B pulses from the incremental encoder on the servo motor is read through the eQEP module.

The microcontroller can be powered by a USB. However, to make it stand-alone, it has an external DC-DC converter to supply it with 3.3V at all times. By removing jumpers JP1, JP2 and JP3, the USB interface becomes galvanically isolated from the board. Since the board is supplied with 3.3V only, jumper JP6 needs to be installed to enable the 5V output ports on the board. The 3.3V DC-DC converter used to supply

power for the board is a custom made circuit of an LM2576 step down switching voltage regulator.

5.6.7 EMI-Box on Rig

The load cell amplifier is mounted on the rig to be physically close to the load cell. The amplifier is sensitive to noise, and therefore the board is mounted inside a shielded box, called the EMI-box. This box is positioned behind the motor on the rig. The inside of the box is shown in figure 44.

The EMI-box has three connections:

1. RJ45 port that supplies the box with 12V and 3.3V, and returns the load cell signal and the endstop signals.
2. D-sub 9-pin male that connects the endstops and load cell.
3. D-sub 9-pin female that outputs the raw (not amplified) load cell signal, to be able to read them with the Dewe43A.

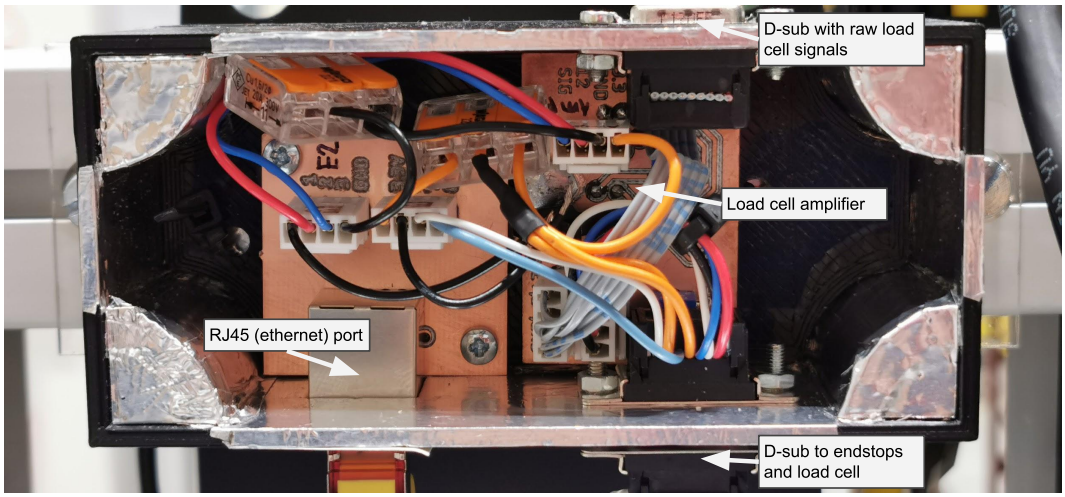

Figure 44: Inside of the electronics box on the rig, called the EMI-box.

5.6.8 Analogue Communication

Ethernet cables are utilised for analogue communication of the rig. Ethernet cables are robust, shielded and have twisted pair wires for better Electromagnetic Compatibility (EMC). An important note is that while Ethernet cables are used, the signals in the cables are analogue, and no digital communication is used (as would normally be the case when using Ethernet).

During the construction of the rig, there were problems with huge interference in the load signal. The load cell amplifier has a low pass filter. However, radiated interference was picked up by the signal cable on the way to the microcontroller.

When checking with an oscilloscope, the voltage spikes were 20 Volts peak-to-peak. To mitigate this issue, two solutions were used:

- Sending analogue signals through Ethernet cables, to reduce the amount of interference picked up.
- A low pass filter directly at the microcontroller input.

The noise picked up by the load cell signal has a frequency of 30 kHz and is in the form of voltage spikes. It only appears when driving the servo motor. Thus the noise originates from the servo system. As the noise emitted by the servo driver cannot easily be reduced, the problem was worked around using the previously discussed points; Ethernet cables and low pass filters.

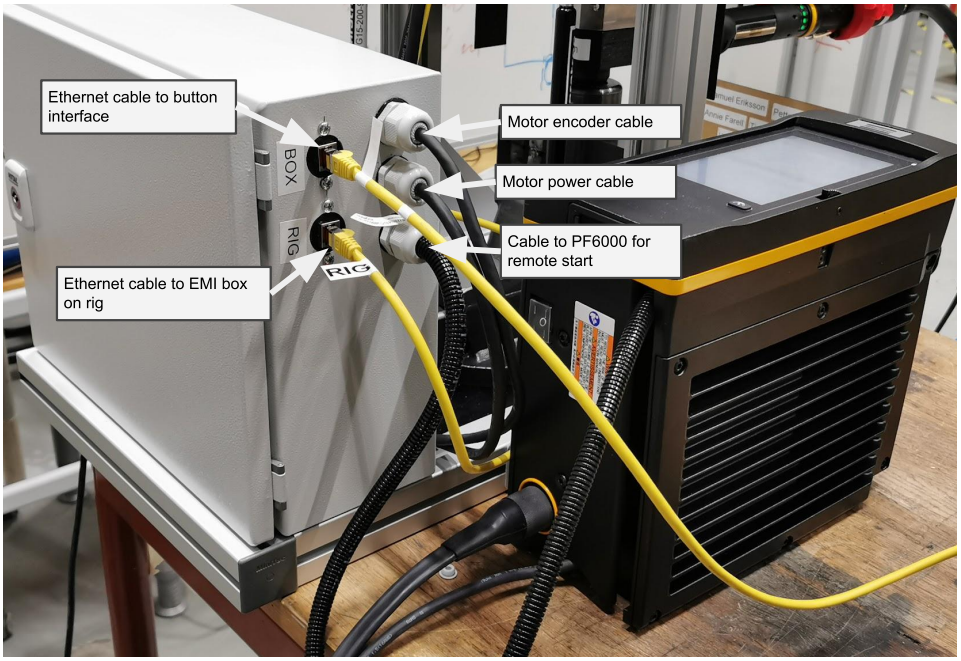

Figure 45: All cables that run from the electrical cabinet.

5.7 Control Scheme

The motor is controlled by using a cascaded motion controller. The outer loop is controlling the motor angle, and the inner loop is controlling the motor velocity using PWM. The velocity controller is inside of the servo driver from HIWIN, while the angle controller is developed by using error feedback with a P-controller. The reference for the angle controller is made by the operator model, which uses the measured force acting on the operator as input. The whole control structure are illustrated in figure 46 below.

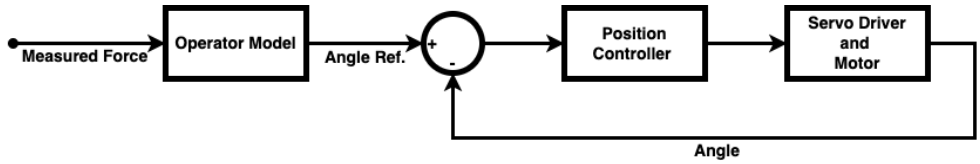

Figure 46: Control scheme of motor assembly, from building the reference to driving the motor.

5.7.1 Operator Model

The operator model is based on the mass-spring-damper model described in section 2.1.3. Instead of using physical masses, springs and dampers, the operator model is built as an artificial system generating a signal to the motor to simulate the mass-spring-damper system. The input for the operator model is the force acting on the operator, and the output is the angle on the tool that this force would have generated in a real mass-spring-damper system.

In continuous time the mass-spring-damper operator model can be described by the equation

$$\phi = \frac{1/r_0}{ms^2 + ds + k} F. \tag{3}$$

The model is optimised by using measured data from a real tightening sequence provided by the R&D at Atlas Copco. Angular displacement and handle force is captured by using a small encoder and a force sensor. The tightening strategy used is *Turbo Tight*® set for 30 Nm torque for all provided tightenings. Even though the data provided is captured from the same operator and the same tightening strategy, the data sets differ from one another. This can be seen in figure 47 below, where data for five different tightenings are plotted along with each other.

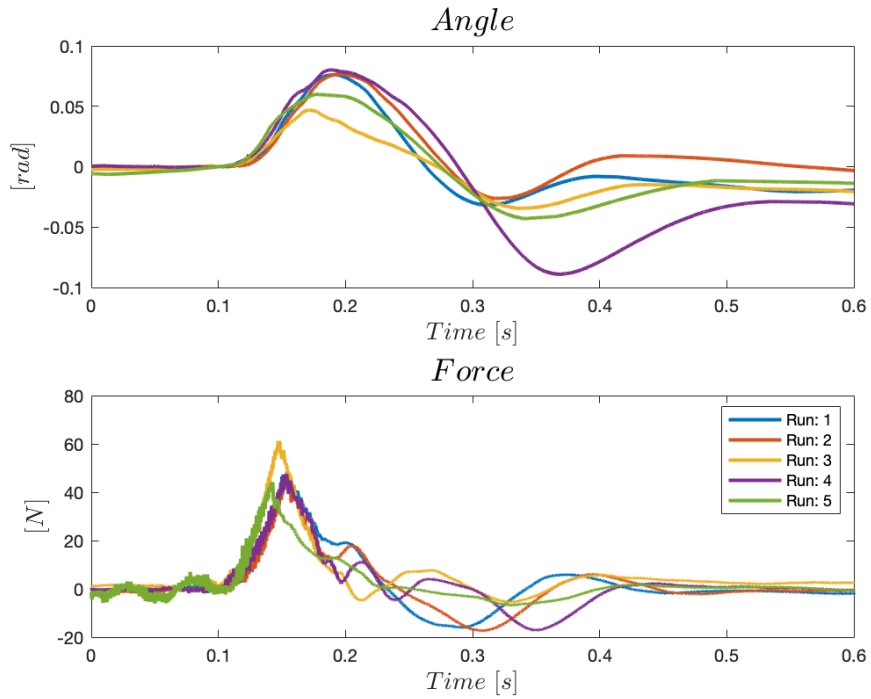

Figure 47: Five different human tightenings using the same operator and tightening strategy (Turbo Tight 30 Nm).

Since the data differ from one another, the operator model is optimised by using the data from one run and then verified by using the data from a second run. As stated in section 2.1.3, the operator act almost equal to a mass-spring-damper system for approximately 200 ms after the force has started acting on the operator. Because of this, it is only 200 ms of the data that is used to identify the model parameters. By using the system estimation toolbox in MATLAB, the parameters of the operator model are optimised to fit one set of data (one tightening sequence). The tool used is the "tfest()" command in MATLAB, which optimises a continuous-time transfer function with a user-specified number of poles and zeros. In this case, the tool returns a transfer function of the form

$$\phi = \frac{a_0}{s^2 + b_1 s + b_0} F, \tag{4}$$

where a_0, b_0 and b_1 all have numerical values. Since the placement of the force sensor, r_0 is known, the numerical values of the mass, spring constant and damping constant can be extracted from the numerical representation of the transfer function.

If assuming $r_0 = 0.37m$, the following values of the transfer function parameters can be calculated, see table 3 below. With these parameter settings, the following model response is generated, see figure 48. Here the model response is plotted against the

estimation data and is given a model FIT, which represents how well the model fits the recorded data. The model FIT is calculated as

$$FIT = 100\frac{1 - \|(Y - \hat{Y})\|}{\|(Y - \bar{Y})\|} \tag{5}$$

where Y is the recorded data and $\hat{Y}$ is the data produced by the model, $\bar{Y}$ is the mean value of the recorded data and the $\|Y\|$ is the euclidean norm (or 2-norm) of Y. A FIT value of 100% means that the model produces the exact same result as the recorded data.

Table 3: Estimated parameters while assuming $r_0 = 0.37m$.

Parameter	Estimated Value
m	0.301 [kg]
d	31.77 [Ns/m]
k	1043 [N/m]

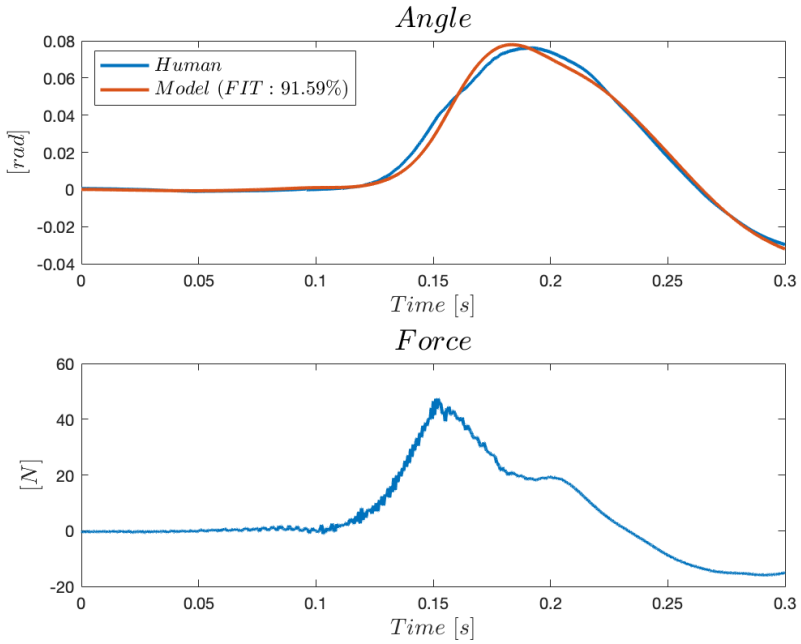

Figure 48: Operator model response compared to the identification data from Turbo Tight 30Nm (containing 200ms of the tightening sequence).

The optimised model is then verified with another set of data from the same operator. The validation data contains a whole tightening sequence. The model response with the validation data can be seen in figure 49 below.

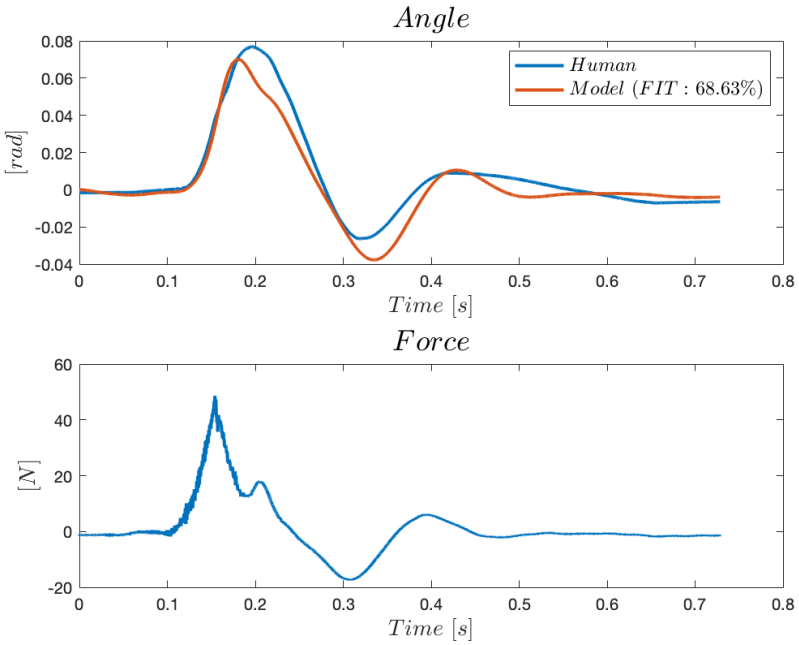

Figure 49: Operator model response compared to the validation data, containing the whole tightening sequence (Turbo Tight 30 Nm).

5.7.2 Embedded Implementation

The operator model used in the microcontroller is generated from the optimised parameters. The operator model is built by a MATLAB script that builds a continuous-time transfer function of the operator model, based on the optimised parameters in table 3.It is required that the model is converted from continuous-time to discrete-time to implement the operator model into the microcontroller. In order to do this, the MATLAB command *'c2d()'* is used. The discrete-time transfer function generated is then used in Simulink with a transfer function block. The transfer function takes the measured force as input and generates a reference angle as output, just as figure 46 shows. Since the model is generated from the calculated mass, spring constant and damping constant, it makes it easy to change the characteristics of the operator model. By changing the value of some parameters and recompiling the code, the operator model is updated and has different characteristics than the previous one.

5.8 Software

One of the early requirements on the software of the rig was to not use any too expensive software. In particular, the stakeholders asked us not to use a too wide range of MATLAB extensions as they only have access to a certain set, and if these would be exceeded, there is a hefty price tag on acquiring keys to the ones not already in the subscription.

This made it a goal of the project to develop a completely stand-alone system, which would not need any additional software to function. Simulink Coder [38] and Embedded Coder [39] can be used to generate stand-alone C-code via Simulink. This means that the software can be developed completely in Simulink but still result in a stand-alone product. This C-code can then be opened in an embedded software IDE, i.e. Code Composer Studio, which is specially developed for TI microcontrollers such as the C2000 used in the test rig if changes to it need to be made manually.

The resulting Simulink block diagram can be seen in figure 50.

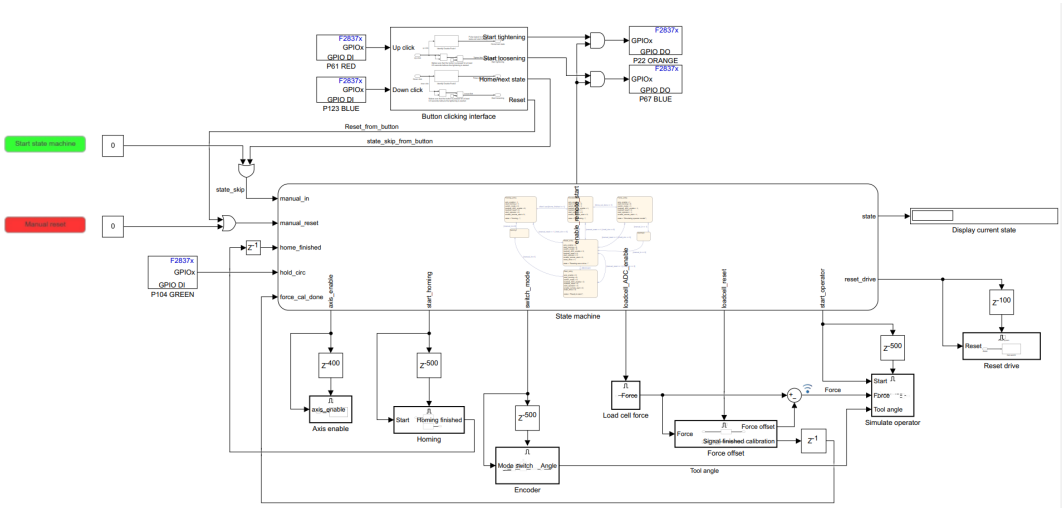

Figure 50: Overview of final block diagram representing the software of the test rig.

An interesting aspect of the block structure is that on the activation line to each of the subsystems (the one connected on the top edge), a delay block is present. This is due to a complication regarding the activation and deactivation of the subsystems. If a subsystem is outputting *High* on a GPIO-output and is deactivated during this action, the GPIO-output will continue outputting *High* until the subsystem is activated and updated again. To solve this the delay blocks were implemented, both for activation and deactivation, so that the subsystems are given time to enable/disable all signals before being activated/deactivated.

5.8.1 Code Structure

It was decided to implement the software as a state machine. This would allow different operations to happen in order and with a clear structure. It also helps that the rig was to be developed as a stand-alone product. A state machine is simple to control with minimal input, which was necessary as no major interface with a user will be implemented.

The state-machine block can be seen in figure 51. This block works by setting it up internally, as seen in figure 52, where the blocks are states and the arrows are

transition paths with corresponding transition criteria. These criteria are dependent on inputs to the state machine, i.e., the input arrows seen on the left in figure 51. This means that if the state machine is located in a state with a transition with criteria that gets fulfilled, it will transfer over to the next state pointed to by the transition arrow.

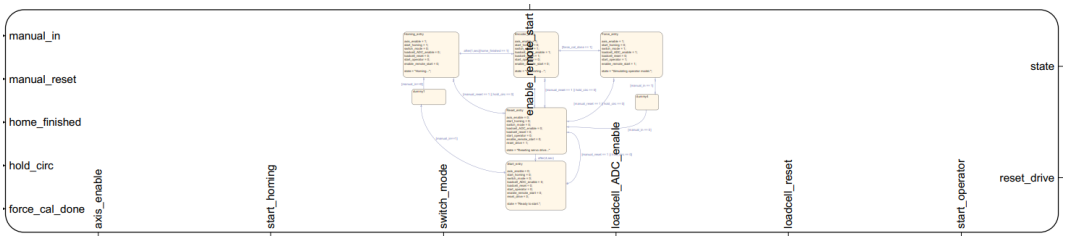

Figure 51: State-machine block in Simulink with its corresponding in-/outputs.

On entry to a new state, the outputs of the state machine are changed according to the state setup, as can be seen within the blocks of figure 52. This is then used to activate the different subsystems of the software, e.g., if the first variable *axis_enable* is set to 1 from the state machine, the *Axis enable* subsystem is activated, and if it is set to 0, the subsystem is disabled. Through this mechanism, it is easy to enable and disable the different functions of the software when executing different operations. Functions and operations are explained further below.

The state machine has a reset state that is always entered at the start of the program. If the reset signal is activated in any state, the reset state is entered and the servo drive is reset, and thus the motor is turned off. If the holding circuit is powered off, the reset state is also entered. After the reset state, the start state comes. The state machine will wait in this state until the rocker switch is double-clicked or the start button is pressed in Simulink.

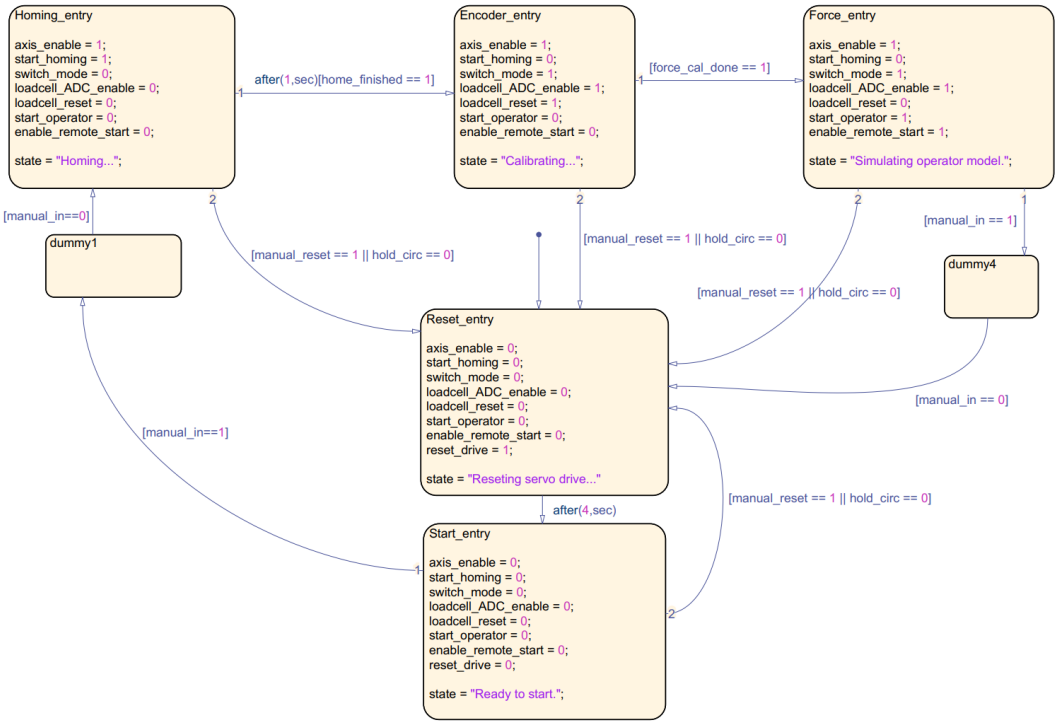

Figure 52: State-machine internals.

5.8.2 Axis Enable

The *Axis enable* subsystem is of quite simple proportions. It has two system inputs, *axis_enable* which is the signal responsible for activating the servo-driver, and the enabling signal for the subsystem itself. These can be seen in figure 53a. In figure 53b, it is further evident that this is a simple subsystem. Here, only the activation block of the system and a GPIO-output is present. The GPIO corresponds to the pin that is connected to the servo driver's axis enable-pin via its input board, the electronics of which is explained further in section 5.6.2. This means that if the input of the *Axis enable* subsystem is set to *High*, and the system is active, it sets the *Axis enable* variable in the servo-driver to *High* also.

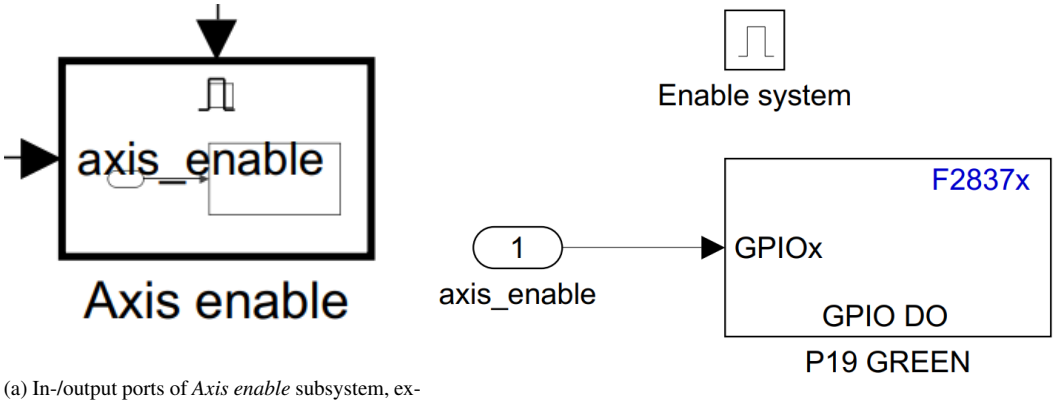

(a) In-/output ports of *Axis enable* subsystem, external view.

(b) Internal view of *Axis enable* subsystem.

Figure 53: *Axis enable* subsystem.

In table 4 the pin-map for the subsystem can be found.

Table 4: Pin-map for the *Axis enable* subsystem.

Block name	**Type**	**Pin**
P19 GREEN	GPIO-Output	P19

5.8.3 Homing

Homing is the sequence that executes before any initiated tightening can begin. This is so the tool arm and the tool can find the home position, i.e., be centred (between the endstops) to avoid any rig collisions. This subsystem can be seen in figure 54.

It has two system inputs and one system output. The inputs are *start*, which initiates the homing sequence, and the second one is the enabling signal of the subsystem. The output is *Homing finished*, which corresponds to the end of the homing process. In figure 54b, it is evident that this subsystem is also simple, consisting of a GPIO-input and a GPIO-output. The output activates the homing sequence when the system input *start* is set to *High* and the system is active. The homing software is located on the servo drive, which only needs an activation signal. The GPIO-input reads when the homing sequence has finished by reading output 2 from the servo drive and then conveying this as a system output.

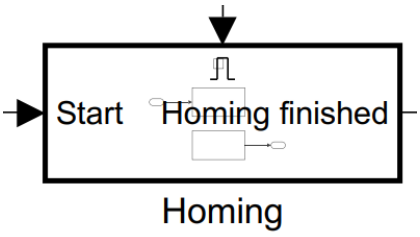

(a) In-/output ports of *Homing* subsystem, external view.

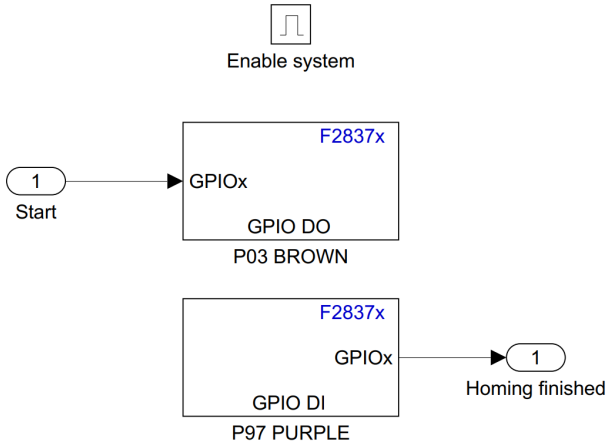

(b) Internal view of *Homing* subsystem.

Figure 54: *Homing* subsystem.

In table 5 the pin-map for the subsystem can be found.

Table 5: Pin-map for the *Homing* subsystem.

Block name	**Type**	**Pin**
P03 BROWN	GPIO-Output	P03
P97 PURPLE	GPIO-Input	P97

5.8.4 Encoder

After the homing sequence is completed the encoder needs to be initialised in the software, and the angle of the encoder must be set to 0 rad. This is performed by the *Encoder* subsystem, which can be seen in figure 55.

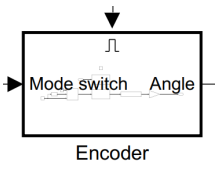

(a) In-/output ports of *Encoder* subsystem, external view.

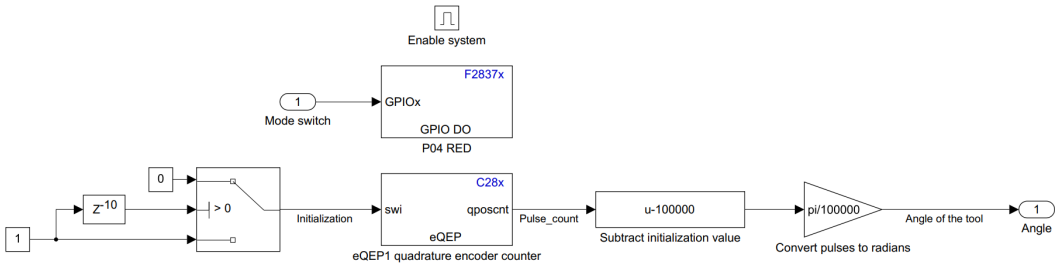

(b) Internal view of *Encoder* subsystem.

Figure 55: *Encoder* subsystem.

The subsystem has two system inputs and one system output. The inputs are *Mode switch*, which changes the mode of the servo drive from position mode to velocity mode. The second input is the enabling signal of the subsystem. The output is the angle of the encoder. As can be seen in figure 55b, the *Mode switch* input sets a GPIO-output to *High*. The GPIO corresponds to the pin that is connected to the servo drive's "switch to secondary mode"-pin via its input board, the electronics of which is explained further in section 5.6.2. The driver is configured so that the primary mode is position mode and the secondary mode is velocity mode. This is because the homing can only be performed in position mode.

From figure 55b it can be seen that, for the initialisation of the encoder, a switch block is used together with a delay and two constants to send a ten sample long *High* pulse when the encoder subsystem is enabled. The pulse goes into the microcontrollers encoder block, when the encoder block receives the pulse it initialises the position counter value to 100000. The value is initialised to 100000 to ensure that it will never reach 0 or the maximum value of the counter, $2^{32} - 1$, during operation, resulting in an overflow. The output of the encoder block is the value of the position counter, 100000 is subtracted from the output so that it equals 0 in the position after the homing sequence. The output is then scaled by pi/100000, from the 10000 pulses per motor revolution and a gear ratio of 20, so that the output, *Angle*, is in radians for the output shaft of the gearbox.

In table 6 the pin-map for the subsystem can be found.

Table 6: Pin-map for the *Encoder* subsystem.

Block name	**Type**	**Pin**
P04 RED	GPIO-Output	P04
eQEP	5V Quadrature Interface	

5.8.5 Load Cell Force

The *Load cell force* subsystem is responsible for measuring the force of the load cell, and the *Force offset* subsystem calibrates the load cell. Both subsystems are visible in figure 56.

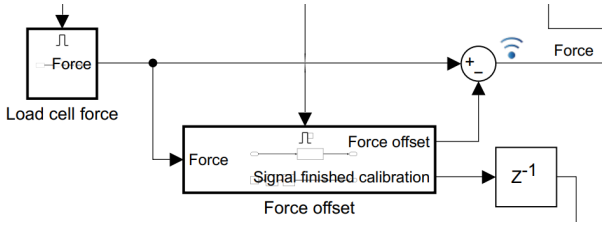

Figure 56: External view of *Load cell force* and *Force offset* subsystems.

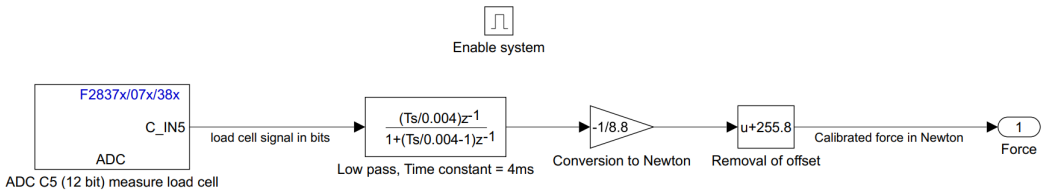

Figure 57: Internal view of *Load cell force* subsystem.

In figure 57 the internal structure of the *Load cell force* subsystem can be seen. The subsystem has one input and one output. The input is the enabling signal of the subsystem, and the output is the uncalibrated force measured by the load cell. As can be seen in figure figure 57, the signal from the load cell is measured with an ADC pin on the microcontroller. A digital low pass filter with a cutoff frequency of 250 Hz is used to remove noise in the sensor signal. The signal is then scaled to convert the signal from a value between 0 and 4095 into a force in Newton. The scaling factor was determined by placing different weights on the load cell and then using curve fitting to determine the relationship between the measured signal and the force on the load cell. After the signal has been scaled, an offset value of 255.8 is added to the signal to compensate for the offset in the measured signal. By adding the offset value, the signal is close to 0 N when no force is applied to the load cell.

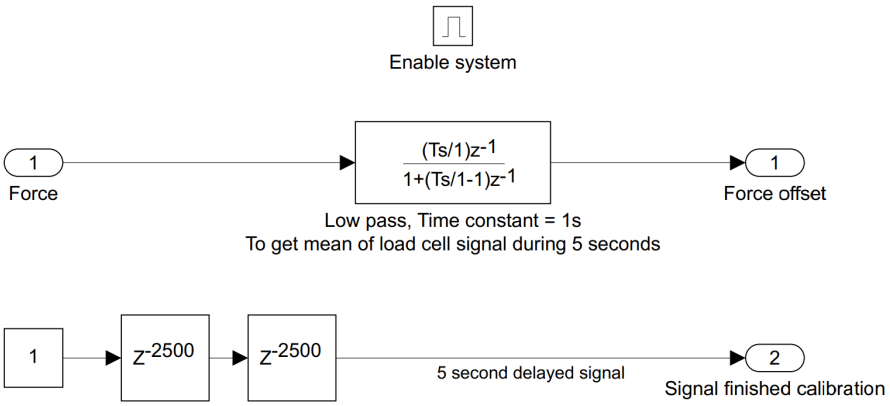

Figure 58: Internal view of *Force offset* subsystem.

In figure 58 the internal structure of the *Force offset* subsystem can be seen. The subsystem has two inputs and two outputs. The first input is the enabling signal of the subsystem, and the second input is the uncalibrated *Force* signal from the *Load cell force* subsystem. The first output is the *force offset*, i.e. the offset the force signal has to 0 N. The second output, *Signal finished calibration*, is a signal that the load cell calibration is finished.

At the same time as the encoder is being initialised, the *Force offset* subsystem calibrates the load cell. The calibration ensures that the force signal is 0 N when

no force is applied. As mentioned earlier, a fixed offset value is added to the signal to get the signal close to 0 N. However, when using different nutrunners in the test rig, the fixed offset value will not be sufficient to get the signal to 0 N and hence it needs to be calibrated. In figure 58 it can be seen that the force signal is passed through a digital low-pass filter with a cut-off frequency of 1 Hz. This reduces most of the variations in the force signal so that a static force is outputted. As can be seen in figure 56, the *Force offset* is subtracted from the uncalibrated *Force* signal. This results in the force signal after the subtraction being equal to 0 N when no force is applied. The constant together with the delay in the *Force offset* subsystem, seen in figure 58, results in a 1 being outputted on *Signal finished calibration* after 5000 samples. When this occurs, the *Force offset* subsystem is deactivated, and the last value of *Force offset* is held. When the subsystem is deactivated, the calibration is completed, and the state machine moves into the next state.

In table 7 the pin-map for the subsystem can be found.

Table 7: Pin-map for *Load cell force* subsystem.

Block name	**Type**	**Pin**
ADC	ADC	ADCINC5

5.8.6 Simulate Operator

The *Simulate operator* subsystem is responsible for the control strategy and has four system inputs and no system outputs. These are, from the bottom up in figure 59a, *Tool angle*, *Force*, *Start*, and lastly the enabling signal for the subsystem. These correspond to the measured and calculated displacement angle of the tool from the *Encoder* subsystem, the measured and calibrated force of the force gauge coming from the *Load cell force* subsystem, the start signal from the state-machine, and the enabling signal from the state-machine, respectively.

This subsystem's internals represent the control strategy shown in figure 46 almost one to one, if disregarded a couple of filters and safety features. In figure 59b the *Force* signal corresponds to the *Measured Force* from figure 46, and *Tool angle* corresponds to the *Angle* feedback for the control loop, also in figure 46.

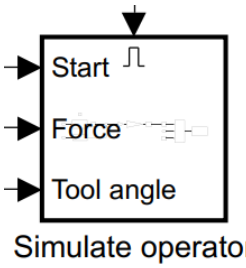

(a) In-/output ports of *Simulate operator* subsystem, external view.

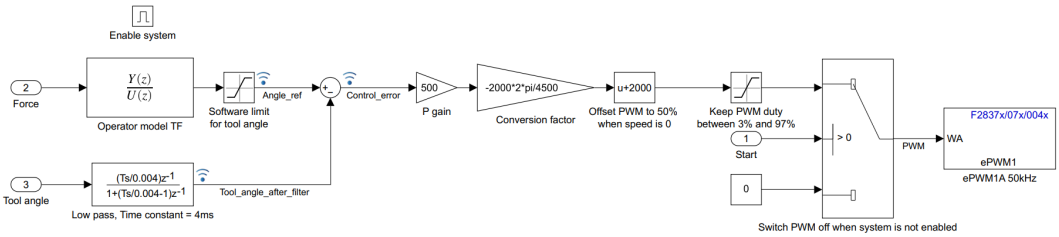

(b) Internal view of *Simulate operator* subsystem.

Figure 59: *Simulate operator* subsystem.

By going from left to right in figure 59b, the first blocks encountered are two transfer functions. The upper one is the operator model, with a force as input and the reference angle as output, and the lower one is a low pass filter for the feedback angle. Following the operator model, a saturation block is present. This saturation block works as a soft stop for the displacement angle, implemented via software. It makes sure the reference is not set to a value higher than the available angular displacement, limited by the mechanical design of the rig. This is to avoid a rig collision.

Following, continuing from left to right is the feedback subtraction and P-controller. The gain block represents the entire controller, as it is of such a simple nature. The following few blocks are purely a translation of angular displacement to a discrete value between 0 and 4000, as this is what the ePWM (enhanced PWM) block is set to accept. 4000 represents 100% duty cycle forward, and 0 represents 100% reverse. The speed on the motor, which 100% duty cycle represents, is set in the servo driver software Lightening, which is explained further in section 5.8.8.

The scaling works like the following. By first scaling the angle from radians to a value corresponding to a -2000–2000 scale, then shifting it up to the 0–4000 scale by addition of 2000. This translated angle is then sent into the ePWM block. However, a switch is utilised to ensure that the signal is shut down when the subsystem is deactivated. This defaults to sending 0 during deactivation so as not to activate the motor outside of the *Simulate operator* subsystem.

The reason why this does not cause the servo drive to go in full reverse instead of stopping completely, as explained before, is because that was only half true. A

safety feature is present that will not allow the servo drive to activate the motor if the ePWM signal is set to 100%, no matter the direction. I.e., it will not drive the motor if the signal is set to 0 or 4000. This is also the reason for the second saturation block in the subsystem, the one following the scaling. This makes sure that the input to the ePWM from the control loop is never 0 nor 4000, as this would abruptly stop the motor from almost full speed. Something very undesirable like this would interrupt the test data and possibly cause damage to the rig and tool.

The ePWM block is configured according to the list below. The settings not mentioned are set to default. The module only sets what pins will be activated, while the timer period determines the granularity with which it is possible to define the duty cycle. A larger timer period means a higher granularity. The timer register consists of 16 bits and can therefore go up to 64000 if necessary. Configuration list:

- *Module*: ePWM1(A)
- *Timer period units*: Clock cycles
- *Timer period*: 4000
- *Counting mode*: Down

The timer period also determines the ePWM frequency, as the unit type is set to clock cycles. This is determined through a quick calculation according to

$$\text{ePWM freq.} = \frac{\text{Clock speed}}{\text{Timer period}}, \tag{6}$$

where it is evident that there is always a trade-off between granularity and ePWM frequency, as a lower timer period results in a higher frequency. The clock speed is in this case set to 200 MHz, which results in

$$\text{ePWM freq.} = \frac{200\text{MHz}}{4000} = \mathbf{50kHz}.$$

200MHz clock speed is default for the CPU, however, not for the slower peripherals such as the ePWM modules. These have a separate setting that slows down their clock speed, which has been set with a prescaler of 1 according to

$$\text{EPWMCLKDIV} = \frac{\text{SYSCLKOUT}}{1},$$

where EPWMCLKDIV is *EPWM dlock divider* and SYSCLKOUT is the *CPU Clock Speed*. This is to allow for a higher ePWM frequency. The prescaler default is 2, which would halve the EPWMCLKDIV, which indirectly would halve the ePWM frequency and cause problems with compatibility between the C2000 and the servo drive, as the servo drive requires high frequencies to operate. The default pulse speed for the servo drive is *High Speed Pulse command*, which is frequencies between 4 MHz and 500 kHz, but *Low Speed Pulse command* is used for pulses under 500 kHz. This allowed a PWM frequency of 50 kHz. How low frequencies the drive can accept is not known, as it is not stated in the servo drive manual.

In table 8 the pin-map for the subsystem can be found.

Table 8: Pin-map for the *Simulate operator* subsystem.

Block name	Type	Pin
ePWM1	ePWM	PWM1A

5.8.7 Button Interfacing

The *Button clicking interface* subsystem is responsible for registering when a button on the remote control has been pressed. The subsystem has two inputs and four outputs. The inputs are *Up click* and *Down click*, which are connected to the GPIO-inputs that corresponds to the up and down click on the remote control. The first output is *Start tightening*, which sends a signal to a GPIO-output that controls the remote start of the Power Focus via the interface board described in section 5.6.4. The second output is *Start loosening*, which, similarly to *Start tightening*, sends a signal to the Power Focus to start loosening. The third output, *Home/next state*, sends a signal to the state machine to move to the next state. Finally, the fourth output, *Reset*, sends a signal to the state machine to go to the reset state.

If the tightening or loosening button has been depressed for more than half a second, the subsystem will send a signal to tighten or loosen the nut respectively. If the tightening or loosening button has been double-clicked, the subsystem will send a signal to the state machine to move to the next state or move to the reset state respectively. In figure 60 the *Button clicking interface* subsystem can be seen.

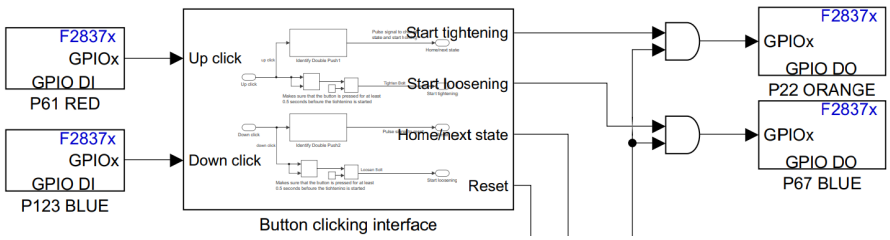

Figure 60: External view of *Button clicking interface* subsystem.

In figure 61 the internal structure for the *Button clicking interface* subsystem can be seen. The structure for the up and down click are identical, and thus only the up click structure will be described in detail. As can be seen in figure 61, a discrete integrator together with a relational operator is used to determine when the button has been pressed for more than half a second. When this occurs, the output, *Start tightening*, is set to 1. The discrete integrator is reset when it detects a falling edge, i.e. when the button is released. Thus setting the output, *Start tightening* to 0.

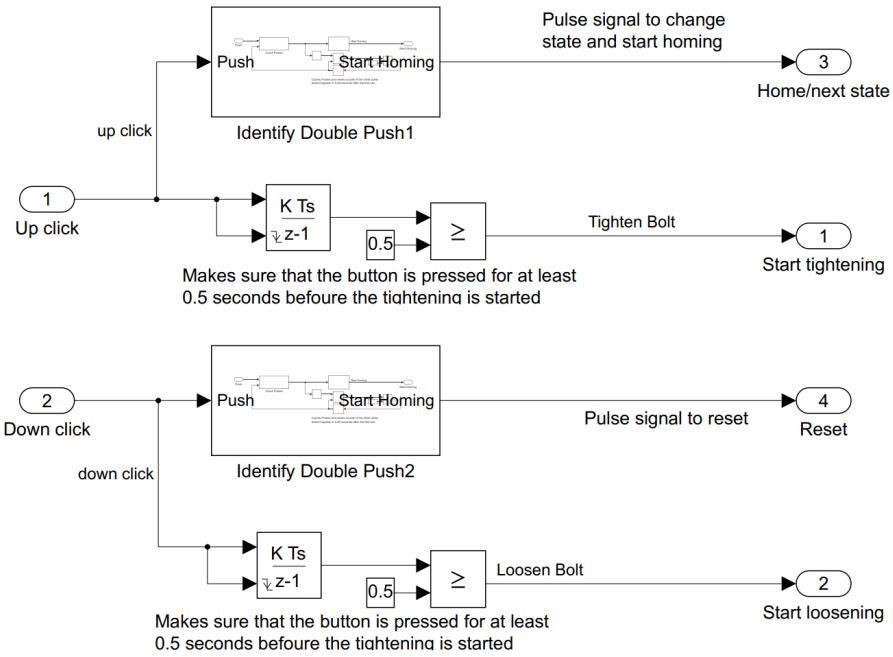

Figure 61: Internal view of *Button clicking interface* subsystem.

In figure 62 the internal structure for the *Identify double push* subsystem can be seen. The *Count pulses* subsystem counts how many times the button has been pressed and outputs the counter value on the output, *U*. If a signal is sent to the *Reset* input of the *Counter Pulses* subsystem, the counter value is reset to 0. The MATLAB function block has the counter value, *U*, as an input and outputs a 1 on the output, *y*, if the input is greater than or equal to 2. This results in a signal to move to the next state being outputted when the button has been double-clicked. The reason for using a MATLAB function was that the regular relational operator did not work correctly on this particular signal while using the external mode. The discrete integrator together with the relational operator results in the *Count pulses* subsystem being reset if a second pulse does not appear 0.49 seconds after the first pulse. This is to ensure that a double-click and a long press to start tightening or loosening cannot happen simultaneously. The saturation block is set to 1, and the delay of one sample time is to ensure that that there is no algebraic loop.

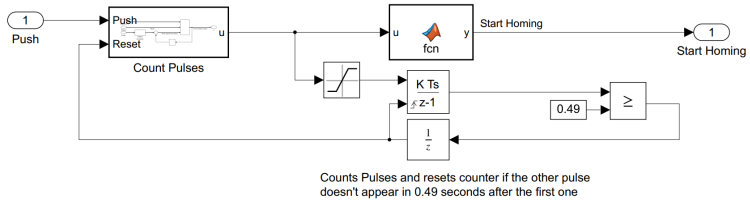

Figure 62: Internal view of *Identify double push* subsystem.

In figure 63, the internal structure for the *Count pulses* subsystem can be seen. The *Detect increase* block outputs a 1 if there has been an increase in the input compared to the last sample, i.e. if the button has been pressed. The delay and the sum block works like a holding circuit, feedbacking the current counter value. The delay ensures that there is no algebraic loop. When a reset pulse is received, the switch block switches to the input with the constant and thus, the counter value is reset.

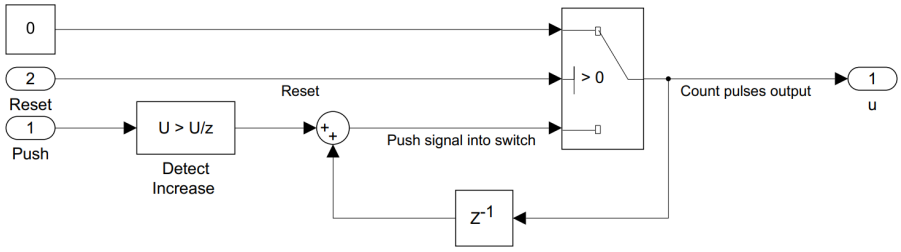

Figure 63: Internal view of *Count pulses* subsystem.

In table 9 the pin-map for the subsystem can be found.

Table 9: Pin-map for the *Button clicking interface* subsystem.

Block name	**Type**	**Pin**
P61 RED	GPIO-input	P61
P123 BLUE	GPIO-input	P123
P22 ORANGE	GPIO-output	P22
P67 BLUE	GPIO-output	P67

5.8.8 Servo Drive Software: Lightening

The servo drive has its own software called Lightening [35]. The software is distributed by Hiwin Mikrosystem and is free to use. When using lightening, the servo drive must be powered on and connected to the computer running lightening with a USB cable. This section briefly covers the important aspects of lightening regarding the project. All details about lightening can be found in the servo drive manual, provided by Hiwin Mikrosystem.[35]

Figure 64 shows the main window in lightening and the names of the main menus. The menus are explained in more detail in the list below, and what settings are used in each menu is also explained:

- *Configuration center:* What motor and encoder that the servo drive is using are defined. This only needs to be done once, as long as the motor or encoder is not changed. In this menu you can also change the primary and secondary operation mode, as well as the inputs for each mode and their scaling. In our case the primary operation mode is position mode, and the secondary mode is velocity mode. For velocity mode the input is PWM with 50% duty cycle corresponding to zero speed. A higher duty cycle gives positive speed, negative duty cycle gives negative speed.
- *Auto tune center:* The servo drive does a sinusoidal sweep that identifies system parameters to adjust control gains. If the parameters of the system are changed, e.g., the mass, the auto tune must be run again to ensure stability of the system.
- *Performance center:* Here the motor can be controlled manually, e.g., by jogging. The gains of the controller can be changed, to make the motor more or less stiff. The easiest way is to change the common gain (CG), but individual gains can also be changed. It is also possible to scope all signals available to the servo drive; motor angle, current, velocity, etc.
- *Application center:* Here the homing sequence is defined. It is configured to first home the left side, then right side, and then to center the motor in-between the limit switches.
- *Protection center:* The maximum speed and acceleration of of the motor can be defined, to limit the speed for safety reasons. It is configured for 4500 rpm as maximum speed.
- *I/O center:* Define the function for each input and output. How each port is configured is written in section 5.6.1. The limit switch inputs are inverted because they are normally closed for safety. Also, the input "Switch HI/LO pulse command" is inverted, because it is not connected to any GPIO pin and must always be on (to make the driver accept the PWM signal).
- *Parameter saving/loading:* A very useful feature is that the parameters on the servo drive can be saved to a file, and later loaded to the drive again. This allows for experimenting with changing parameters, and if something goes south, the drive can be reverted to a previously functional state by loading a previously saved file. To save any changes to the servo drive permanently (meaning that they remain after the servo drive is powered off) the RAM must be flashed to the servo drive memory.

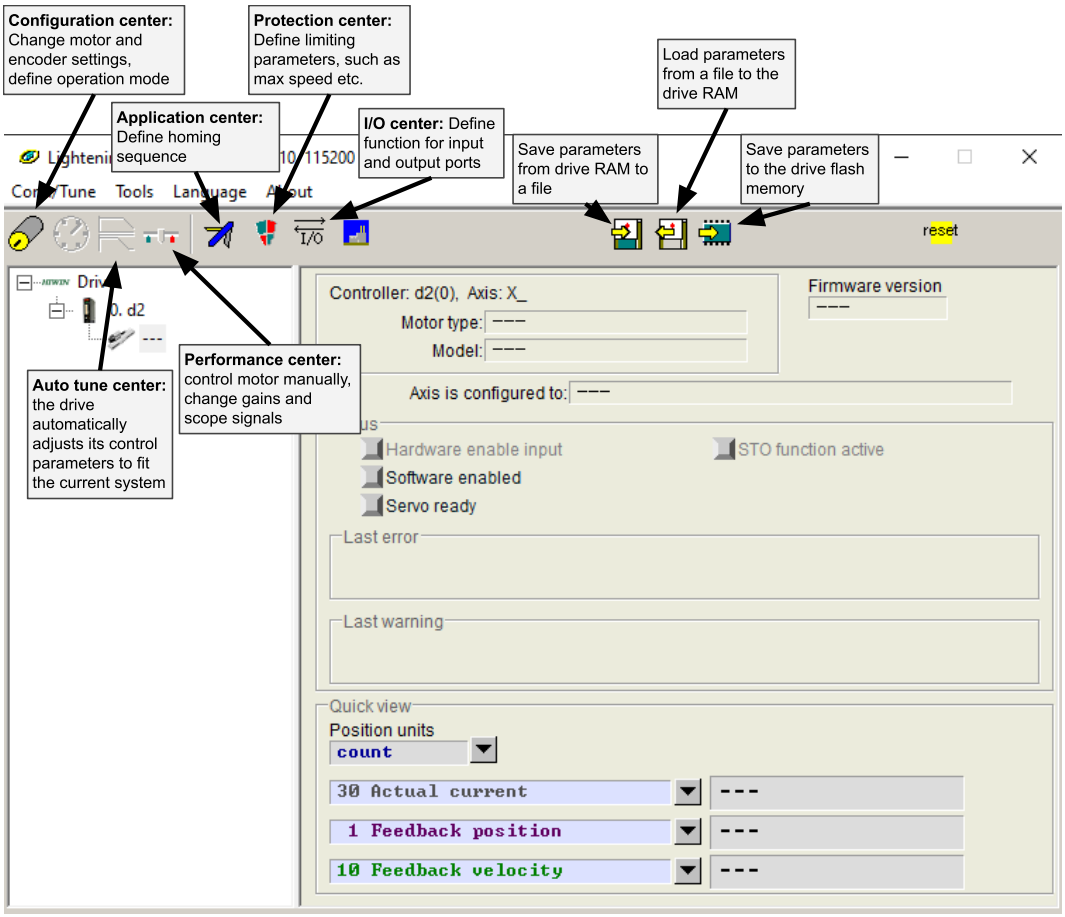

Figure 64: Main window in Lightening.

5.9 Safety Features

In the following sections, the different safety features implemented in the test rig are described.

5.9.1 Emergency Stop Button

The emergency stop button stops all operations from proceeding if pressed. This is achieved both through analogue and software implementations explained in section 5.6.3 and 5.6.4. When the emergency stop button is pressed, the holding circuit is deactivated and turns off the power to the servo motor. This causes the state machine to go into the reset state, no matter what the current state is. In the reset state, Axis Enable is deactivated, the remote triggering of the nutrunner is turned off, and the servo driver is reset.

5.9.2 Reference Limit in Software

The reference limit acts as a safeguard to limit the angular displacement of the arm to $\pm\frac{\pi}{4}$ rad, to prevent collisions with the rig frame. In section 5.8.6 it is explained how this is designed.

5.9.3 Limit Switches

The limit switches act as a software stop if the arm collides with the frame. As mentioned in section 5.6.1, the switches are connected to inputs of the servo driver. When one of the limit switches is pressed, the servo driver will not allow the servo motor to rotate further in that direction. If anything tries to rotate, the motor will apply a torque to counteract the movement. The servo motor is free to move in the opposite direction.

5.9.4 Hardware Stop

To prevent damage to the test rig if the arm were to collide with the frame, hardware stops were implemented. As mentioned in section 5.2.1, the stops were made from 2 mm thick sheet metal that was bent for added strength. The stops were attached to the linear rails so that the arm could collide with the stop instead of the frame. 3D-printed bumpers made from Thermoplastic polyurethane were installed on the arm to reduce the impact.

6 Verification

Before the rig could be compared with the stakeholder requirements, it had to be verified that it works as expected. This section presents the process of testing the system, both by each subsystem itself and for the whole assembly. Tests on reference tracking, repetitiveness and rig performance compared to a human operator were made, which are further explained below.

6.1 Part Verification of Subsystems

The test rig was verified during the building process and when the rig was complete. Each subsystem was built and verified before it was assembled with the other subsystems, ensuring that the assembled parts performed as expected. Subsystems such as the motor and driver, the linear rails, the microcontroller, and the DC-DC converters were first tested on their own before they were assembled. The 12V–3.3V DC-DC converter was, for example, tested by withdrawing a current of 1000 mA, making sure that the voltage was stable at 3.3V even for larger loads.

By following this approach, it was easy to find and locate issues in the mechanical and electrical parts of the rig. The same approach was used in the building process of the software used on the microcontroller. Before the state machine was built and implemented, each of the states was tested and built separately. Even the subprograms inside each state were tested by themselves before adding other features. As in the case of the mechanical and electrical parts of the system, this approach also made it easier to find and locate issues within the code.

6.2 Complete Rig Verification

When the rig was assembled with all including components and software, it was verified by checking the ability to:

- follow the reference generated by the operator model,
- generate repetitive tests,
- match data collected from a human operator.

These verifying tests were made on a sequence of several tightenings. In order to see how well the rig perform during these tests, the RMSE value is used. The RMSE value is calculated as

$$RMSE = \sqrt{\sum_{i=1}^{n} \frac{(\hat{y}_i - y_i)^2}{n}}, \tag{7}$$

and gives an indication on how well a signal follows the expected value. Here $\hat{y}$ is the measured value and y is the actual value of the signal (or the expected value of the signal).

6.2.1 Reference Tracking

While testing the ability of the rig to follow the reference, the measured angle of the tool arm was compared to the reference angle generated by the operator model. This was done for several tightening strategies such as *Turbo Tight*® (TT) 30 Nm, TT 70 Nm, *Quick Step*® (QS) 70 Nm and a slow configuration of QS 50 Nm. It was also tested how the controller parameters such as the common gain (the servo drive gain) and the controller gain of the P-controller affects the reference tracking performance. This was done only for tightenings using the TT 30 Nm strategy. For the other tightening strategies, the common gain and the controller gain was set as the initial settings (common gain = 0.2, controller gain = 500).

6.2.2 Repetitiveness

To test the ability of the rig to generate repetitive test results, a test series of several tightenings were made. The angle and the force acting on the tool were tracked for each tightening and then compared to one another to see how the two signals differ between each tightening. These tests were made with the initial settings on the common gain and the controller gain. The repetitiveness was tested for TT 30 Nm, TT 70 Nm, QS 70 Nm and a slow configuration of QS 50 Nm.

6.2.3 Human vs. Machine

One of the most important parts of testing was to ensure that the rig sufficiently simulates a human operator. In order to test this, operator data used for the identification of the operator model was compared to rig data generated with the same tightening strategy. Since the operator data provided by Atlas included runs on TT 30 Nm, this strategy was chosen for the verifying tests. Just as in the case of reference tracking, the common gain and the controller gain were adjusted to see how they affected the rig performance. Several tightenings for each setting was made, where each test run was compared to the operator data and hence given a RMSE value. The force from the operator data was compared to the measured force from the test rig, while the angle from the operator data was compared to both the measured angle of the rig and the reference angle generated by the operator model.

7 Results

The section of results presents the final test rig, the verification of the performance of the test rig, and how it fulfilled the stakeholder requirements given in the beginning of the project.

7.1 Final Rig

Below in figure 65 is an image of all components included in the final test rig. To the right, the test rig itself can be seen and also the nutrunner that has been attached to the rig. A box containing all the necessary electronics can also be seen at the back of the rig. The box prevents the electronics from disturbing the signals from the sensors and also protects the operator from any contact with the high AC voltage. The Power focus 6000 is the controller where different tightening programs can be selected and has been connected to the microcontroller that is stored inside the electronic box. The button interface is also connected to the microcontroller. It has two buttons for controlling the power to the motor, one for turning on the power and one for turning off the power. It also has an emergency stop button and a remote control that is used to control the test rig and nutrunner.

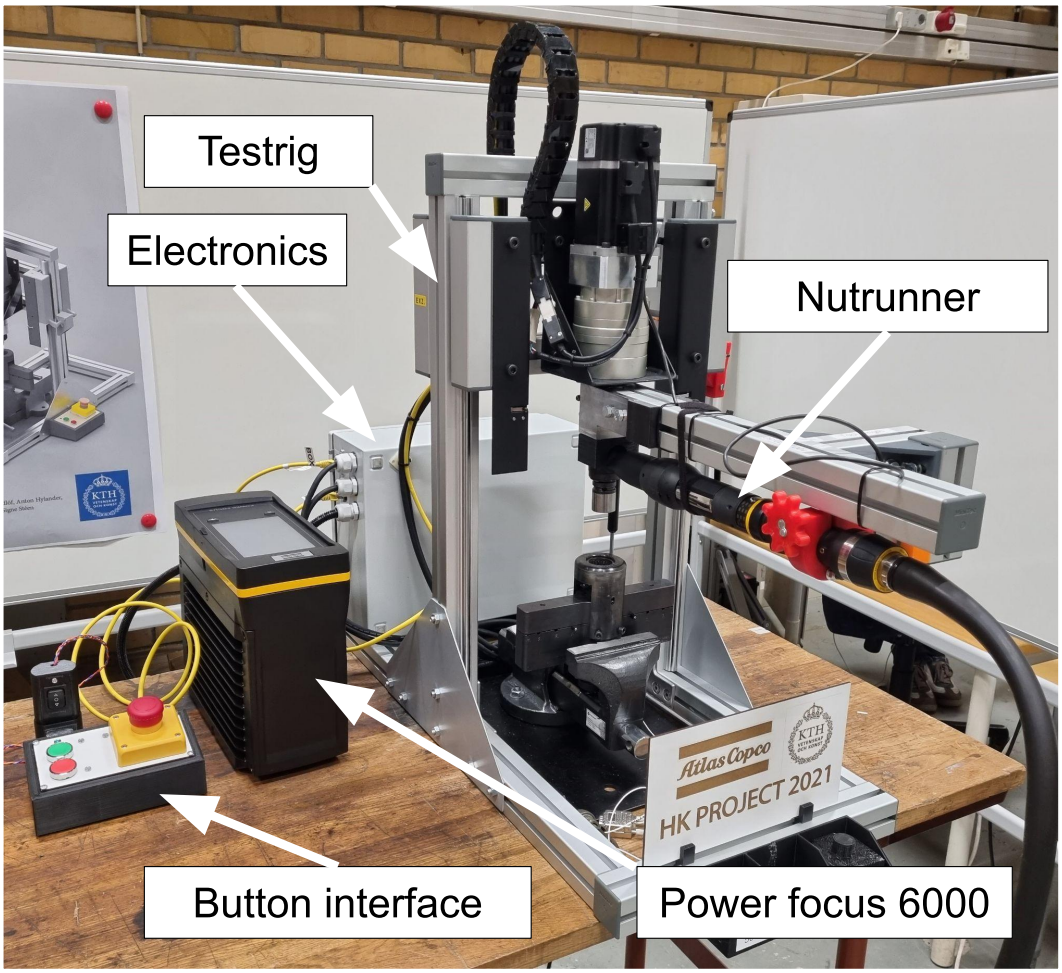

Figure 65: All components included in the final test rig.

Table 10 shows general specifications for the test rig. Maximum output torque is the peak torque that can be generated on the output shaft of the gearbox and should only be generated in time intervals of one second. The maximum output speed is also the maximum rotational speed of the output shaft of the gearbox.

Table 10: General specifications for the final test rig.

Specification	Value	Unit
Height	755	mm
Width	380	mm
Length	840	mm
Max output torque	144	Nm
Max output speed	150	rpm
Input voltage (AC)	230	V
Encoder resolution	10000	pulses/rev
Sampling frequency (microcontroller)	1000	Hz

7.2 Verification of Performance

The final assembly of the rig was tested for the three test cases described in section 6.2. The ability to follow the reference, the repetitiveness, and rig performance compared to a human operator has been verified.

7.2.1 Reference Tracking

The ability of the rig to follow the reference signal generated by the operator model was evaluated for several test runs and controller settings. Table 11 below shows the mean RMSE values between the reference angle and the measured angle for several tightenings with different controller settings and different tightening strategies. The settings of the beam test joint were also varied between the test runs (as can be seen in the table). Figure 66 below shows the response of one of these tightenings for each control setting and tightening strategy. The blue line represents the measured angle, while the dotted orange line represents the reference angle generated by the operator model.

Table 11: Mean RMSE values between the reference angle generated by the operator model and the measured angle of the motor, for different settings of the common gain and P-controller gain.

Tightening Strategy	Beam Joint Setting	No. Runs	Common Gain	P-value	RMSE
TT30	Hard	7	0.6	500	0.0211
TT30	Hard	6	0.6	750	0.0153
TT30	Hard	9	0.2	500	0.0134
TT30	Hard	6	0.4	500	0.0210
TT30	Hard	5	0.2	1500	0.0100
TT70	Mid	6	0.2	500	0.0277
QS70	Mid	8	0.2	500	0.0389
QS50 (Slow)	Mid	7	0.2	500	0.0307

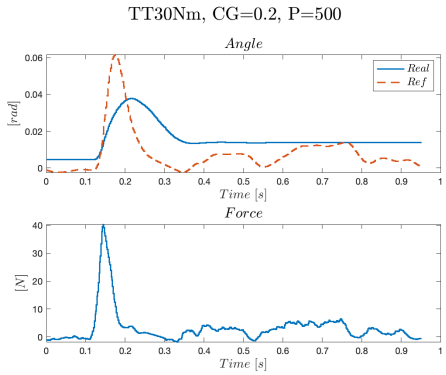

(a) Turbo Tight 30 Nm, CG=0.2 and P=500.

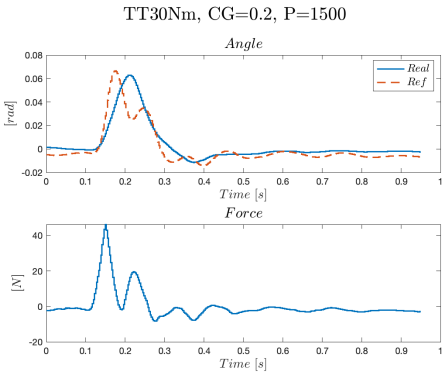

(b) Turbo Tight 30 Nm, CG=0.2 and P=1500.

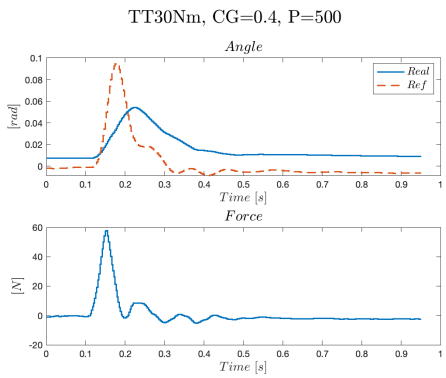

(c) Turbo Tight 30 Nm, CG=0.4 and P=500.

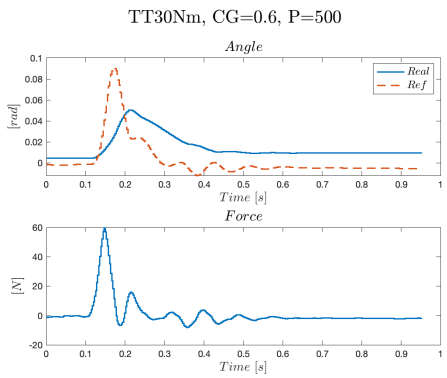

(d) Turbo Tight 30 Nm, CG=0.6 and P=500.

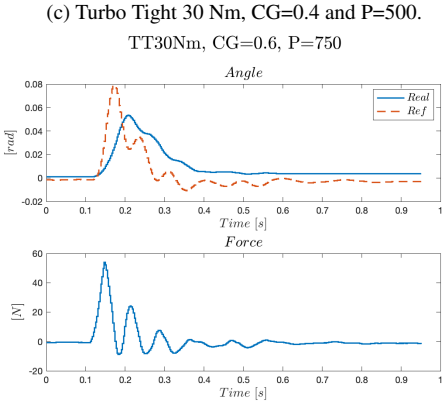

(e) Turbo Tight 30 Nm, CG=0.6 and P=750.

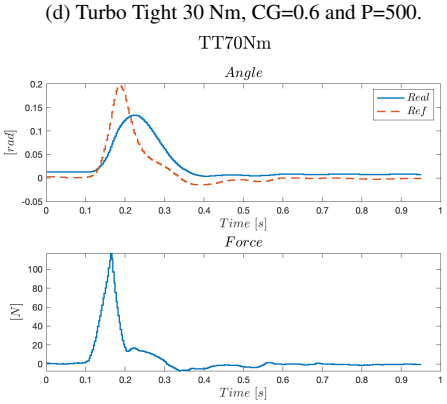

(f) Turbo Tight 70 Nm, CG=0.2 and P=500.

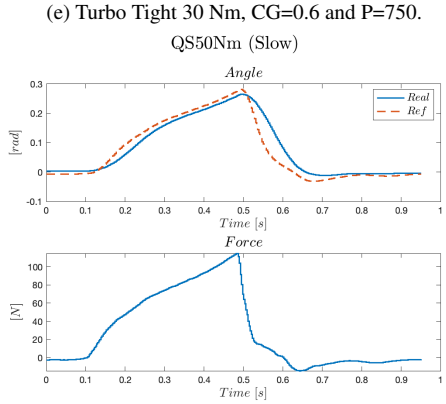

(g) Quick Step 50 Nm (slow), CG=0.2 and P=500.

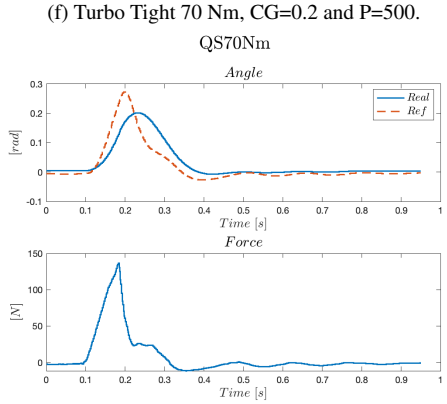

(h) Quick Step 70 Nm, CG=0.2 and P=500.

Figure 66: Test rig response while using different settings of the common gain and the controller gain for different tightening strategies. Blue line shows the measured value and the dotted orange line shows the reference generated by the operator model.

7.2.2 Repetitiveness

The repetitiveness was tested by making several tightenings with the same controller settings. The common gain and the controller gain were set as initial (common gain = 0.2, controller gain = 500). All tightenings made for each tightening strategy were plotted together, see figure 67. This shows how each tightening differs from one another.

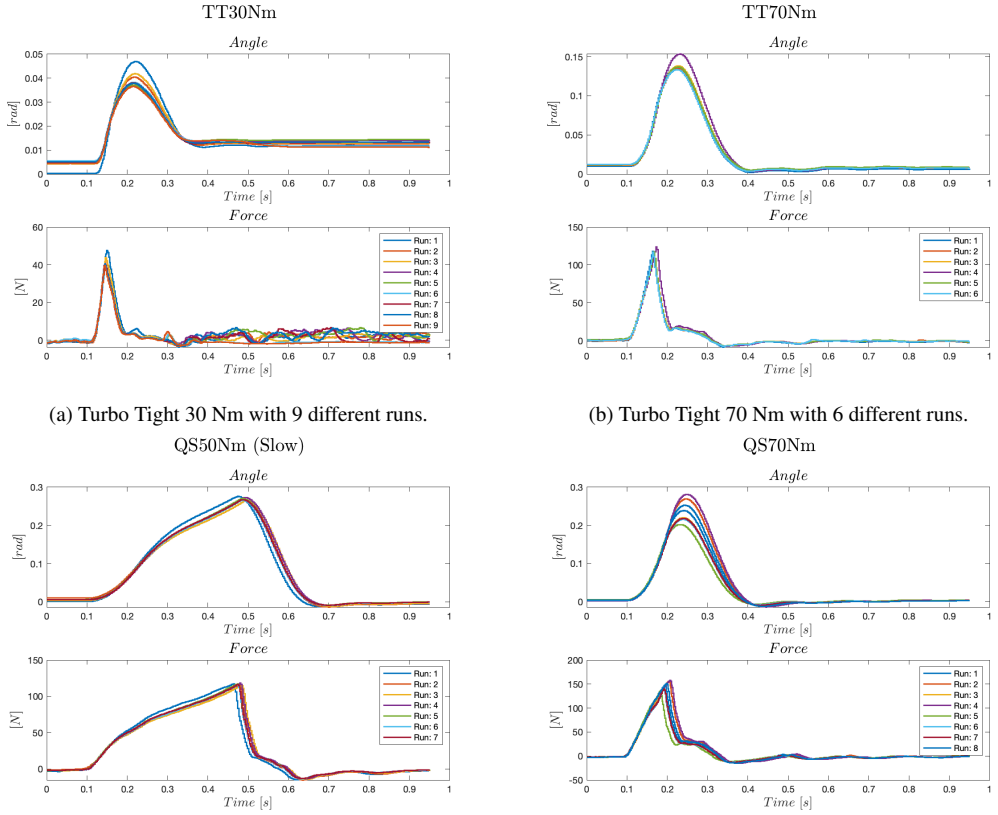

(a) Turbo Tight 30 Nm with 9 different runs.

(b) Turbo Tight 70 Nm with 6 different runs.

(c) Quick Step 50 Nm with 7 different runs.

(d) Quick Step 70 Nm with 8 different runs.

Figure 67: Test rig response for several tightening sequences while using different tightening strategies (Common gain and controller gain is set as initial, CG=0.2 and P=500).

7.2.3 Human vs. Machine

The rig response was compared to the identification data used to identify the operator model in section 5.7.1. Several runs with different control settings for tightenings with TT 30 Nm was made. RMSE values for the measured force, angle and the reference angle were generated for each test run. In table 12 below, the mean RMSE values of all test runs are presented. It can be seen that the RMSE value for the reference is smaller than the RMSE value of the actual angle of the tool. This means that the reference angle follows the measured angle from the human operator data more precisely than the actual angle of the tool follows the measured angle from the human operator. Figure 68 below shows the response of one of these tightenings for

each control setting with TT 30 Nm. The blue lines show the measured angle and force from the test rig, while the black lines show the angle and force from a real operator (the identification data presented in section 5.7.1).

Table 12: Mean RMSE values for different signals with different settings on the common gain and P-controller gain compared to the model identification data.

Common Gain	P-value	No. Runs	$RMSE_{Force}$	$RMSE_{Angle}$	$RMSE_{Ref.Angle}$
0.6	500	7	7.048	0.0289	0.0145
0.6	750	6	7.264	0.0234	0.0148
0.2	500	8	6.471	0.0284	0.0192
0.4	500	6	6.418	0.0290	0.0142
0.2	1500	5	6.536	0.0160	0.0139

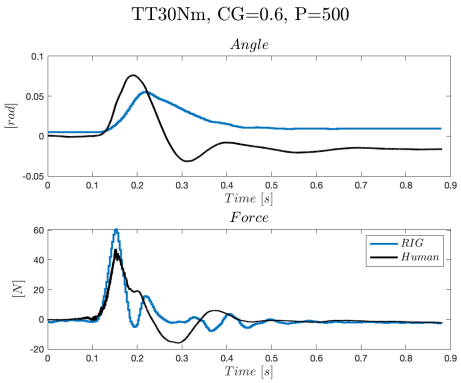

(a) Turbo Tight 30 Nm, CG=0.6 and P=500.

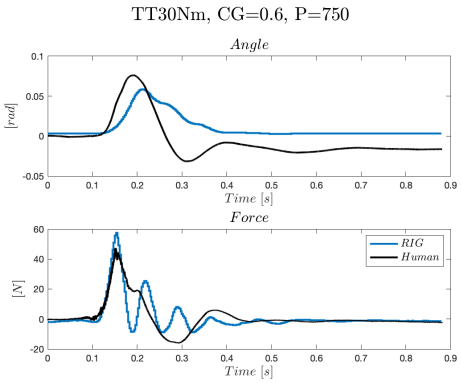

(b) Turbo Tight 30 Nm, CG=0.6 and P=750.

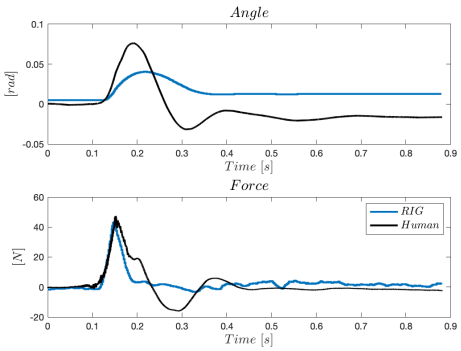

(c) Turbo Tight 30 Nm, CG=0.2 and P=500.

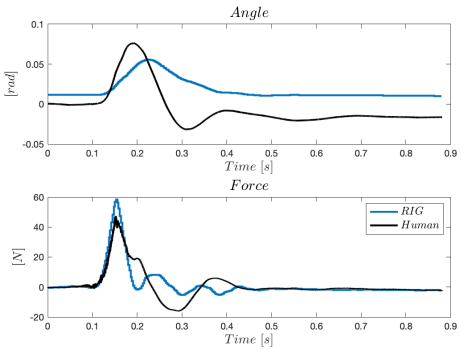

(d) Turbo Tight 30 Nm, CG=0.4 and P=500.

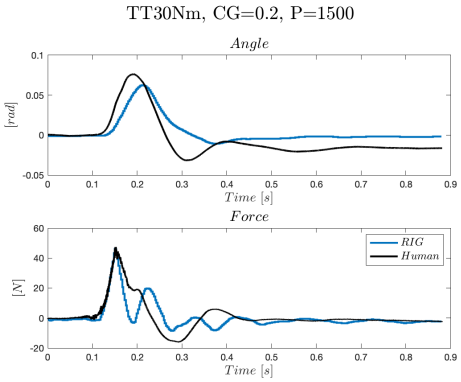

(e) Turbo Tight 30 Nm, CG=0.2 and P=1500.

Figure 68: Test rig response with different settings on the common gain and the controller gain for Turbo Tight 30 Nm, compared to operator data provided by Atlas.

7.3 Stakeholder Requirements

The goal has been to meet as many requirements of those listed from the section 1.3 as possible. Regarding the requirements of the operator model, the test rig can simulate a human operator accurately compared to data from Atlas Copco. There may be differences between different human operators, which results in difficulties for the test rig to correspond to all human operators. The section 7.2.1 confirms that this requirement is met. The test results are repetitive and accurate and have been

improved with this test rig compared to Atlas Copco's current test rig, which the results in section 7.2.2 show.

Regarding the physical requirements, the test rig is designed to be robust enough to withstand heavy vibrations, and to withstand up to 100 Nm, but has not yet been verified. The test rig adjusts for height differences during bolt tightening (see section 5.3). An Inline Rotary Torque Transducer (IRTT) between the tool and the bolt and a beam test joint will fit in the rig, which are described in section 5.4.2. The test rig can also perform various tightening strategies, such as Quickstep and TurboTight, and exceeds 60° rotary (angular) displacement (up to almost 180°). The rig functions with the following three angle tools: STR series ETV STR61-50-10, ETV STR61-70-13, ETV STR61-100-13. As for measurements, the rig can accurately measure reaction torque on the nut and reaction force to the operator, see section 7.2.1.

Regarding safety measures, the rig can protect against finger injuries as there is no need to be in contact with the rig during test runs. Instead, the rig is operated through a remote control, where there is also an emergency stop for the rig. The emergency stop ensures that all operations of the test rig can be interrupted in the event of an emergency. The noise levels are also below harmful threshold. For further descriptions regarding the safety features of the rig, see section 5.9.

Other wishes from the stakeholders at Atlas Copco that are fulfilled by the rig are that the rig is movable with the help of only two people, has low manufacturing complexity, is easy to maintain and has an independent installation of the tool. The project stayed within reasonable limits in terms of costs, and a BOM is attached in appendix G.

Wishes from the stakeholders that were not fulfilled are that the rig does not work with pistol grip tools, and it cannot test different operator positions (at this moment it can test horizontal operator positions). The status of each requirement or wish are stated in table 13 below.

Table 13: Status of the stakeholder requirements and wishes.

Requirement/Wish	Comment	Status
Simulate a human operator		OK
Enable repetitive and accurate test results		OK
Being able to test new tightening strategies		OK
Be robust enough to operate during heavy vibrations	Not verified.	N/A
An IRTT must fit between the tool and the bolt		OK

Be robust enough to withstand extreme cases (reaction torques up to 100 Nm)	The maximum torque the motor is able to handle (with the gearbox) is 144 Nm > 100 Nm. If applied with 100 Nm in the current operator model, the angular displacement would be $\approx 40^\circ$ which is smaller then the current software limit of 45°.	OK
Fit a beam test joint		OK
Adjust for height difference from bolt tightening		OK
Work for different tightening strategies	Not tested for Tensor Pulse.	OK
Be able to send data to a Dewe43	A D-sub port is integrated in the rig in order to provide signals to the Dewe43. It has not been tested.	N/A
Work with three different angle tools: STR series ETV STR61-50-10, ETV STR61-70-13, ETV STR61-100-13		OK
60° rotary (angular) displacement	Almost total angular displacement of 180°.	OK
Have a lifespan of >10 000 test runs	Not verified.	N/A
Movable by two people		OK
Short list of components and/or low manufacturing complexity		OK
Easy maintenance	Includes few parts that requires maintenance.	OK
Independent installation of tool (ease of use)	The tool is easy changed by loosening one fastening point.	OK
Accurately measure reaction torque on nut	Not verified.	N/A
Accurately measure vibrations of the tool	Not verified.	N/A
Accurately measure reaction force to the operator		OK
Work with pistol grip tools	Delimited.	NO
Simulate different types of operators	Easy to change the whole operator model, or to only change a few parameters inside the mass-spring-damper model.	OK
Different operator positions can be tested, horizontally and vertically	Delimited.	NO
Protect against injuries, e.g. finger injuries, while running the test rig	With the control panel separated from the rig it should be possible to place the rig inside a cage when tests are performed.	OK
Have an emergency system that stops all operations	The emergency system shuts down the motor and forbids the power focus to make a tightening. Even when the emergency button is released the system has to be restarted by pushing the green button.	OK
Noise levels below harmful threshold	The loudest component is the nutrunner.	OK
Enable component and implementation costs within budget	There was no hard budget limit, but it should be limited to around 25 000 SEK.	OK

8 Discussion and Conclusions

From the results, the following discussion regarding different parts of the project of the test rig can be made. The same titles apply to this section as to the section 7.

8.1 Final Rig

When the rig was designed and built one of the main concerns was if the rig was sturdy enough to withstand pulses of high torques and higher torques for a long period of time. Therefore when building the rig, the dimensions of all the fasteners were well-sized, and an extra support structure was added to the rig. This was proven to be enough when the rig was tested with tightening techniques of 70 Nm. The rig, however, needs to be securely mounted to the table or the ground to avoid flexing in the bottom structure. The rig's capability of withstanding heavy vibrations was not fully investigated, but since the construction is well-dimensioned, the rig should at least for a shorter period be able to withstand heavy vibrations.

The implementation makes it possible to produce test series that can make several tightenings just by adding some rows of code, which is discussed further in section 9. How the rig would withstand these long series of testing considering the fatigue of crucial parts was however not fully investigated.

8.2 Verification of Performance

The operator model is only based on one tightening sequence and only for one single operator. In order to improve the model, more angle/force data needs to be captured. But for the given operator data, the simulated mass-spring-damper system is very similar in its reaction.

8.2.1 Reference Tracking

The reference is calculated from the applied force at the handle. From the results, it can be seen that the reference changes between runs with different regulator gains, which can be seen in figure 66. This is not good since the reference should only be dependent on the tool tightening and the operator parameters. How this can be improved is discussed in section 9.

A fundamental problem with this controller design is that the control of the system affects the measured force and therefore also the reference, as it is calculated from the force. In a control loop, the reference is usually not affected by the system, but is set to some value by e.g., a person. When the reference is affected by the system, the system might become unstable if the reference starts oscillating (because of some effect from the system). This must be investigated to see how it can be solved.

The oscillations might also be because of the large inertia of the tool arm, which is discussed in section 8.2.3.

8.2.2 Repetitiveness

The repetitiveness of the rig is good compared to the repetitiveness of a human operator. By watching the plots in figure 66 it can be seen that the angle and force generated in the rig follow the same pattern for all tightening strategies tested, generating almost the same results for each test with the same tightening strategy. Compared to the plot with operator data in figure 47, it can be seen that the rig from a repetitiveness perspective performs a lot better than a human operator used for testing. Even though it is the same operator and the same tightening strategy used in every test with the human operator, the resulting data is more random and unpredictable compared to the rig data. The human data differs a lot between different tightenings.

Repetitive tests are extremely important while testing new tightening strategies, tool updates, or evaluating existing tools. If the testing equipment is not able to produce repetitive tests, it is difficult to determine if the tool works properly, if changes made in the control of the tool is affecting the test results or if it is caused by the testing equipment. From this perspective, the rig works significantly better than tests with a human operator since the response from the rig is much more predictive than the response of a human operator. The rig is also able to produce almost identical test results between different tightenings.

8.2.3 Human vs. Machine

The results of the human comparison, see figure 68, shows that the rig does not always act as a human arm would. There are oscillations when using high gains, and there are large differences between the human and the machine, especially when comparing the tool angle. By watching the RMSE values in table 12, it can be seen that the angle reference matches the human angle better than the actual angle measured in the rig. As discussed in section 8.2.1, the rig is not able to follow the reference accurately, which is probably the reason for a better fit between the reference angle and the human angle compared to the actual angle of the rig.

Even though the rig is not able to accurately simulate the human angle during a tightening, it still captures the peak force on the tool handle similar to a human operator. What happens after this peak force differs between the different controller settings. The best fit in angle is measured for a common gain of 0.2 and a controller gain of 1500. The force, in this case, shows slightly oscillatory behaviour after the peak force has occurred. This is probably due to the inertia of the rotating parts of the rig. The optimised operator model had a mass of $\approx 0.3\ kg$. With a radius of 0.37 m to the tool handle, this corresponds to an inertia of $\approx 0.0411\ kgm^2$. This means

that if the rotating parts of the rig have a total inertia larger than $\approx 0.0411\ kgm^2$, the servo motor needs to help the tool accelerate the system to follow the angle reference accurately. If accelerating the system by using the servo motor, the measured force on the tool handle will decrease. This makes the servo motor decrease its angle, which causes the measured force on the tool handle to increase. This causes oscillatory behaviour inside the system.

The inertia for just the servo motor and the gearbox after gearing is calculated to $\approx 0.0848\ kgm^2$, which is much larger than the inertia of the operator model. The rig also includes other parts, which means that the total inertia of the moving components of the rig is even larger than $\approx 0.0848\ kgm^2$. This means that the oscillatory behaviour seen when using a larger controller gain (and hence better following the reference angle) is probably caused by the large inertia of the rig.

8.3 Stakeholder Requirements

The stakeholders' requirements were well defined at an early stage of the project. It enabled clearer objectives and how the test rig should be designed. However, it became clear quite early on that some of the additional wishes of the stakeholders at Atlas Copco would make the project too extensive in relation to the time limit. The fact that some of the wishes are not fulfilled is also not something that affects the test rig's performance, and can instead be used to further develop the rig in the future. These and other future work recommendations are further described in section 9. The rig is built to meet all requirements stated in section 1.3, but all requirements have not been able to be verified. The status of each requirement or wish are stated in table 13 in section 7.3. From this, it can be concluded that the project was successful and gives a firm foundation for further development of the rig or immediate testing of tools.

9 Future Work

This section contains areas that can be improved and other recommended future work.

9.1 Further Verification

Human operators are all very different, as can be seen in figure 47. The rig has only been compared to a single data set from a single human operator. Further verification is recommended, by using different operator parameters (mass, spring constant, damping) and seeing how that affects the reaction force of the rig. It can also be tested if the rig performs better for some combination of operator parameters, which have not yet been tested.

9.2 Suggested Improvements

The following section will cover suggested improvements of the rig.

9.2.1 Control Strategy

The controller is quite fast, but still has problems following the reference when using TurboTight®, as can be seen in figure 66. Increasing controller gains leads to instability, and thus another controller strategy must be implemented. A start would be a 2DOF PID controller, preferably with discrete pole placement to ensure good stability. Another idea is to feedback not only force and angle, but also velocity and acceleration to get more information about the system, which might result in a more stable controller.

For the design of the next controller, a suggestion would be to find the rig's transfer function. This would allow for precise pole placement, ensuring stability and robustness. Finding the transfer function could be done analytically or through an experimental method. An example of an experimental method could be sinusoidal sweeps. By recording the amplitude and phase response of the rig when running the motor with a frequency gradient sinusoidal reference, the bode diagrams, and therefore the transfer functions, are known. When doing this, it is also possible to choose what input and output are desired from the transfer function, which allows for very simple implementation at the later stages.

Using the internal position controller in the servo drive could be another possibility. The servo drive has a built-in high performance position controller. When using the driver in position mode it however only accepts pulses as a reference. One pulse equals one encoder step, so pulses must be sent continuously and quickly to the driver to update the reference. Because of time constraints, and limited experience

within the area, the implemented control structure was instead the one with a cascade controlled velocity mode servo drive, and the position control was put aside. It is however a controller with smaller delay and higher performance. Hence why it deserves further investigation.

9.2.2 Increased Torque Performance

The current rig is limited to torques up to 144 Nm. There are, however, a few ways to increase this limit. One way is just simply to change the motor for a one with higher rated torque or to buy a gearbox with a higher gear reduction ratio. Changing the gearbox might, however, impact the performance of the rig since it would also affect the output speed as a higher torque results in a reduced speed. How the rig would be affected by lowering the output speed has not been investigated. A third alternative to increase the torque capability would be to integrate passive components to the rig, such as passive springs and dampers. One alternative is to place a torsional spring between the motor mount and the custom adapter which is connected to the beam. This would stiffen up the beam and enable the rig to withstand higher torques, depending on how stiff torsional spring is added. Regular springs and dampers can also be integrated directly onto the beam. However, there is not any appropriate structure existing today that the spring and damper could be mounted on, so that needs to be investigated as well. But to keep the wide range of motion for the beam that it has in its current state, the best alternative would be to either add a torsional spring or improve the motor or gearbox.

9.2.3 Robustness

The main issue encountered during this project was the noise generated by the servo drive. To combat this, both active and passive low pass filters were used on those signals that got affected. The low pass filters do, however, have a bad impact on the performance of the rig, as the signals become slower (limited by the cutoff frequency). To be able to increase the robustness and performance by removing the low pass filters, the disturbances from the servo drive, motor cables and servo motor need to be decreased drastically. Some investigations were made in this area, but not that many conclusions could be drawn. The noise seems to arise from the high frequency pulses that are sent out by the servo drive to the motor. The high frequency pulses then propagate in the motor cable until it reaches the motor. The motor cable used is 5 m long, and reducing the length of this cable should result in less noise. There is no need for the cable to be more than 1.5 m long. By routing the motor cable separately from other sensitive cables would also result in less induced voltage spikes in other conductors. Another thing discussed was to place a line reactor, also called choke, in series with the motor cable, which should smooth out the spikes generated

from the pulses. The use of ferrite rings in strategic places was also discussed but not fully implemented which leaves room for improvements.

9.2.4 Interface

The user interface of the rig is currently quite under developed. There is a need for an interface since the operator needs to step through each of the processes in the state machine described in section 5.8.1. If the state machine stops in a certain step or some errors appear, the operator has no chance of noticing this. A couple of LEDs for indicating the current state would be a great improvement, and any kind of display to be able to display any eventual errors that might occur. A screen would also be beneficial if an *Automatic Test Series* would be implemented, which is described further in section 9.2.5.

9.2.5 Automatic Test Series

The current rig is capable of many tightenings in the tight consecutive time frame. It does, however, require manual input from an operator to do so. An improvement that could prove useful would be to develop a system in the software for performing a test series instead of singular tightenings at a time. This would probably benefit from an improved user interface as well, but that is discussed more in section 9.2.4.

Some things to consider if this were to be implemented are some extra safety measures, as the rig could be left without supervision. A few software stops should probably be included. One of them should be a current sensor, measuring the current through the motor, sending its information to the microcontroller where it is then possible to develop a software stop if the current is above a certain maximum threshold.

9.2.6 Improved Operator Model

The rig currently uses a mass-spring-damper system as the operator model, which works well for ergonomic assessment. However, the operator model can be improved to more accurately simulate the behaviour of a human operator. Improvements for the operator model could be to include the human reaction time, as described in section 2.1.1. There is also a possibility to implement several mass-spring-damper systems with different parameters in the state machine, and then switch between them for different phases of the tightening as the human operator's dynamics change.

Probably the most realistic operator model would be an active model, for example, the Huxley model. By using an active model, the model will probably be an accurate representation even after the first 200 milliseconds. Contrary to the mass-spring-damper system, as discussed in section 2.1.3. However, with the increase of the

operator models complexity, additional computing power might be needed. Also, a more complex active model might not be needed for ergonomic assessment.

References

[1] *ETP STB34-06-I06-W 8433 3018 75 ServAid*. URL: https://servaid.atlascopco.com/AssertWeb/sv/AtlasCopco/Catalogue/2408.

[2] *ETV STB34-30-10-W 8433 3018 35 ServAid*. URL: https://servaid.atlascopco.com/AssertWeb/sv/AtlasCopco/Catalogue/2405.

[3] Akul Joshi, Ming Leu, and Susan Murray. "Ergonomic analysis of fastening vibration based on ISO Standard 5349 (2001)". In: *Applied Ergonomics* 43.6 (Nov. 2012), pp. 1051–1057. ISSN: 18729126. DOI: 10.1016/j.apergo.2012.03.005.

[4] *Methods of Tightening Threaded Fasteners*. URL: https://www.boltscience.com/pages/tighten.htm.

[5] *Pocket Guide Power Focus 6000 - Atlas Copco Sweden*. URL: https://www.atlascopco.com/sv-se/itba/about-industrialtechnique/brochures-and-catalogs/pocket-guides.

[6] Atlas Copco. *The art of Ergonomics*. URL: https://www.atlascopco.com/content/dam/atlas-copco/industrial-technique/ergonomics/documents/Pocket%20Guide%20Ergonomics%209833858701_L.pdf.

[7] Atlas Copco. "Pocket Guide The Art of Ergonomics". In: (). URL: https://www.atlascopco.com/sv-se/itba/about-industrialtechnique/brochures-and-catalogs/pocket-guides.

[8] Atlas Copco. *Pocket Guide Vibrations*. URL: https://www.atlascopco.com/sv-se/itba/about-industrialtechnique/brochures-and-catalogs/pocket-guides.

[9] Safety Executive. *Hand-arm vibration at work: A brief guide for employers*. Tech. rep.

[10] Canadian Center for Occupational Health CCOHS and Safety. *Raynaud's Phenomenon : OSH Answers*. URL: https://www.ccohs.ca/oshanswers/diseases/raynaud.html.

[11] Bo Lindqvist and Lars Skogsberg. *Power tool ergonomics : evaluation of power tools*. Atlas Copco, 2007. ISBN: 9789163199004.

[12] OrthoInfo. *Carpal Tunnel Syndrome Symptoms and Treatment*. URL: https://orthoinfo.aaos.org/en/diseases--conditions/carpal-tunnel-syndrome/.

[13] Sonex Health. *Carpal Tunnel Syndrome - Symptoms and Treatment - OrthoInfo - AAOS*. URL: https://orthoinfo.aaos.org/en/diseases--conditions/carpal-tunnel-syndrome/.

[14] Jia Hua Lin, Raymond W. McGorry, and Rammohan V. Maikala. "The effects of joint torque, pace and work:Rest ratio on powered hand tool operations". In: *Ergonomics* 55.3 (Mar. 2012), pp. 361–370. ISSN: 00140139. DOI: 10.1080/00140139.2011.639905.

[15] Maria Boberg. *Automated Test-Rig Report*. Tech. rep.

[16] Industrial Ergonomics, Seoungyeon A Oh, and Robert G Radwin. *The effects of power hand tool dynamics and workstation design on handle kinematics and muscle activity*. Tech. rep. 1997, pp. 59–74.

[17] Jia Hua Lin, Robert G. Radwin, and Terry G. Richard. "A single-degree-of-freedom dynamic model predicts the range of human responses to impulsive forces produced by power hand tools". In: *Journal of Biomechanics* 36.12 (2003), pp. 1845–1852. ISSN: 00219290. DOI: 10.1016/S0021-9290(03)00214-8.

[18] *Active vs. Passive Vibration Isolation - Vibration Engineering Consultants*. URL: https://vibeng.com/active-vs-passive-vibration-isolation/.

[19] Masaaki Kawana and Taro Shimogo. "Active suspension of truck seat". In: *Shock and Vibration* 5.1 (Jan. 1998), pp. 35–41. ISSN: 1070-9622.

[20] *Tech highlight: fully active suspension in new Audi A8 | OpenRoad Auto Group*. URL: https://openroadautogroup.com/blog/tech-highlight-fully-active-suspension-new-audi-a8.

[21] *(PDF) Study and Comparison on Linear Electromagnetic Shock Absorbers among other Available Intelligent Vibration Dampers*. URL: https://www.researchgate.net/publication/342709899_Study_and_Comparison_on_Linear_Electromagnetic_Shock_Absorbers_among_other_Available_Intelligent_Vibration_Dampers.

[22] Bart L.J. Gysen et al. "Active electromagnetic suspension system for improved vehicle dynamics". In: *IEEE Transactions on Vehicular Technology* 59.3 (Mar. 2010), pp. 1156–1163. DOI: 10.1109/TVT.2009.2038706.

[23] *Permanent Magnet Synchronous Motor : Construction & Its Working*. URL: https://www.elprocus.com/what-is-a-permanent-magnet-synchronous-motor-its-working/.

[24] Shritama Mukherji. *EXPLORING TORQUE AND DEFLECTION RESPONSE CHARACTERISTICS TO EVALUATE THE ERGONOMICS OF DC TORQUE TOOLS VIA A TOOL TEST RIG*. Tech. rep. 2008.

[25] Haluk Ay, Anthony Luscher, and Carolyn Sommerich. "A dynamic simulator for the ergonomics evaluation of powered torque tools for human assembly". In: *Assembly Automation* 37.1 (2017), pp. 1–12. ISSN: 01445154. DOI: 10.1108/AA-12-2015-126.

[26] Johansson Hans. *Elektroteknik*. 1st ed. Vol. 1. Stockholm: Kungl Tekniska Högskolan, 2013, pp. 5–22.

[27] Johansson Hans. *Elektroteknik*. 1st ed. Vol. 1. Stockholm: Kungl Tekniska Högskolan, 2013, pp. 1–63.

[28] MathWorks. *Remove High-Frequency Noise in Measured Data*. URL: https://se.mathworks.com/products/embedded-coder.html (visited on 12/19/2021).

[29] maximintegrated. *GUIDE TO ANTI-ALIASING FILTER BASIC*. URL: https://www.maximintegrated.com/en/design/technical-documents/tutorials/9/928.html (visited on 12/19/2021).

[30] *DEWE-43A | USB Data Acquisition System (DAQ) | Dewesoft*. URL: https://dewesoft.com/products/daq-systems/dewe-43.

[31] *DEWE-43A-ISO.png (1244×720)*. URL: https://www.zse.de/db_pics/shop_content/1280x720-c/DEWE-43A-ISO.png.

[32] Jan David Quesel et al. "How to model and prove hybrid systems with KeYmaera: a tutorial on safety". In: *International Journal on Software Tools for Technology Transfer* 18.1 (2016), pp. 67–91. ISSN: 14332787. DOI: 10.1007/s10009-015-0367-0.

[33] HIWIN MIKROSYSTEM. *D2T Drive - Controller & Drive - Products | Hiwin Mikrosystem Corp.* Nov. 23, 2021. URL: https://www.hiwinmikro.tw/en/product/controller-drive/drive-d2t (visited on 11/23/2021).

[34] HIWIN MIKROSYSTEM. *FR Series - AC Servo Motor - Products | Hiwin Mikrosystem Corp.* Nov. 23, 2021. URL: https://www.hiwinmikro.tw/en/product/ac-servo-motor/ac-servo-motor-fr-series (visited on 11/23/2021).

[35] *Download | Hiwin Mikrosystem Corp.* URL: https://www.hiwinmikro.tw/en/download?file=002a758f-b411-4b83-af7e-6a002ec3a0fe.

[36] *INA126 data sheet, product information and support | TI.com*. URL: https://www.ti.com/product/INA126.

[37] *LAUNCHXL-F28379D Development kit | TI.com*. URL: https://www.ti.com/tool/LAUNCHXL-F28379D.

[38] MathWorks. *Generate C and C++ code from Simulink and Stateflow models*. URL: https://se.mathworks.com/products/simulink-coder.html (visited on 12/02/2021).

[39] MathWorks. *Generate C and C++ code optimized for embedded systems*. URL: https://se.mathworks.com/products/embedded-coder.html (visited on 11/23/2021).

A Complete schematic

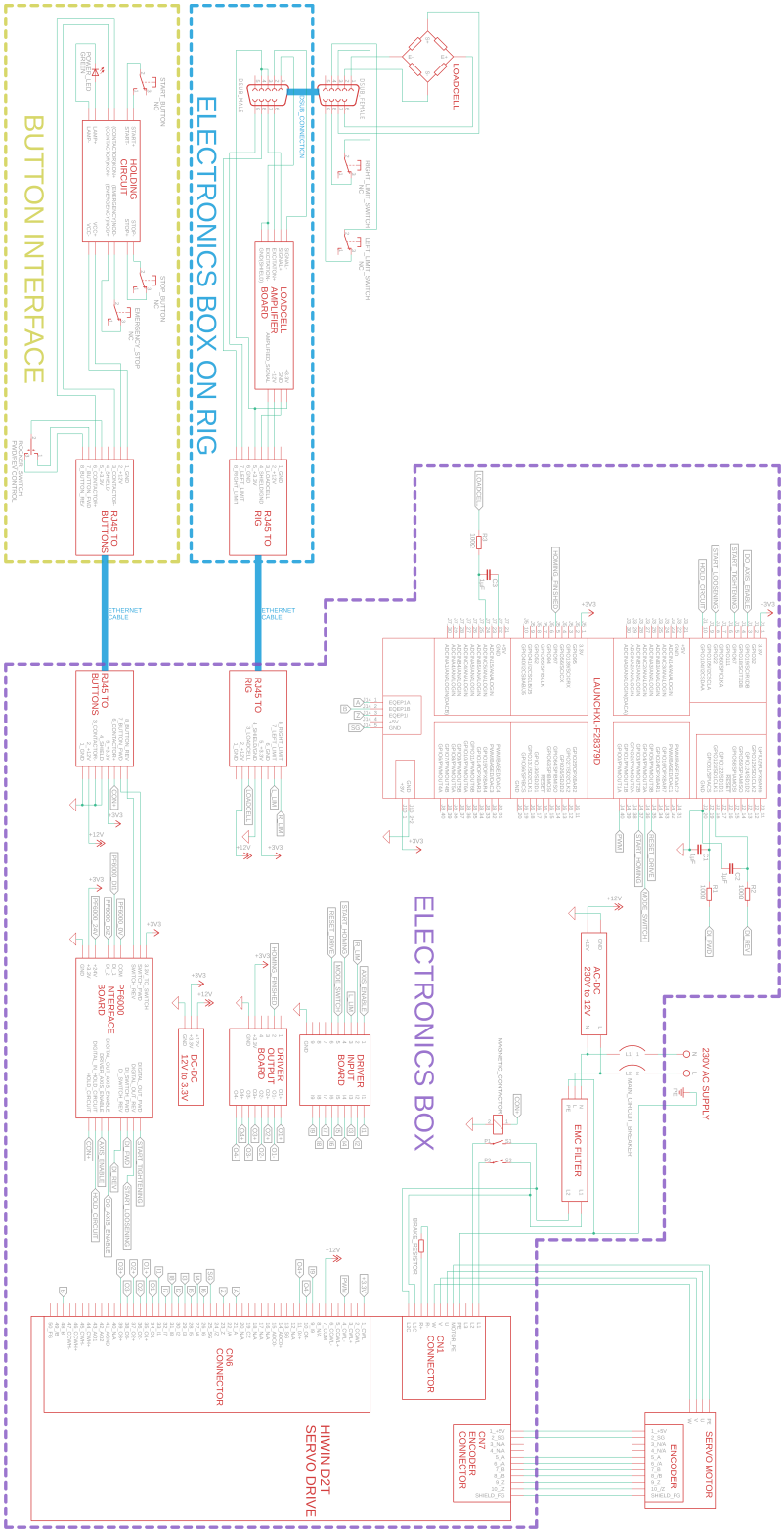

B GANTT - Fall Term

C Pros and Cons for the concepts

The entire list of pro's and con's from the evaluation of the initial three concepts.

Pros of Concept 1:

+ The height of the rig is movable, which enables the rig to follow the tool down during bolt tightening and to fit different types of beam test joints.
+ This height regulation also enables the rig to fit different types of beam test joints and various sensors.
+ The attachment construction makes it easy to change beam test joints and to change the tool.
+ The construction enables the tool to rotate $\approx \pm 90^{\circ}$ around its rotation axis.

Cons Concept 1:

- To generate torque directly on the tool head requires a strong motor, which can be very expensive, or a high gear ratio, which require a lot of space.
- The control system needs to be precise fast and in order to measure the small angle changes at the tool head and have time to apply enough motor torque.
- The beam that the tool is attached too can be heavy. This can affect the inertia and the results of the tests.
- The concept will require a large gear ratio, which can increase the inertia of the system a lot, as the inertia of the motor is proportional to the gear ratio squared.

Pros Concept 2:

+ Easy to use semi-active system which has been proven to work (section 2.3).
+ With correct settings on the pneumatic cylinder and for small tool angles it can simulate a human arm well.
+ Using a pneumatic cylinder semi-actively is robust for extreme cases, since it does not need be actively controlled and requires no power during test runs.
+ The curved rail enables the tool to rotate several degrees around its rotation axis.

Cons Concept 2:

- Semi-active systems limits the modelling of a human operator. For example, the stiffness and damping can change during rundown which is hard to simulate with pneumatic.

- Large forces will occur on the attachment points on the cylinder, which can affect the robustness.
- Friction forces in the rail might affect the test results, and if the nut is not perfectly centred the linear bearing might bind up.

Pros Concept 3:

+ The placement of the motor enables lower torque requirements on the motor, compared to concept 1. The price of the motor would be lower.
+ A passive system with springs and dampers can be implemented parallel to the active system. This would also decrees the torque requirement on the motor.

Cons Concept 3:

- The tool has limited rotation range since the tool attachment point in the wagon has limited vertical translation space.
- Forces of the components on the attachments point between the tool and the wagon are high, which can affect the robustness.
- As for concept 1, the inertia of the motor will have a large effect on the total system inertia, as there is a high gear ratio.

D Servo Motor Datasheet

5.3.5 AC servo motor FRMS 750 W

Table 5.7 **Technical data FRMS 750 W**

Motor data	Symbol	Unit	FRMS752 _ _08_
Nominal voltage	V	VAC	220
Nominal power	W	W	750
Nominal torque	T_C	Nm	2.4
Nominal current	I_C	A_{eff}	5.1
Peak torque for 1 sec.	T_P	Nm	7.2
Peak current for 1 sec.	I_P	A_{eff}	15.3
Nominal speed	n_N	rpm	3,000
Maximum speed for 1 sec.	n_{max}	rpm	4,500
Torque constant	K_T	Nm/A_{eff}	0.47
Voltage constant	K_e	V_{eff}/(1,000 rpm)	28.4
Winding resistance [1]	R	Ω	0.813
Winding inductance [1]	L	mH	3.4
Mass inertia of rotor	J	$kgm^2 \times 10^{-4}$	1.4
Mass inertia of rotor with brake	J	$kgm^2 \times 10^{-4}$	1.46
Motor weight	M	kg	2.66
Motor weight with brake	M	kg	3.32
Motor insulation class			A
Motor brake (optional) [2]			
Braking torque (static)	T_b	Nm	2.4
Power supply	V	VDC	24 ± 10 %
Power consumption	A	A	0.4
Rated input	W	W	8.6
Response time open	t_O	ms	45.0
Response time close	t_R	ms	10.0

[1] Measured between phase–phase
[2] The motor brakes are holding brakes only, not operating brakes

Torque-speed curve FRMS 750 W:

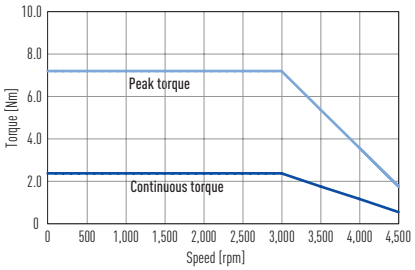

Dimensions FRMS 750 W:

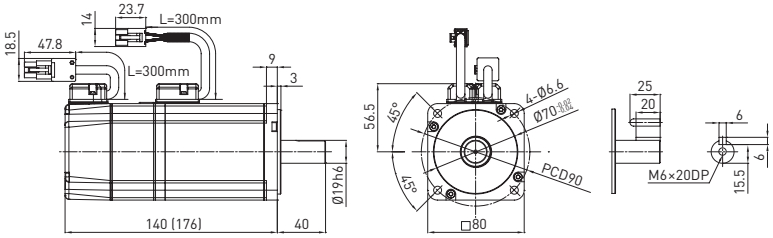

Values in brackets apply
to model with motor brake

E Gearbox Datasheet

VRL-SERIES Inline shaft

VRL-090 – 1-Stage Specifications

Frame Size	090									
Stage	1-Stage									
Ratio	Unit	Note	3	4	5	6	7	8	9	10
Nominal Output Torque	[Nm]	*1	50	75	75	75	75	75	50	50
Maximum Acceleration Torque	[Nm]	*2	80	125	125	125	125	125	80	80
Emergency Stop Torque	[Nm]	*3	200	250	250	250	250	250	200	200
Nominal Input Speed	[rpm]	*4	3000							
Maximum Input Speed	[rpm]	*5	6000							
No Load Running Torque	[Nm]	*6	0.35							
Permitted Radial Load	[N]	*7	810	890	960	1000	1100	1100	1200	1200
Permitted Axial Load	[N]	*8	930	1100	1200	1300	1300	1400	1500	1600
Maximum Radial Load	[N]	*9	2400							
Maximum Axial Load	[N]	*10	2200							
Moment of Inertia (≤Ø 8)	[kgcm2]	--	--	--	--	--	--	--	--	--
Moment of Inertia (≤ Ø 14)	[kgcm2]	--	0.720	0.490	0.400	0.360	0.320	0.310	0.290	0.290
Moment of Inertia (≤ Ø 19)	--	--	1.200	0.950	0.860	0.820	0.790	0.770	0.760	0.750
Moment of Inertia (≤ Ø 28)	[kgcm2]	--	3.200	3.000	2.900	2.800	2.800	2.800	2.800	2.800
Efficiency	[%]	*11	95							
Torsional Rigidity	[Nm/arc-min]	*12	10							
Maximum Torsional Backlash	[arc-min]	--	≤ 5							
Noise Level	[dB]	*13	67							
Protection Class	--	*14	IP54 (IP65)							
Ambient Temperature	[°C]	--	0-40							
Permitted Housing Temperature	[°C]	--	90							
Weight	[kg]	*15	3.5							

VRL-090 – 2-Stage Specifications

Frame Size	090									
Stage	2-Stage									
Ratio	Unit	Note	15	16	20	25	28	30	35	40
Nominal Output Torque	[Nm]	*1	50	75	75	75	75	50	75	75
Maximum Acceleration Torque	[Nm]	*2	80	125	125	125	125	80	125	125
Emergency Stop Torque	[Nm]	*3	200	250	250	250	250	200	250	250
Nominal Input Speed	[rpm]	*4	3000							
Maximum Input Speed	[rpm]	*5	6000							
No Load Running Torque	[Nm]	*6	0.06							
Permitted Radial Load	[N]	*7	1400	1400	1500	1600	1700	1700	1800	1900
Permitted Axial Load	[N]	*8	1900	1900	2100	2200	2200	2200	2200	2200
Maximum Radial Load	[N]	*9	2400							
Maximum Axial Load	[N]	*10	2200							
Moment of Inertia (≤Ø 8)	[kgcm2]	--	0.130	0.150	0.130	0.120	0.140	0.100	0.120	0.099
Moment of Inertia (≤ Ø 14)	[kgcm2]	--	0.280	0.300	0.280	0.280	0.290	0.250	0.270	0.250
Moment of Inertia (≤ Ø 19)	--	--	0.720	0.740	0.720	0.710	0.730	0.700	0.710	0.700
Moment of Inertia (≤ Ø 28)	[kgcm2]	--	2.700	2.800	2.700	2.700	2.700	2.600	2.700	2.600
Efficiency	[%]	*11	90							
Torsional Rigidity	[Nm/arc-min]	*12	10							
Maximum Torsional Backlash	[arc-min]	--	≤ 5							
Noise Level	[dB]	*13	67							
Protection Class	--	*14	IP54 (IP65)							
Ambient Temperature	[°C]	--	0-40							
Permitted Housing Temperature	[°C]	--	90							
Weight	[kg]	*15	4							

F Further explanation of requirements

Table 14: A table expanding on what the different attributes regard and involve.

Test-rig attribute	Explanation
Low moment of inertia	The moment of inertia of the moving assembly, be it the arm and shaft of concept 1 or the carriages and arm of concept 4.
Repetitiveness	How well the test-rigs would be able to duplicate results between experiments.
Extreme cases	How the test-rigs perform during experiments where with extreme loads.
Easy access to nut	How easy it is to change or adjust the nut
Easy access to tool	How easy it is to access the tool and to change it to another type.
Robustness	The test rig should be steady for heavy forces.
Vibration resistance	The test rig should be able to handle large vibrations from the tightenings but how well vibration resistance was for the concepts was not calculated.
IRTT Compatibility	The test rig should provide space to fit an IRTT sensor between the beam test joint and the tool head.
Vertical adjustment	The test rig should enable the tool to move vertically during tightening and loosening. Vertical movement is also an important factor in the accessibility of changing tools.
Component availability	How easy it is to get access to necessary components to assembly the test rig. Delivery time off components is highly important.
Mobility	How easy it is to move the test rig to another location.

G Bill Of Materials (BOM)

Note: the costs are without VAT.

Piece	Article nr.	Description	Comment	Unit cost	Units	Total Cost
Aratron						
Profile 45x45 UL, length = 380	20.1063/0	380		65	3	195
Profile 45x45 UL, length = 750	20.1063/0	750		129	2	258
Profile 45x45 UL, length = 222	20.1063/0	222		38	2	76
Profile 45x45 UL, length = 131	20.1063/0	131		23	1	23
Profile 45x45 UL, length = 110	20.1063/0	110		19	1	19
Profile 45x45 UL, length = 500	20.1063/0	500		86	1	86
Rail 45, length = 650	28.0006/0	650		434	2	868
Slide LW 45	28.0091/0	Carriage		1761	2	3522
Mounting angle 45 GD	21.1133/0	Connector		39	5	195
MiniTec Power lock fastener 45	21.1018/0	Connector	Some surplus	39	12	468
T sheet VA	21.0019/0	Connector		130	2	260
End cap 45x45 Z grey	22.1004/1	Cosmetic	Some surplus	9	12	108
Adapter plate between gearbox and servo	19DD M6 PCD90R			494	1	494
Gearbox, n=20	VRL-090C-020-K5-19	With keyway		3415	1	3415
750W Motor	1 040 726	FRMS7520508A		2038	1	2038
Motor Driver	1 041 247	D2-1023-E-C0		6837	1	6837
Power cord 5m	1 038 704	HVPS04AA05MB		232	1	232
Encoder cable 5m	1 038 705	HVE13IAB05MB		413	1	413
Cutting of profiles				80	10	800
EMC-filter for servo driver	D2-EMC3			387	1	387
						0
						0
Aratron (round 2)						
Nuts (suqare,with springs), M8	1071710	LÄNK		7	12	84
Nuts (suqare,with springs), M6	1069122	LÄNK		7	20	140
Gas springs	1025891	LÄNK		411	2	822
Angle connector	1009384			53	4	212
Pressure adjustment in gas springs	1073578			40	2	80
RS Components Sweden						
Breaking resistor 110Ω 100W	185-2423	LÄNK		115	1	115
Endstop switches	616-0524	LÄNK		59	3	177
Elfa						
Contactor, 2NO, 12V, 25A, 6.25kVA, Finder	136-70-322			268	1	268
Emergency stop, 2NC, Röd / Gul, IP65, IDEC	302-21-437			384	1	384
Key switch, 1 pole, Lorlin	135-04-482			85	1	85
Circuit breaker C, 6A, 500V, IP20	110-83-834			333	1	333
Switching power supply, 60W, 12V, 5A	300-60-595			177	1	177
Load cell amplifier	301-45-509			102	2	204
Hall effect sensor	173-49-087			51	2	102
Accelerometer ADXL345	301-39-029			167	1	167
Rocker switch CR, 1NO, ON-OFF, Black/Green	301-61-424			13	2	26
Elfa (round 2)						
Led lamp, Green, 8.1mm, 12V	133-71-150	LÄNK		41,4	1	41,4
RCBO 10A 2 poles	110-47-908	LÄNK		877,2	1	877,2
Relay for circuit board	301-18-686	LÄNK		43,9	2	87,8
Electrical cabinet 155x380x300mm	302-32-166	LÄNK		890	1	890
Pushbutton, green	135-12-322	LÄNK		146	1	146
Pushbutton, red	135-12-323	LÄNK		142	1	142
DIN-35-rail	150-63-508	LÄNK		34,1	1	34,1
Elfa (round 3)						
RJ45 contacts	301-38-983			48	3	144
Rocker switch (ON)-OFF-(ON)	135-03-45			43,29	1	43,29
Pushbutton	302-21-591			41	1	41
Ethernet cable	301-25-203			50,3	1	50,3
Elfa (round 4)						
WR-MJ modular contact, RJ45	301-27-254			23,4	6	140,4
Contact block for pushbutton, 1NO	302-21-459			83,9	1	83,9
Pushbutton 1NO OFF-(ON) Black	135-27-538			64,1	1	64,1
Patch cable, RJ45 kontakt - RJ45 kontakt, Cat 6, 2m	301-25-203			50,3	1	50,3
Aluminium tape, 50mm x 50m	302-21-408			208	1	208
					Total:	27113,79

H Project Poster

Atlas Copco

HK Project

An **automated** platform for **repetetive** ergonomic assessment of hand-held power tools

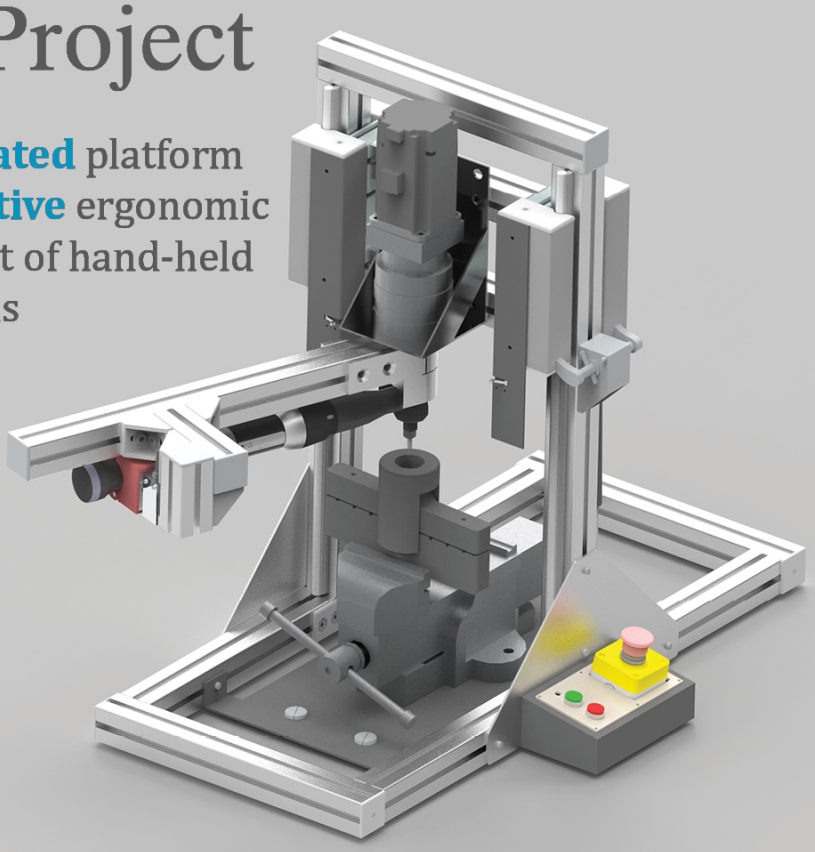

Samuel Eriksson, Petter Falkenstrand, Annie Farell, Tim Gidlöf, Anton Hylander, William Marin, Denis Ramsden, Erik Rudqvist, Signe Stéen

December 2021

KTH VETENSKAP OCH KONST